Universitat Autònoma de Barcelona

Analysis of miRNA expression in Alzheimer's disease. Potential use as early biomarkers

Dolores J. Siedlecki Wullich

Institut de Neurociències

Departament de Bioquímica i Biologia Molecular

Unitat de Bioquímica, Facultat de Medicina

Universitat Autònoma de Barcelona

"Analysis of miRNA expression in Alzheimer's disease. Potential use as early biomarkers"

Dolores J. Siedlecki Wullich

TESIS DOCTORAL

Bellaterra, 2018

Institut de Neurociències
Departament de Bioquímica i Biologia Molecular
Unitat de Bioquímica, Facultat de Medicina
Universitat Autònoma de Barcelona

"Analysis of miRNA expression in Alzheimer's disease. Potential use as early biomarkers"

"Análisis de la expresión de miRNAs en la enfermedad de Alzheimer. Potencial uso como biomarcadores tempranos"

Memoria de tesis doctoral presentada por Dolores J. Siedlecki Wullich para optar al grado de Doctora en Neurociencias por la Universitat Autonòma de Barcelona.

Trabajo realizado en la Unidad de Bioquímica y Biología Molecular de la Facultad de Medicina del Departamento de Bioquímica y Biología Molecular de la Universitat Autònoma de Barcelona, y en el Instituto de Neurociencias de la Universitat Autònoma de Barcelona, bajo la dirección de los Doctores José Rodríguez Álvarez y Alfredo J. Miñano-Molina.

El trabajo realizado en esta tesis doctoral ha estado financiado por los siguientes proyectos de investigación: Ministerio de Economía y Competitividad (MINECO), *Molecular mechanisms involved in glutamatergic synapses dysfunction in early stages of Alzheimer disease* (SAF2014-59697-R), Fundació La Marato de TV3, *Searching new biomarkers and therapeutic targets related to cognitive deficits in early stages of Alzheimer's Disease* (Marato TV3 2013-343), Centro de Investigación Biomédica en Red de Enfermedades Neurodegenerativas (CIBERNED) (CB/06/0005/0042), y el proyecto colaborativo de CIBERNED, *Study of exosomal microRNA from CSF as a biomarker for frontotemporal dementia and as a tool to understand the biological basis of the pathology.*

Bellaterra, 28 de septiembre de 2018

Doctoranda	Director de tesis	Director de tesis
Dolores J. Siedlecki Wullich	José Rodríguez Álvarez	Alfredo J. Miñano-Molina

«Cuando está de veras viva,
la memoria no contempla la historia,
sino que nos invita a hacerla.
Es contradictoria, como nosotros.
Nunca está quieta:
como nosotros, cambia»
Eduardo Galeano

INTRODUCTION

More than one hundred years have passed since Santiago Ramón y Cajal defended the doctrine of the neuron during his acceptance of the Nobel Prize: the brain tissue was made up of individual cells (neurons) that establish contacts between them[1]. Nowadays, we know that those connections, called synapses, are complex and dynamic structures formed by multiple cell types, and it is in this network where our knowledge and memories are supported. Memory is who we are, is the accumulation of our lived experiences, of everything that has shaped our personality, our desires and dreams. Life, as Gabriel García Márquez said, *"…is not the one we lived, but the one we remember (…)".*

Thus, if memory is who we are, dementia is a syndrome that threatens our identity producing structural and functional changes in the brain that gradually impairs memory, affecting thinking abilities and personality. Alzheimer's disease (AD) is the most common type of dementia, accounting for an estimated 60 to 70% of cases.

Although memory loss is one of the first symptoms of the pathology, when this symptom appears, the disease has been developing silently for many years. When AD is diagnosed, neuronal death is already extensive in areas such as the entorhinal cortex and the hippocampus, making it difficult for available treatments to have an effect beyond delaying the progression of the disease for a short period of time. Unfortunately, there is no effective treatment able to stop AD progression.

It is for this reason that in recent years, efforts to develop and validate AD biomarkers have increased. A diagnosis that incorporates the identification of biomarkers in blood or cerebrospinal fluid, could significantly improve the tools already available, promoting an early detection of the disease.

In this scenario, we aim to study the mechanisms underlying early synaptic dysfunction associated to AD, and to identify blood biomarkers capable of differentiating early stages of the AD pathology, therefore, allowing the use of new potential treatments. In addition, an early diagnosis of the disease could give a new opportunity to therapies that have failed in past clinical trials, maybe due to an improper time of application: too late in the development of the disease. An earlier diagnosis could be the key to achieve the preservation of patients' normal brain function.

1. Alzheimer’s disease

The numbers of the disease

According to *World Alzheimer Report 2016*, 47 million people are living with dementia worldwide. Dementia prevalence reaches almost 50% in people older than 85 years, and due to population aging, it is expected that 131 million persons will be affected by this syndrome by 2030[2]. This accelerated increase in the number of cases makes it an issue not only for those affected and their families, but also a socio-health problem of first magnitude.

Dementia is a general term that describes a syndrome characterized by cognitive or/and behavioral affectation that disturbs daily life. Within the wide range of symptoms covered, the most characteristic is memory impairment, which occurs when brain structures related to this function, such as entorhinal cortex and hippocampus, are affected[3,4]. Difficulties in the expression and understanding of language, diminished visuospatial skills, difficulty in performing tasks and making decisions or even changes in personality could be also present[5]. These symptoms, which result in severe long-term impairment of cognitive function, are one of the leading causes of disability and dependency among the elderly worldwide. The most frequent forms of dementia include dementia with Lewy bodies, vascular dementia, frontotemporal dementia, Parkinson's disease, and the one with the highest prevalence: Alzheimer's disease (AD), which affects 60 to 70 percent of demented people[2,6].

Dementia is not a normal part of aging, but age is a main risk factor. The increase in life expectancy is turning AD into an epidemic, as the prevalence increase exponentially with age, reaching about 30 percent prevalence in people over 85 years[7–9]. The consequences of the disease are devastating for entire families, since it has an impact not only on the patient, but also on their relatives and caregivers, increasing the numbers of those affected directly and indirectly by the disease[10].

In 2016, the worldwide cost of dementia was estimated in US$948 billion, including costs of informal, social and medical care. With an annual growth rate of almost 16 per cent, it is expected that dementia cost will rise above a US$ trillion this year and

US$ 2 trillion by 2030[11,12]. Unfortunately, the budget for research is far below that intended to alleviate the effects of this disease. Although an early diagnosis could save only in the USA US$ 7 trillion, for every $9,700 that National Institutes of Health spend on medical care for people with AD, only $100 are used for AD research[13].

AD genetics and neuropathological aspects

AD is histopathologically characterized by the accumulation and deposition of amyloid-β peptides (Aβ), forming extracellular amyloid plaques, and abnormally hyperphosphorylated species of tau, a microtubule-associated protein, forming intraneuronal neurofibrillary tangles (NFTs)[14] and aggregated in paired helical filaments (PHFs)[15] (Figure 1). These pathological hallmarks, mostly found in hippocampus and cortical regions, are accompanied by synaptic dysfunction and neuronal death. In initial stages of the disease, loss of synapses correlates with early memory decline[16–18].

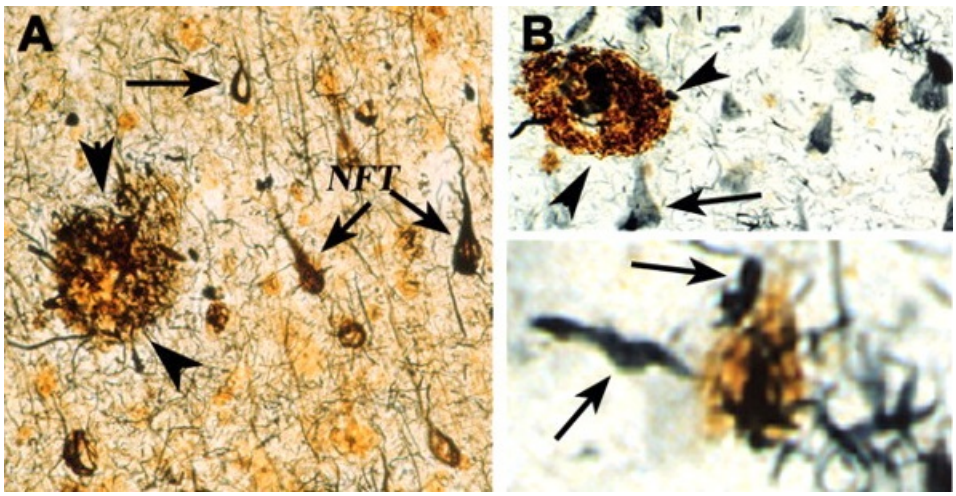

Figure 1: Pathological hallmarks of AD. β-amyloid plaques (arrowheads) and neurofibrillary tangles (arrows) in AD brain (Bielschowsky silver stain) (A). Tau and β-amyloid PHF-containing neurites associated with amyloid deposits labeled by anti-PHF antibody (B). (Figure from Nixon 2007[15])

In 1906 the neuropathologist Aloysius “Alois” Alzheimer described the clinical and neuropathological characteristics that still define the disease that was named after him a few years later by Emil Kraepelin. After the histopathological analysis of the brain of Auguste Deter, a patient who had suffered from delusions, auditory

hallucinations, speech and perception problems and severe memory decline, Alzheimer described for the first time the neurofibrillary tangle pathology. Moreover, he detected neuritic plaques, already known by that time, but that had never been observed in someone as young as Auguste, who was 51 years old when she was admitted to the Frankfurt hospital. It was Alzheimer who linked the presence of senile plaques to dementia condition[19–21].

AD is a complex syndrome where environmental and genetic factors have their implication, and which can be classified in early onset AD (EOAD) and late onset (LOAD). EOAD, also known as familial AD, is the form of AD originally identified by Alzheimer that affects adults under 65 years, often before age 55 years, who inherit the disease in an autosomal dominant fashion. Familial AD share the same histopathological characteristics described by Alzheimer with the LOAD or sporadic AD, that affects usually people over 65 years.

Early and late onset AD

EOAD constitutes from 1 to 5 percent of AD cases and is caused by mostly autosomal dominantly inherited mutations in three genes involved in the amyloid precursor protein (APP) processing: APP, presenilin-1 (PSEN1), and presenilin-2 (PSEN2)[7,22–24] More than 200 mutations in these 3 genes have been described and linked to the disease[25,26]. Mutations in PSEN1 account for most EOAD cases[25] (30 to 70 percent of cases)[27]. Familial AD is usually associated with a faster progression of the disease[23].

On the other hand, from 95 to 99 percent of AD cases can be classified as LOAD or sporadic AD, where the best known genetic risk factor is the genotype of the apolipoprotein E (APOE) alleles: APOE2, APOE3, or APOE4. APOE is a major lipid transporter highly expressed in the brain which allows lipids, cholesterol, and other hydrophobic molecules uptake and redistribution within cells, critical in the maintenance of myelin and neuronal membranes[9,28,29]. It has been shown that cholesterol mobilization, transport and elimination could affect the progression of LOAD[30,31]. While homozygosis for the APOE2 allele is linked to preserved cognitive function, APOE4 allele correlates with increased risk and earlier AD onset[32].

Heterozygosis for APOE4 allele increases the risk by a factor of 3, while homozygosis increase the risk by a factor of 8-10[28,33] compared to E4 non-carriers.

While other genes implicated in cholesterol metabolism, mitochondria dysfunction, innate immune and inflammatory reactions and endocytosis have been associated to LOAD[34], age remains the greatest and indisputable risk factor for AD. Though more discussed, sex could be another risk factor[35,36]. Only in Europe there are nearly 9 million people affected by AD of which almost 6 million are women [37]. Whereas some reports point that the increasing incidence of AD with age shows no difference between men and women[38], other studies show an interaction between APOE4 and sex with a stronger effect of APOE4 allele in females than in males[39–41]. Physiological factors linked to sex, such as menopause or pregnancy, or predisposition to other diseases, such as vascular diseases, have been pointed as potential differential risk factors that might interact with APOE4[9,13,42,43]. Even social elements, such as unequal access to education, could be taken into account as playing factors in AD sex prevalence differences[43].

Although the mechanisms by which APOE4 affects AD pathogenesis remain unclear, it has been shown that its implication in cholesterol homeostasis, β-amyloid peptides (Aβ) deposition and soluble oligomeric Aβ (oAβ) formation could affect the progression of LOAD[28,30,31,33].

APP processing and amyloid cascade hypothesis

APP is *an essential* type I transmembrane protein with a large extracellular domain and a short intracellular domain that plays a crucial role in AD pathogenesis since Aβ, which are accumulated and deposited as senile plaques in AD patients' brains, are a product of its processing. APP could be cleaved either by the α-secretase or by the β-site APP cleaving enzyme-1 (BACE1 or β–secretase) to initiate nonamyloidogenic or amyloidogenic pathways, respectively. The nonamyloidogenic pathway starts with APP cleavage in the middle of the Aβ region by α-secretase releasing a large amyloid precursor protein ectodomain (sAPPα) and a shorter 83-residue carboxy-terminal fragment (CTF). This CTF is then cleavage by γ-secretase generating an extracellular p3 fragment and a C-terminal APP intracellular domain fragment (AICD)[44]. The APP amyloidogenic processing consists in a sequential

proteolytic cleavage: first β-secretase cleaves APP in the N-terminal side of the Aβ sequence, generating a C-terminal fragment that is then cleaved by γ-secretase releasing an AICD and extracellular Aβ peptides[45]. Hence, γ-secretase has an important role in APP processing, since it participates in both amyloidogenic and nonamyloidogenic pathways. γ-secretase is a large enzyme formed by multiple subunits of which the catalytic subunit is presenilin, a multi-pass transmembrane protein that cleavages different type I transmembrane proteins. As mentioned before, APP and PSEN mutations has been linked to neurodegeneration processes and pointed as a main cause of FAD[46–48]. Many of these mutations altered the balance between Aβ species generated *in vivo* after APP processing, increasing Aβ42/Aβ40 ratio[46,49]. While Aβ40 has been proposed to have an anti-amyloidogenic role[50], Aβ42 and Aβ43 are particularly hydrophobic species that express high potential of self-aggregation contributing to amyloid plaques formation[51,52]. Aβ accumulation and deposition into plaques is the earliest event in *the amyloid cascade hypothesis*[53], proposed as the primary cause driving all of the other pathological features including disrupted calcium homeostasis, intracellular NFT formation, inflammation, loss of synaptic connections and cell death (Figure 2). However, in the last decades has also emerged that oAβ but not amyloid plaques initiates the pathological cascade. It has been shown that oAβ toxicity is higher compared to fibrils and non-aggregated monomers and is its presence which negatively affect hippocampal long-term potentiation (LTP) and can even disrupt synaptic plasticity[54] constituting a key pathogenic event in early neurodegenerative processes linked to AD[55–57]. Though it is unquestionable that Aβ plays a critical role in AD neuropathology, several evidences indicate that amyloid plaques accumulation in the brain does not correlate with cognitive impairment, and even people with widespread amyloid plaque neuropathology could exhibit normal cognitive function[58]. If oAβ could not fully explain this multifactorial pathology, it seems reasonable to think of multiple players as part of the same complex process.

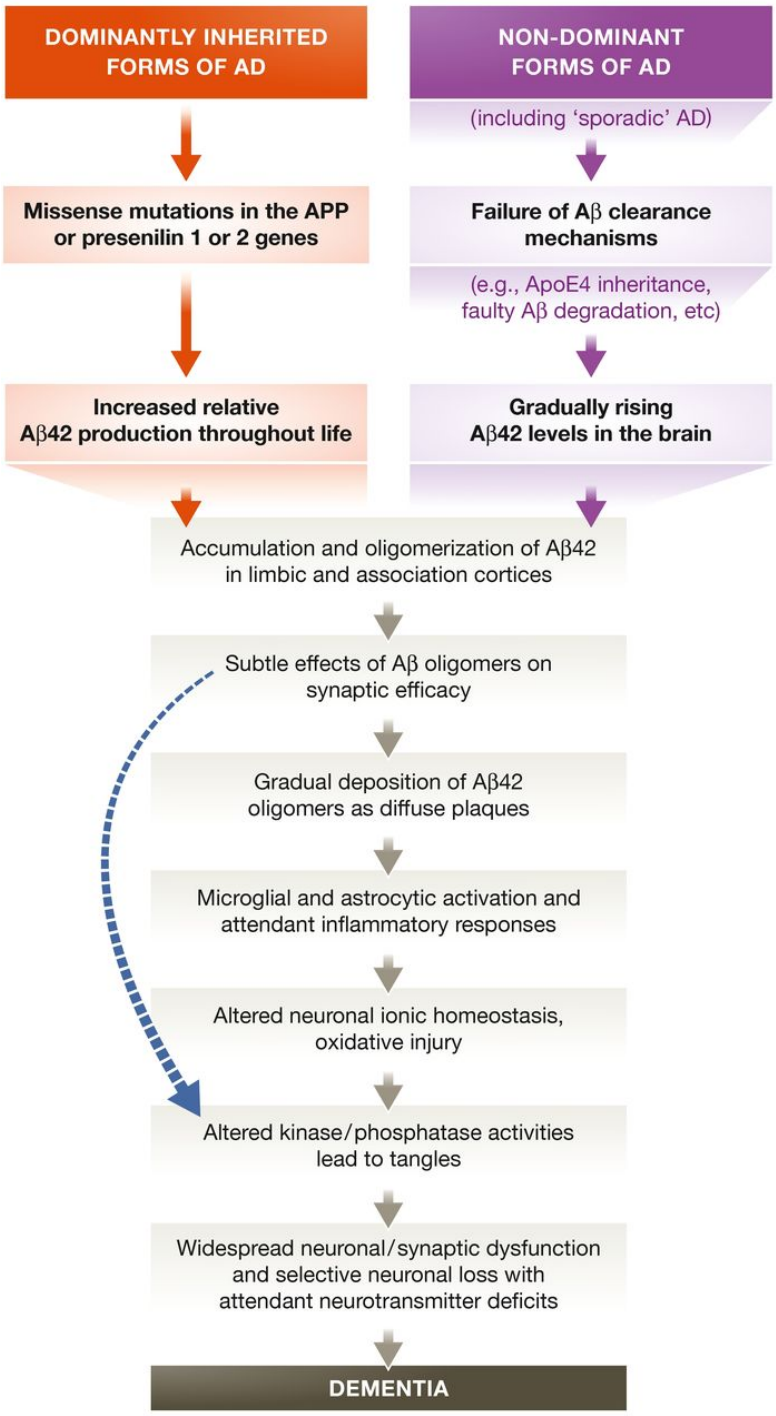

Figure 2: The amyloid cascade hypothesis. From APP processing and oAβ generation through the amiloidogenic pathway, to neuronal death and dementia, AD is characterized by a cascade of events of which synapse afection is one of the earliest (from Selkoe & Hardy 2016[59]) .

Tau pathology

Tau aggregation forming neurofibrillary tangles is the other main hallmark of AD brains. Tau is a microtubule-associated protein (MAP) encoded by the *MAPT* gene located in chromosome 17 that regulates the polymerization, stability and re-organization of axonal microtubules[60,61]. Tau biological activity is regulated by its phosphorylation state, characteristically increased in AD and other tauopathies. Under pathological conditions, tau localization is not limited to axons, as in normal conditions, but is redistributed to the cell body and neurites. Tau hyperphosphorylation decreases its affinity for microtubules and consequently its assembly activity that results in the breakdown of the microtubule network. Moreover, hyperphosphorylation facilitates tau aggregation and NFTs formation, contributing to signaling impairment and neurodegeneration[61–63]. Of note, several evidence suggests that toxic effects induced by Aβ may be mediated by tau[52,64–66]. Tau dysfunction has been also linked to degeneration since mutations in *MAPT* is known to cause Parkinsonism linked to chromosome 17 (FTDP-17), and other missense mutations in this gene have also been related to inherited frontotemporal dementia, corticobasal degeneration, progressive supranuclear palsy and Pick's disease[60,61,67].

AD pathological classification and cognitive impairment correlation

Unlike what occurs with the presence of amyloid plaques in the brain, NFT tau pathology does correspond to cognitive decline[55,68] and while neurite plaques are irregularly distributed, NFT pathological progress pattern is well characterized and shows minor inter-individual variations[69]. NFT pathology initiates in the entorhinal cortex (EC), continues with hippocampus affection, reaches subcortical limbic region and in final pathological stages it spreads to association cortices and most neocortical areas[69,70]. This characteristic pattern allowed Braak and Braak to establish the mostly used pathology classification that settled 6 pathological stages known as Braak stages[69–71] (Figure 3). Braak stages I–II are designed as *transentorhinal stages* as is this the first affected region with slight compromise of the hippocampus (CA1 and subiculum) as well. This early stages might represent preclinical phase of AD. Stages III-IV are characterized by limbic affection and still-low isocortical involvement. Clinically could correspond to incipient AD or mild

cognitive impairment (MCI). At later stages (Braak V–VI) the pathology includes all the changes noted in earlier stages and also is widely spread throughout the neocortex severely affecting frontal and occipital cortices. Moreover, in these final stages, considerable loss of neurons is observed and cognitively match with fully developed AD[69,71].

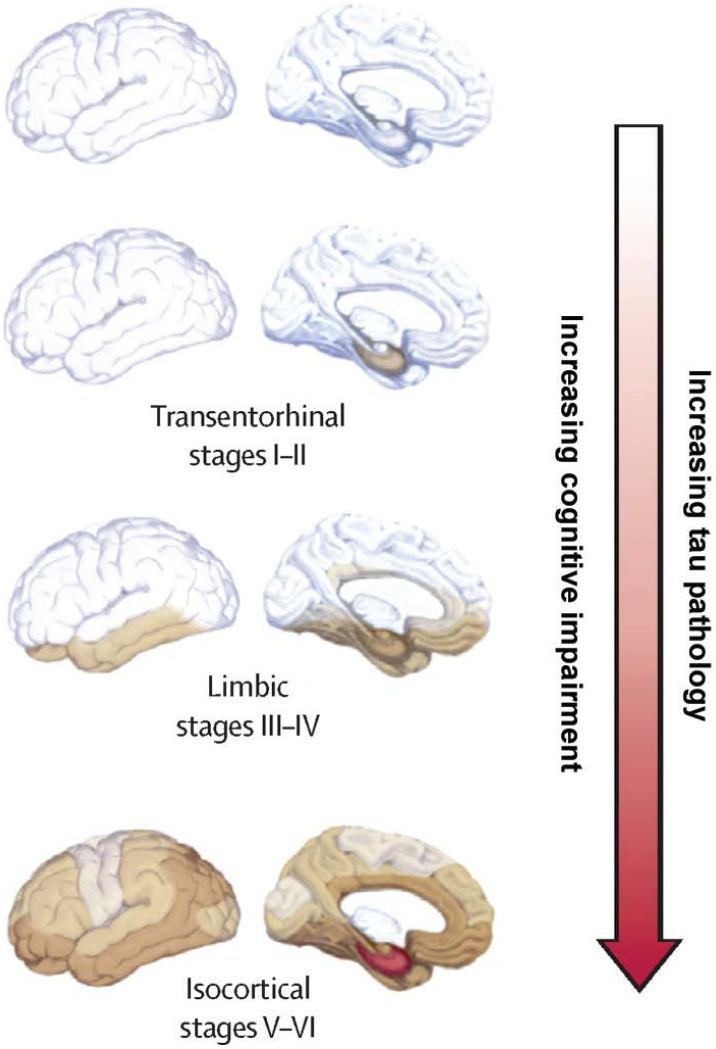

Figure 3: Progression of tau pathology during AD and correlation with cognitive state. Classification in 6 stages according to Braak and Braak staging[69,70]. (Figure from Villemagne 2015[72])

Recent evidence in experimental models of AD suggest that this progression pattern could be determined by tau misfolding transmission between cells using stablished neural circuits[73].

Both tau[74] and oAβ[75] have been proposed to be involved in synaptic plasticity impairment in early AD, through the balance alteration between long-term potentiation (LTP) and long-term depression (LTD).

Synaptic plasticity and glutamatergic synaptic transmission

LTP and LTD are the most widely studied forms of synaptic plasticity, that are believe to underlie learning and memory[76–79]. The most prevalent forms of these processes are induced by Ca2+ influx through postsynaptic N-methyl-D-aspartate receptors (NMDAR), which, in turn, regulates the recruitment or removal of synaptic α-amino-3-hydroxy-5-methylisoxazole-4-propionic acid receptors (AMPAR), strengthening or weakening synapses, respectively[76,80]. Transient activation of NMDAR initiates a wave of synaptic activity that is expressed as a persistent increase in synaptic transmission through AMPAR. The opening of a large number of AMPAR produces important membrane depolarization that finally could lead to an action potential response in the postsynaptic neuron. Moreover, postsynaptic depolarization produces Mg^{2+} ions removal from NMDAR channel, allowing a strong Ca^{2+} influx through activated NMDAR. Increased intracellular Ca^{2+} levels activate several protein kinases, such as protein kinase A (PKA), protein kinase C (PKC) and calcium/ calmodulin-dependent protein kinase II (CaMKII), triggering important signaling cascades[81]. Calcium rise also mediates presynaptic LTP processes that mainly involve voltage-gated Ca^{2+} channels (VGCC)[82] that eventually increase glutamate release from the presynaptic terminals.

LTP can be divided into three components: a transient phase that depends on fast signaling mechanisms, called short-term potentiation (STP), and a sustained period that includes early LTP (E-LTP) and late LTP (L-LTP)[79,83–85]. Early and late phases of sustained LTP are defined by differentiated mechanisms: E-LTP is a brief phase, independent of PKA and *de novo* protein synthesis that can be induced with a single period of high frequency stimulation (HFS). Whereas L-LTP is long lasting, requires multiple HFS events for its induction[86], is PKA-dependent and involves new gene expression and protein synthesis that leads to additional structural changes such as growth and remodeling of preexisting synapses and also new synapses formation [87]. At the gene expression level, L-LTP requires the activation of a complex signaling network that involves several protein kinases including PKA, CaMKII, CaMKIV and

mitogen-activated protein kinase (MAPK) that leads to cAMP response element binding protein (CREB) dependent gene expression.

It is known the central role that NMDAR have in synaptic plasticity, and that AMPAR localization is closely related to them. Nonetheless it has also been shown that L-LTP requires synaptic recruitment of calcium permeable AMPAR and that one of the main mechanisms of LTD induction is the removal of these receptors from the postsynaptic membrane, indicating that AMPAR are important players in these processes[78,88–91]. Besides to the number of receptors at synapses, it has been reported that synaptic transmission is regulated by phosphorylation of AMPAR subunits, which determine their activity and trafficking[92,93].

AMPAR as key players in glutamatergic synaptic transmission

The study of AMPAR trafficking and function has focused the attention of many groups due to the evident role they have in health and disease, modulating excitatory transmission in the central nervous system (CNS).

AMPAR structure is well characterized: they are tetrameric ionotropic receptors formed by combination of 4 subunits (GluA1 to GluA4) which combination determines the main properties of the receptor. In this way, changes in the subunit composition constitute an effective way to alter synaptic transmission by modification of agonist affinity, activation kinetics or calcium permeability, without affecting the number of receptors[94]. Specifically, the C-terminal region of AMPAR subunits undergo a fine-tuning phosphorylation-desphosphorylation mechanism that regulates functional aspects such as their activity-dependent trafficking to the synapse[78,90,95,96].

Lu and collaborators[97] described that near 80 percent of synaptic and over 95 percent of somatic extrasynaptic receptors in CA1 pyramidal neurons are GluA1/GluA2 heteromers which mainly mediates excitatory synaptic transmission. In addition, it has been reported that GluA1 is mostly involved in activity-dependent synaptic targeting of AMPAR while GluA2 and GluA4 are more related to basal synaptic transmission maintenance[90,95,97].

Interestingly, GluA1 intracellular C-terminal region has several serine residues susceptible of being phosphorylated including Ser831 and Ser845. Ser831, phosphorylated by CaMKII, is implicated in the regulation of ion channel conductivity while Ser845 phosphorylation by PKA is related both to AMPAR recruitment to the cell surface during LTP[98,99] and with increased probability of channel opening, and consequently with receptor function potentiation[100]. On the other hand, dephosphorylation of Ser845 by the calcium-dependent phosphatase calcineurin, correlates with AMPAR endocytosis [92], essential for NMDAR-dependent LTD[81,101–103]. Moreover, Lee and collaborators[102] demonstrated that phosphorylation of GluA1 AMPAR subunit is critical for synaptic plasticity processes, since deficits in LTP and LTD induction were observed when GluA1 subunits were mutated in CaMKII and PKA phosphorylation sites in mice. Less is known about the role of Ser818 GluA1 phosphorylation, though it has been suggested that its phosphorylation by PKC is increased during LTP and may have a modulating role facilitating LTP expression[104,105]. Importantly, evidence suggests that GluA1 alone is sufficient for AMPAR trafficking to the synapse surface[97,101], proposing an important activity-dependent role of this subunit during learning and memory processes.

Considering the aforementioned, it is clear that AMPAR trafficking is a dynamic process modulated by LTP and LTD and mediated by fast and long-lasting changes in number, localization and receptor properties. Since AMPAR could be recruited from intracellular reservoirs or could laterally diffuse from extrasynaptic pools to the spine membrane[80], their trafficking also required a huge amount of proteins capable of guiding and retaining receptors at the post-synaptic density (PSD). Thus, the role of scaffolding proteins at the PSD has been largely studied and related to trafficking and mobility of receptors along the cell membrane, protein assembly, synaptic growth and plasticity[106–108].

AMPAR-related proteins at synapses

PSD-95, the most abundant postsynaptic scaffolding protein, contains three protein-protein interaction motifs (PDZ domains) that allow it to interact with a huge diversity of proteins. It is known that it facilitates signal coupling by bringing together cytoplasmic signaling molecules and surface receptors [107,109]. For instance, PSD-95 can interact with supporting transmembrane AMPAR regulatory proteins (TARP)[94]

an also with the A-kinase-anchoring (AKAP) family of proteins. Human AKAP79 and its murine orthologue AKAP150, are scaffolding proteins that controls AMPAR assembling at synapses by keeping kinases and phosphatases responsible for its regulation (PKA, PKC and calcineurin) close to their substrate in the PSD[107,110]. It has been described that AKAP can also control calcium permeable AMPAR delivery to synaptic terminals during NMDAR-dependent LTD[81] pointing out that these protein complexes could have an important role modulating the activity of the receptors involved synaptic plasticity. In the same way, they could have an important role during synaptic function alterations observed in early stages of AD.

Neuronal pentraxins (NP) are another family of AMPAR-interacting proteins mainly expressed in the nervous system, especially in cerebellum and CA3 hippocampal neurons[111,112]. Binding to the membrane-distal N-terminal domain (NTD)[113] of all AMPAR subunits[109,114], they are thought to promote receptor clustering and retention at synapses[90,115]. Neuronal pentraxin 1 (NP1) and neuronal pentraxin 2 (NP2) are secreted from glutamatergic terminals while the neuronal pentraxin receptor (NPR) is a type II transmembrane protein, which has been suggested to facilitate AMPAR interaction with secreted NP[115,116]. NP1 and NP2 are induced in different conditions, whereas NP2 is synaptic activity-dependent; NP1 is induced under low neuronal activity conditions. Therefore, although both pentraxins are believed to affect excitatory transmission, they probably do so through opposite mechanisms[109,112,117,118].

Synaptic dysfunction in AD

Several evidences suggest that cognitive decline observed in early stages of AD could be due, in part, to alterations in synaptic function that occurs before neurodegeneration takes place[119,120]. Total number of synapses in the hippocampus and frontal cortex of early AD patients displays a positive correlation with the Mini-Mental State exam (MMSE) used to evaluate cognitive function, and with other cognitive tests that evaluate hippocampus-dependent tasks such as the delayed word list recall test. These findings indicate that cognitive function impairs as synapses number decreases[18,119,121]. Synaptic loss in AD is well characterized and It has been shown that correlates with cognitive decline linked to AD progression in a clearer way that classical AD hallmarks (amyloid plaques and NFT)[17,57,119,121–123].

In addition, wide loss of synaptic markers are observed in early AD[123] and recent reports indicate that synaptic proteins are able to discriminate between healthy controls and demented subjects with high sensitivity and specificity[124]. Supporting these findings, also significant associations between synaptic proteins and cognitive decline were found in other types of dementia, such as Parkinson's disease or dementia with Lewy bodies[125]. In regard to experimental models of AD, a relationship between deregulation of synaptic proteins levels and early cognitive dysfunction has been suggested[126,127] and a negative effect of oAβ on synapses has also been established [128–130].

APP processing and consequent Aβ generation is promoted by neuronal activity[131]. Under normal conditions, Aβ is able to restore homeostasis tuning down neuronal hyperactivation through LTD-related mechanisms, such as endocytosis of glutamate receptors. However, during pathological processes, Aβ accumulation modulates downstream kinases and phosphatases leading to an excessive internalization of NMDAR and AMPAR[132–134] that impairs normal glutamatergic synaptic transmission. The negative effects of the alteration between LTP and LTD on dendritic spines shape and number has been widely supported[75,129,132–142]. It has been reported that exposure to oAβ decreases stubby and mushroom spines, characteristic of healthy neurons, and leads to formation of aberrant filopodial spines[137,143] therefore, reducing functional synapses[76–79,144]. Thus, evidence suggest that oAβ is specially toxic to glutamatergic synapses, initiating a cellular cascade that leads to synaptic dysfunction and finally to neuronal death[55,57,137,145].

Several studies have shown that oAβ can facilitate the removal of AMPAR from the cell surface, thus the functionality of these receptors could be involved in the early cognitive dysfunction observed in experimental models of AD[93,127].

Glutamatergic synaptic dysfunction: the role of AMPAR in AD

As described above, it is thought that LTP and LTD expression are due to increased or decreased insertion of AMPAR at the PSD, respectively, and to the precise cellular mechanisms that enhanced or reduced the activity of these receptors, including changes in AMPAR subunits conformation[136,146,147]. It is known that these plasticity processes and accordingly excitatory synaptic transmission are strongly

affected in the hippocampus during AD pathology, and since synaptic alterations are also found in AD experimental models, it seems feasible that alterations in AMPAR abundance and function could be important in AD pathogenesis.

Although a better understanding of AMPAR role in AD is needed, important advances have been made during the last decades. Several evidence suggests that oAβ is capable of altering ionotropic glutamate receptors functionality[133,134] and its accumulation has been linked specifically to AMPAR deregulation and early synaptic deficits in AD experimental models, including primary neuronal cultures and transgenic mice models[127,148]. For instance, oAβ diminish surface AMPAR through a decrease in GluA1 Ser-845 phosphorylation. Interestingly, decrease in GluA1 phosphorylation correlates with learning and memory deficits in a transgenic mice model of AD[127].

Endocytosis of AMPAR mediated by Ca^{2+} influx through ionotropic glutamate receptors and consequent deregulation of kinases and phosphatases activity is the main mechanism described by which oAβ could reduce spine density and lead to synaptic failure[132,134,139] (Figure 4). Dephosphorylation of GluA1 subunit reduces LTP-dependent AMPAR anchoring at the synapse and also affects heteromeric AMPAR composition at the cell surface with the functional consequences discussed previously.

Furthermore, NP association with AD pathology is supported by observations in experimental models and in AD cases. Abad and colleagues provided consistent data supporting the implication of NP1 in AD, since a oAβ -dependent increased in NP1 levels was observed in vitro, while NP1 was likewise significantly increased in brain samples from AD patients [112]. Moreover, NP rise correlates with age-associated oAβ accumulation and amyloid plaques formation in hippocampus, while NP levels are not altered in non-affected areas, suggesting a relationship between NP levels and AD pathology[150].

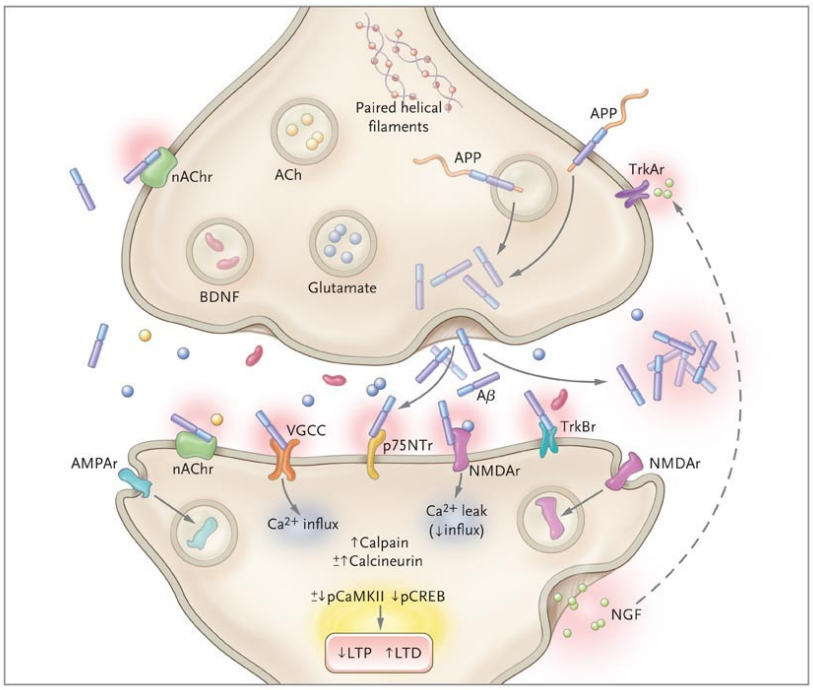

Figure 4: Glutamatergic synaptic dysfunction in AD. The bottom terminal represents a synapse affected by Aβ presence, that leads to glutamate receptor endocytosis, altered balance between LTP and LTD, and finally synaptic plasticity impairment and loss of dendritic spines (from Querfurth and Laferla 2010[24]).

In this context, where a wide range of synaptic proteins are known to be affected, the mechanisms that underlie these changes could be important to understand the onset of the disease. One of these mechanisms could be the posttranscriptional regulation of mRNAs by microRNAs.

2. microRNAs

microRNAs (miRNAs) are the most studied family of the small noncoding RNAs (ncRNAs), a class of functional RNA molecules without protein-coding properties. The first miRNA, *lin-4*, was observed in the nematode *Caenorhabditis elegans* forty years ago[151], however it was not until 1993 when it was discovered that *lin-4* did not code for a protein, as was thought in the first place, but for a small regulatory RNA[152,153]. Since then, over 2600 mature miRNAs have been described only in human[154,155].

With approximately 22 nucleotides (nt) of length, miRNAs post-transcriptionally regulate gene expression by base-pairing interaction, usually to the 3-untranslated region (3-UTR) of target messenger RNAs (mRNAs). Interestingly, it is thought that more than 60 percent of protein-coding genes are controlled by miRNAs[156].

While in plants miRNAs bind to mRNA with almost perfect complementarity, resulting in mRNA degradation[157], animal miRNAs join to mRNA mainly with partial complementarity that, in the vast majority of cases, produce translational repression of the mRNA[156,158,159]. In specific cases it has been described that binding can upregulate translation[160].

miRNAs biogenesis

Since miRNA biogenesis could follow different steps depending on the species, and also different cellular locations or enzymes could be involved in each step, I will focus in mechanisms described in metazoan.

The canonical pathway

The canonical pathway gives rise to the majority of currently identified miRNAs. Briefly, is characterized by two main cleavage steps facilitated by RNase III enzymes: the first one within the nucleus by Drosha, and the second one by cytoplasmic Dicer. The mature miRNA produced at the end of the pathway, exerts its function after being incorporated into the RNA-induced silencing complex (RISC) formed by an Argonaute (Ago) protein and other auxiliary elements such as TRBP and PACT[156,161]. In humans, the Ago protein family comprises four members (Ago1–4), capable of binding to regulatory molecules, mediating all small RNAs (sRNAs) gene-silencing pathways. Ago2 is the only catalytic member, and the PIWI domain confers its endonuclease activity. The other 3 domains that characterized Ago proteins (N, PAZ and MID), perform structural and anchoring functions[156,162].

In animals, miRNA biogenesis is compartmentalized, starting in the nucleus where miRNAs genes are transcribed to a primary miRNA (pri-miRNA) by a RNA polymerase II. Composed by a hairpin structure or terminal loop with imperfectly base-paired and a double-strand RNA (dsRNA) stem flanked by single-strand RNA (ssRNA) segments, the pri-miRNA is subsequently cleaved by the microprocessor

complex, consisting of the RNase III enzyme Drosha and the RNA-binding protein DiGeorge syndrome critical region in gene 8 (DGCR8).

A functional model of this complex has been proposed by Nguyen and collaborators, where Drosha is capable of recognizing the basal elements, while DGCR8 anchors to the apical elements of the pri-miRNA (Figure 5) and guide Drosha to cleave the pri-miRNA 11 base pairs (bp) away from the ssRNA-ddRNA junction, at the base of the hairpin to release the precursor miRNA (pre-miRNA) [156,163–165].

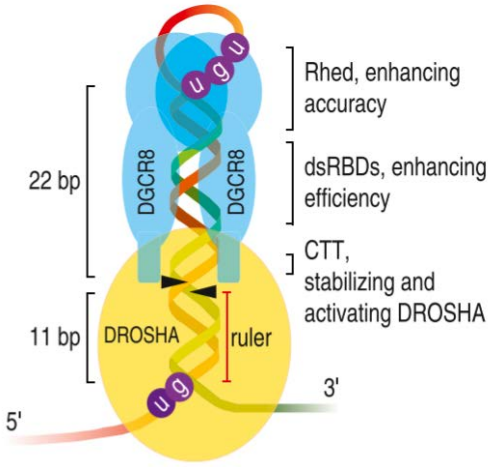

Figure 5: Drosha/DGCR8 complex is a key element in the canonical pathway of miRNA biogenesis. While Drosha recognize basal pri-miRNA elements, DGCR8 anchors to its apical component (from Nguyen et al 2015[163])

It has been shown that DGCR8 function is required for the processing of pri-miRNAs and that its possibly specific for miRNA biogenesis [166]. It is known that this first cleavage carried out by Drosha defines one of the future mature miRNA extremes. Following, the resulting ≈70 nt hairpin structured pre-miRNA bound to an exportin-5 (EXP-5) that recognizes the 2-nt 3-overhang, characteristic of RNase III-mediated processing, and transports the pre-miRNA into the cytoplasm, where is further processed by Dicer, a cytoplasmic RNase III, in complex with the double-stranded RNA-binding protein TRBP. After cleavage, Dicer dissociate from the mature 22-nucleotide miRNA/miRNA* duplex which separates into a guide functional strand and a passenger strand.

Finally, miRNA regulatory function requires the association of the functional strand, complementary to the target mRNA, with an AGO protein in the effector RISC[156,161,163–165]. While the functional strand, by its coupling to the complex, is capable of guiding RISC to mRNAs with partial sequence complementarity mostly in their 3-UTR, inducing mRNA cleavage, translational repression and mRNA

deadenylation, the passenger strand, identified in the nomenclature by an asterisk, is usually degraded[161,162,164,165].

It has been suggested that the thermodynamic stability of the duplex extremes could have a key role in the selection of the strand that will take part in the RISC complex and that a RNA helicase could be involved in the degradation of the passenger strand[164,167].

Non-canonical pathways

As said, most known miRNAs follow the canonical biogenesis pathway, however, next generation sequencing technologies have challenged the linear vision of miRNA processing, revealing numerous subclasses of miRNA-like species which follow alternative biogenesis pathways bypassing some of the miRNAs biogenesis classical steps[156,165].

The main groups are represented in Figure 6.

- Drosha-independent biogenesis : mirtrons

The first non-canonical miRNA maturation pathway described was the Drosha-independent one. Initiate by intron splicing and followed by debranching procesing, it generates pre-miRNA-sized short introns with hairpin structure called *mirtrons* which are exported to the cytoplasm and cleavage by Dicer, following the canonical steps[156,161,165].

In addition, some small nucleolar RNAs (snoRNAs) represent an alternative pre-miRNAs-like source that can be further processed by Dicer, originating mature miRNAs independently from Drosha activity[156,161,165] . Moreover, other forms of mirtrons have been identified and classified depending on the nature of their 3´ and 5´ overhangs: endogenous short interfering RNAs (endo-siRNAs), endogenous short hairpin RNAs (endo-shRNAs) and tRNA[156].

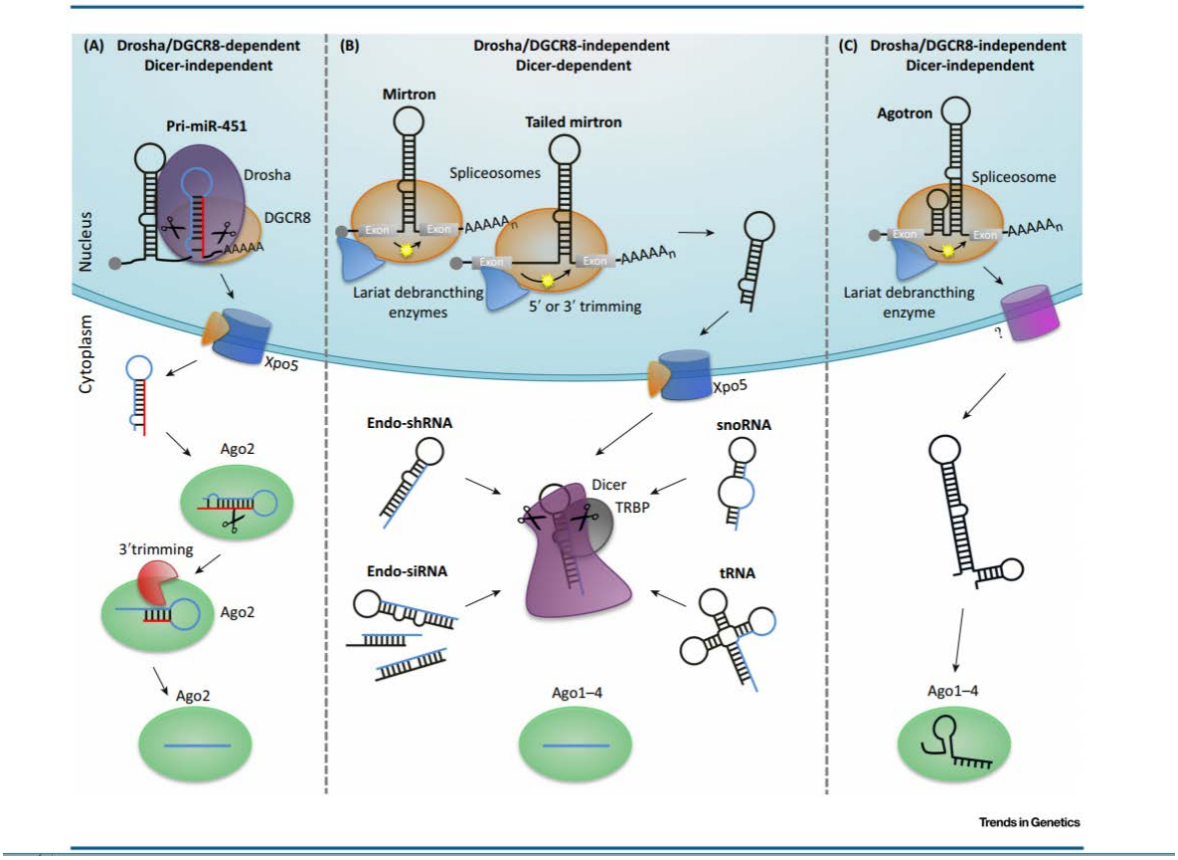

Figure 6: Non canonical pathways in miRNA biogenesis include the generation of mirtrons (B) and agotrons (C). All non-canonical pathways converge in the last step of classical miRNA processing coupling directly Ago proteins in the RISC complex. (From Daugaard 2017[156])

- Dicer-independent biogenesis: the miR-451 case

It is known that the pre-miR-451 hairpin structure derived from pri-miR-451 Drosha-dependent processing contains a 17 bp stem, incompatible with the 22 bp needed to further Dicer processing. This unusual pre-miR thus, completes its maturation process by binding directly to Ago2, which catalyzes hairpin cleavage resulting in mature miR-451 without Dicer-processing need[152,161].

- Drosha-independent/ Dicer-independent biogenesis: agotrons.

The last class of RNA-species that follows non-canonical biogenesis pathway to be described were the *agotrons.* This group of Ago-associated proteins surprisingly bypass both Drosha and Dicer machinery[168,169]. In a similar way as mirtrons, agotrons are originated from short introns, spliced, debranched and exported to the

cytoplasm by a still unknown mechanism. Once in the cytoplasm, agotrons avoid Dicer processing coupling directly to Ago as unprocessed, full-length introns[156]. Regardless of their longer and more complex mature structure, agotrons have been demonstrated to be functional target repressors that behave in a miRNA-like manner. Moreover, it has been suggested that agotrons could work as stabilizing molecules when binding to Ago, since it is know that Ago proteins are unstable while they have no bounded substrates[170]. In addition, they could prevent Ago proteins from binding random RNA degradation products[156,168,169].

All non-canonical pathways converge in the last step of classical miRNA processing, the coupling of the guide strand into RISC to produce, mostly, mRNA translation repression.

Since miRNAs bind to mRNA with partial sequence complementarity, a single miRNA could have hundreds of different targets. In this regard, it is known that over the 60 percent of human protein-coding genes have at least one conserved miRNA-binding site[156]. Even though miRNAs usually bind to the 3-UTR of target mRNAs, occasionally are also able to bind to its coding sequence. This is the case of let-7, which targets Dicer mRNA, creating a negative regulatory feedback loop, but also demonstrating that the regulatory role of miRNAs goes beyond the 3-UTR binding [171]. Additionally, it is known that miRNAs could be modified by transcript editing, a post-transcriptional mechanism through which RNA sequences are modified by deamination of adenosine (A) to inosine (I). These changes in RNA sequences alter the base-pairing and structural properties of the transcript mostly enhancing pri-miRNA Drosha processing, however cases of inhibited Drosha cleavage and following degradation have also been reported[172]. Moreover, edited miRNAs repress different targets than those repressed by unedited miRNAs, thus affecting miRNA target specificity, altering complementarity to target sequences, therefore increasing the diversity of potential tagets[161,173]. Considering the aforementioned, a wide range of possibilities arises for mRNA-miRNAs regulation.

Of note, besides from the typical negative mRNA regulation, it has been described that in particular cases the RISC complex can activate translation of the target mRNA[160] and interestingly, under specific conditions, such as synaptic activity, the repression over the mRNA can be released[174]. This data propose that at least some

miRNAs may be neuronal activity-dependent, suggesting a role of miRNAs in synaptic plasticity modulation.

miRNAs in synaptic plasticity

During the last years the important regulatory labor of miRNAs in diverse biological processes has been largely supported. Almost a 70 percent of identified miRNAs could be found in mammals brain[175,176], and many of them (including miR-9, miR-124, miR 128a/b) have been described to be brain-specific[177,178], consequently, it is expected that miRNAs could play an essential role in brain development, physiology and pathology. Several studies have found highly expressed miRNAs within neuronal dendrites (such as miR-9, *miR-26a,* miR-125b, miR-128, miR-132, miR-134, miR-138, miR-139, miR-218[179–183]) in diverse brain areas, including hippocampus[184–186]. miR-9 has also been detected in axons, together with *miR-15b, miR-16,* miR-135a/b *miR-204 and miR-221 and these miRNAs have been related to* axon growth and branching[181,187,188]*.* The enrichment of particular miRNAs in axons and dendrites suggests their potential role regulating local protein levels, thus synaptic structure and function.

Supporting this idea, cKO models of Dicer and DGCR8, key elements of miRNAs maturation, have demonstrated that loss or reduction of both affects normal synaptic functionality. Compared to controls, KO mice exhibited diminished neuronal size, negatively affected branching and axonal guidance and decreased synaptic connectivity linked to a reduction in the number and size of dendritic spines [189–191].

It is noteworthy that several genes, generally located in different chromosomes, encode many brain-enriched miRNAs. This redundancy suggests the existence of a mechanism capable of guaranteeing the expression of essential miRNAs in case of deleterious mutations of any of the genes that encode them[179].

Interestingly, not only mature miRNAs, but also pre-miRNA have been found within dendrites[184,192–194]. Actually, it has been described that in dendritic spines pre-miRNA levels are higher than mature miRNA levels[184]. In accordance, it has been described the presence of inactive Dicer and its activation after NMDAR stimulation through a calcium-dependent mechanism in mice PSD and dendritic spines[194].

These observations suggest the existence of a rapid local posttranscriptional mechanism that could generate mature miRNAs in an activity-dependent manner, strongly indicating a possible involvement in synaptic plasticity processes.

miR-134: the prototype of activity-dependent miRNA

Despite the progresses achieved in the comprehension of miRNAs neuronal function; its regulation and role during synaptic plasticity is still largely unknown. However, important steps have already been taken, identifying some miRNAs (such as miR-129-5p[195], miR-132, miR-134[174], and miR-485[196]) regulated in an activity-dependent manner which have been linked to synaptic development and plasticity processes. miR-134, a member of the miR379-410 cluster, known to be positively regulated under neuronal activity[197], was the first of this group to be described, and currently is the best characterized. Schratt and collaborators[174] revealed in 2006, miR-134 negatively regulates dendritic spine size in cultured rat hippocampal neurons by targeting the actin cytoskeleton regulator LIM domain kinase 1 (LIMK1). Even more interesting is that the interaction between miR-134-LIMK1 is reversible and it is regulated by synaptic activity. So that in the absence of synaptic activity miR-134 represses LIMK1 translation, however upon synaptic stimulation, and as a consequence of brain-derived neurotrophic factor (BDNF) release, the inhibition on LIMK1 translation is relieved, contributing to dendritic spines development.

In addition, subsequent studies in a mutant mice model lacking the catalytic domain of deacetylase SIRT1 (related to normal brain physiology and neurological disorders) supported miR-134 involvement in synaptic plasticity regulation. Overexpression of miR-134 in the hippocampal CA1 region of these mice, abolished LTP and impaired long-term memory formation during contextual-fear conditioning[198]. Hence, the studies developed by Schratt and colleagues are so far the strongest support of the important role that miRNAs may have in synaptic plasticity.

The identification of this and other miRNAs in the dendrites, raises an increasing picture of the role of miRNAs as synaptic plasticity regulators, and therefore, possible elements in the development of diseases such as AD, where synaptic dysfunction is well described.

miRNAs in AD

As the understanding of the mechanisms of miRNAs in physiological synaptic plasticity progresses, it is impossible to ignore the important role that these regulators may play in pathological processes.

Gene expression profiling studies highlighted deregulation in miRNA expression in an extensive variety of human pathologies[199], including cardiovascular disease[200], neurodegenerative disorders such as Parkinson[201] and especially prolific work has been done in cancer research[202–204]. Numerous studies have already provided evidence of a large number of specific miRNAs misregulated in AD[205], some of which are implicated in the regulation of key genes involved in the pathology, such as APP, BACE1 or PSEN1[205–207].

Several miRNAs have been described to regulate tau phosphorylation (miR-125b[208], miR-132[209], miR-138[210]) and many others are known to be related with BACE1 (miR-29a/b/c[211,212], miR-9[182,211,213], miR-188-3p[214], miR-135b[215],) or APP (miR-101[216], miR-16[217,218], miR-147[219], miR-107[220]) expression.

As mentioned, synaptic dysfunction is an early key event in the mechanisms underlying AD pathology. Although not clearly understood yet, a relationship between synaptic dysfunction in AD and miRNA levels alteration is increasingly supported by studies in the area ([196,224–231]). Besides the effects that miRNAs could have on the regulation of the key genes involved in AD development above mentioned, specific miRNAs could negatively regulate synaptic function through a deregulation of synaptic proteins, such as glutamate receptors and associated proteins, contributing to synaptic deficits.

One of many cases described in bibliography is the case of miR-124, a brain-specific miRNA that besides its suggested role in BACE1 regulation[232], is well established that is able to repress translation of PTPN1[233], a tyrosine-protein phosphatase non-receptor type 1 related to synaptic function. Wang and collaborators[233] described that miR-124 is increased in hippocampus and temporal cortex of AD patients, likewise is increased in the hippocampus of AD transgenic mice (Tg2576) which exhibited synaptic transmission and memory deficits.

Consistently, they found that both, hippocampal neurons treated with oAβ1-42 and mice N2a/APP cells producing high levels of oAβ, revealed a significant increase of miR-124 levels. Interestingly, PTPN1 downregulation through miR-124 overexpression was shown to mimic AD-phenotype while miR-124 inhibition rescued synaptic dysfunction and memory impairment. In this study they also described that PTPN1 knockdown leads to hyperphosphorylation of GluA2, affecting AMPAR trafficking to the cell surface, therefore impairing synaptic transmission. These results strongly indicate a direct function of miR-124 in AD pathology, suggesting that many other candidates may also regulate synaptic levels of proteins related to AD onset.

Beyond the interest that miRNAs have as regulatory molecules, it is remarkable that these small RNAs could be detected in circulating biofluids, opening a new scenario in their use as biomarkers, miRNAs have some features that make them suitable to be considered as biomarkers for disease.

miRNAs as biomarkers

Despite the great efforts made in the search for therapies against AD, there is still no treatment capable of prevent or reverse the pathology process, however, the huge incidence increase during the last decades and estimations make essential to accelerate the search for effective treatments but also for diagnostic tools to facilitate early detection of the disease.

In regard to potential therapies research, so far, several clinical trials have failed possibly due to the limited knowledge about the underlying mechanisms involved in AD progression, but also due to the lack of accessible and reliable diagnostic tools during early preclinical stages that determined that most studies are done in late-stage AD patients. Considering that the pathological process in AD brain starts long before the symptoms appearance, at least 10-20 years earlier, targeting the disease in its synaptic phase, before neuronal death occurs, could be an essential step to achieve better therapeutic results.

Currently, only a few biomarkers can be used to differentiate preclinical AD from AD: cerebrospinal fluid (CSF) signature of low $A\beta_{1-42}$ and high total tau or

hyperphosphorylated tau concentrations and accumulation of Aβ in the brain detected by positron emission tomography [234–237]. Although the identification of these AD biomarkers is possible in cognitively normal individuals, they have a clear limitation in routine clinical screenings due to their invasiveness and economic limitations.

In this scenario, detection of specific miRNAs in circulating biological fluids, including CSF and blood, has a great potential to be used as biomarkers of AD. They can be obtain using non-invasive procedures (especially for serum and plasma) are measured by simple and affordable techniques such as qPCR, making promising their routine use in clinics (Figure 7).

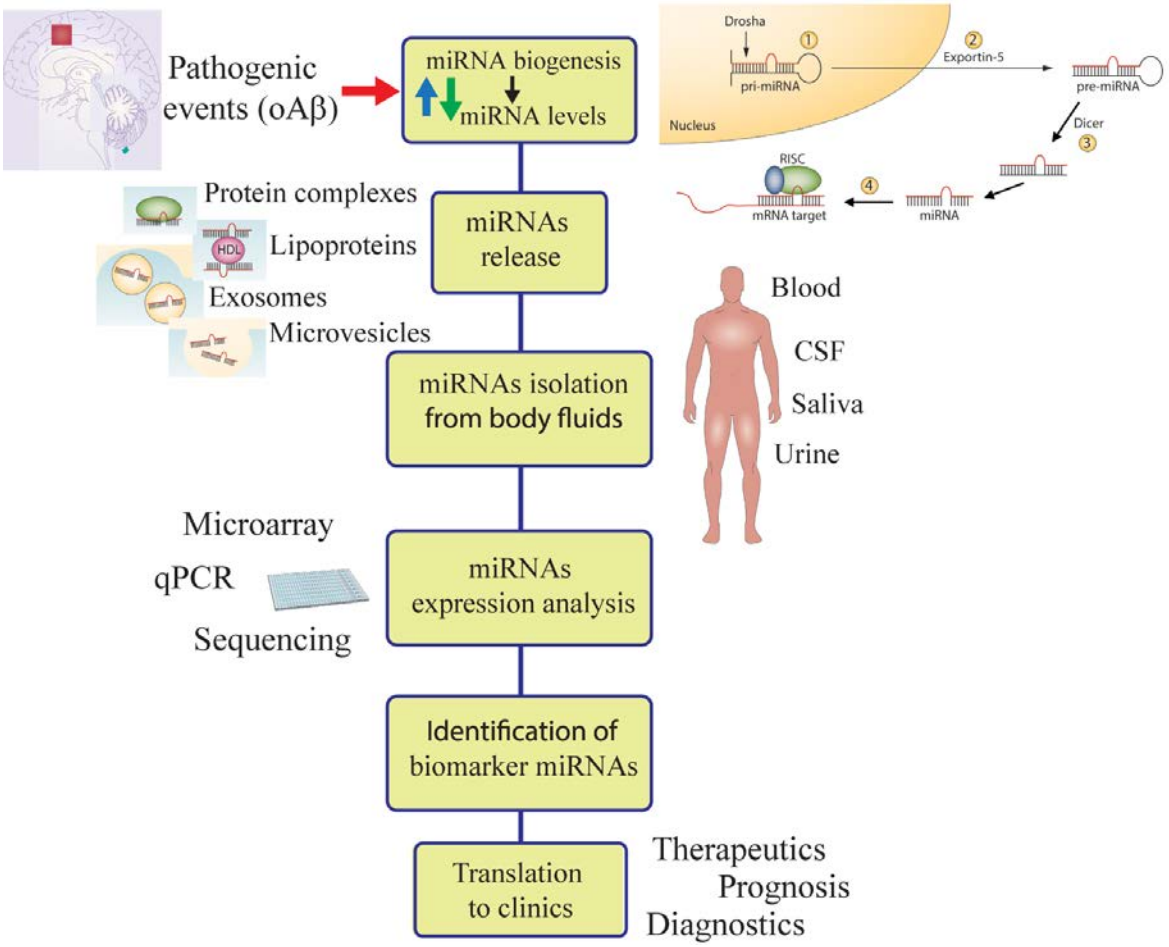

Figure 7: miRNAs detection and possible translation to clinics. miRNAs are release to biological fluids (such as CSF and blood) from where they can be easily obtain through non-invasive procedures. They can be measured by simple and affordable techniques including RTqPCR and next generation sequencing, making it possible its use in clinic routine screenings.

miRNAs are stable in clinical samples since they could be released from cells in membrane-bound vesicles, including exosomes and microvesicles [238], either can be in a non-membrane-bound form, associated to Ago2 complexes [239,240]. Both forms were suggested to confer stability to circulating miRNAs, protecting them from blood RNase activity thus, from degradation [241,242].

Of special relevance is miRNA use as biomarkers of mild cognitive impairment (MCI) and early stages of AD. MCI is a condition common to other dementias where synaptic deficits start to be evident in form of slight affection of thinking abilities. A big percentage of MCI cases are expected to progress to dementia in 5 years, however it has been also reported that some MCI patients could remain stable and others can even recover normal cognitive function[243]. In this prodromal phase is where a biomarker could be more useful differentiating cognitively normal people from MCI or early AD patients.

Lately, extensive interest has focused on identifying alterations in specific circulating miRNAs levels that could be used as AD biomarkers [224,242,244–247], however few data exists about changes in plasma levels of miRNAs related to synaptic protein function in AD [242,248].

Much remains to be known about the proteins and the mechanisms that mediate synaptic and cognitive impairment at early stages of AD. Nonetheless, the study of the main players and modulatory elements that determine the alteration in glutamatergic transmission seems a good start to get a little closer to the understanding of this complex disease. Focusing our efforts on understanding the initial steps that trigger the cascade of events that finally leads to massive neurodegeneration might be critical to increase the probability of developing effective therapies to slow down, stop or reverse AD.

AIMS

This doctoral thesis aims at the identification of synaptic-related miRNAs altered in early stages of AD pathology as a tool for understanding synaptic function deregulation in early AD stages. Understanding the molecular mechanisms in which miRNAs could be involved, may allow the Identification of potential therapeutic targets related to synaptic phase of the disease. Especially exciting is the final purpose of suggesting a circulating plasma miRNA related to synaptic proteins that may be considered as potential biomarker for AD pathology.

To this aim we determine smaller objectives:

- Evaluate synaptic-related miRNAs expression in human tissue of different brain areas during AD progression (Microarray analysis and RTqPCR validation).
- Determine if selected miRNAs are deregulated in experimental models of the disease (APP transgenic mice and in vitro models).
- Assess candidate miRNAs levels in plasma samples and define the diagnostic value of evaluated miRNAs in MCI and AD stages.

-

METHODS

1. Human samples

Human plasma samples

Plasma samples analyzed in this study are from two different cohorts. First one provided by Fundació ACE (Barcelona, Spain) includes 14 HC, 26 MCI and 56 AD patients. The second one was recruited at the Memory Unit of the Hospital Sant Pau (Barcelona, Spain) and consists of 24 HC and 27 FTD patients. Participants were clinically diagnosed by neurologists and classified according to internationally accepted diagnostic criteria. Demographic and clinical characteristics of cohorts 1 and 2 are summarized in Table 1. FTD participants include 19 patients with possible or probable behavioral variant[249] and 6 with semantic variant of primary progressive aphasia[250]. Two patients with FTD were additionally diagnosed with concomitant ALS according to El Escorial criteria[251].

Cohort 1				Cohort 2	
	HC	**MCI**	**AD**	**HC**	**FTD**
Cohort size	14	26	56	24	27
Males/Females	7/7	10/16	15/41	11/13	17/10
Age (years)	68,29±8,991	72,0 ±8,495	77,77±6,688	67.03±5.05	68.87±7.48
GDS	2,07±0,26	3,15±0,37	4,64±1,02	1±0	3.76±0.99
MMSE	29,21±1,051	26,92±2,226	16,05±7,230	28.5±1.69	25.5±3.76

Table 1: Human plasma samples information from cohorts 1 and 2. HC: Cognitively healthy control. MCI: Mild cognitive impairment. AD: Alzheimer's Disease. FTD: Frontotemporal dementia. MMSE: Mini Mental State Examination. GDS: Global Deterioratio Scale. All data are shown as mean ± SD.

Human tissue samples

Human brain samples were provided by 3 different Spanish centers: Fundación Cien (Instituto de Salud Carlos III, Spain). Hospital Clinic-IDIBAPS, and Bellvitge University Hospital (Universitat de Barcelona, Spain). Neuropathology was classified according to Braak staging for neurofibrillary tangles as described[71]. Tissue samples from controls and individuals that displayed neurofibrillary tangle pathology corresponding to early (Braak I-II), mild cognitive impairment (Braak III-IV) and final AD (Braak V-VI) stages were analyzed. Demographic and clinical characteristics of

the subjects are listed in Table 2. Entorhinal cortex (n=21), hippocampus (n=61), prefrontal cortex (37) and cerebellum (n=37) were analyzed for miRNA levels. For protein analysis, the same samples described in Table 2 were used, except for hippocampus: from the 61 samples listed, only the 37 samples matching prefrontal cortex and cerebellum samples were analyzed.

Braak stage	Control	Presymptomatic ADâ‰¤II	MCI ADIII-IV	AD ADV-VI
		Entorhinal cortex		
Cohort size	7	4	5	5
M/F	4/3	1/3	3/2	0/5
Age (years)	68.1±6.9	81.7±5.5	88.2±6.7	83.5±3.1
PMD (h)	8.7±5.5	5.6±1.1	5±2.6	4.7±2.3
RIN	5.7±0.9	6.0±0.8	6.2±0.7	6.5±0.8
		Hippocampus		
Cohort size	12	19	12	18
M/F	7/5	10/9	8/4	6/12
Age (years)	60.7±11.9	72±13.2	85±5.9	81.2±5.9
PMD (h)	7.5±4.5	6.0±2.8	6.1±2.3	6.8±4.8
RIN	5.8±0.7	6.4±0.9	6.2±0.7	6.3±1
		Prefrontal Cortex		
Cohort size	7	8	11	11
M/F	4/3	3/5	8/3	1/10
Age (years)	68.14±6.98	78.63±12.69	85.36±6.05	82.36±5.16
PMD (h)	8.7±5.5	6.6±1.8	6.3±2.4	5.2±1.4
RIN	5.6±1.2	7.1±0.9	6.3±1.1	6.9±1.1
		Cerebellum		
Cohort size	7	8	11	11
M/F	4/3	3/5	8/3	1/10
Age (years)	68.14±6.98	78.63±12.69	85.36±6.05	82.36±5.16
PMD (h)	8.7±5.5	6.6±1.8	6.3±2.4	5.2±1.4
RIN	5.6±1.2	7.1±0.9	6.3±1.1	6.9±1.1

Table 2: Human tissue samples information. M: Male.F: Female. PMD: Postmortem delay. RIN: RNA integrity number. Entorhinal cortex, hippocampus, prefrontal cortex and cerebellum samples analyzed for miRNA and protein levels are listed. All data are shown as mean ± SD.

2. Experimental models

$APP_{Sw,Ind}$ transgenic mice

$APP_{Sw,Ind}$ transgenic mice (line J9; C57BL/6 background) expressing the mutant human APP695 isoform harboring the FAD-linked Swedish (K670N/M671L)/Indiana (V717F) mutations under the expression of the neuronal PDGFβ promoter were previously described[252,253]. Mice were age-matched littermate males obtained by crossing heterozygous $APP_{Sw,Ind}$ to non-transgenic (WT) mice (C57BL/6 background). Experimental design is summarized in Table 3.

	WT			$APP_{Sw,Ind}$		
	Naive	2d	5d	Naive	2d	5d
6M	4	4	4	6	6	6
9M	4	4	4	6	6	6

Table 3: Experimental groups consisted of WT and $APP_{Sw,Ind\ mice}$ at 6 an 9 month of age, trained at the MWM and euthanized 2 or 5 days after training.

$APP_{Sw,Ind}$ phenotype includes increased APP expression in an age-dependent manner, synaptic function impairment and hippocampal-dependent spatial memory deficits (6 month mice) before accumulation of intracellular amyloid plaques (9 month mice)[252–254].

All mice were housed in the same room and kept on a 12 h light/dark schedule and given *ad libitu*m access to food and water.

Behavioral test: Morris water maze

The Morris water maze was performed as were performed by Judit España as previously described[253]. Experimental procedures were performed in accordance with institutional and national guidelines following approval by the Animal Care and Ethical Committee (CEEAH) of the Universitat Autònoma de Barcelona following the European Union guidelines.

Primary hippocampal neuronal cultures

Hippocampal neurons were obtained from C57BL-6J/RccHsd (Harlan, now Envigo) P0-P1 newborn mice pups. Brains were extracted and place in dish containing cold **dissection solution**. Hemispheres were separated and meninges were carefully removed. Hippocampi were dissected and transferred to the pre-warmed **enzymatic solution** (containing papain), and further incubated at 37°C in a tube rotator for 30 minutes to allow tissue digestion. After this time, enzymatic solution was removed without disturbing tissue, and **inactivation solution** was added to the hippocampi and let stand for 2 minutes. Next, inactivation solution was aspirated and mechanical dissociation was completed using pre-warmed **serum media** and a glass Pasteur pipette. Cell suspension was finally filtered through a nylon mesh (40 µm pore size) to eliminate cell clumps and then centrifuged for 5 minutes at 1000 rpm. The supernatant was discarded while the cell pellet was resuspended in **serum media**. Live cells were counted in a hemocytometer and seeded at specified density (125,000 cells/ml for luciferase assay, 250,000 cells/ml for molecular and biochemical assays) in **Poly-D-lysine pretreated plates (**24 well plates and 35 mm diameter plates, respectively) containing **supplemented Neurobasal-A medium**. Neurons were maintained in a humidified incubator at 37ºC with 5% CO2, and the culture medium was changed 24 hours after seeding by replacing half of the conditioned medium with fresh medium. 72 hours after seeding, glial growth is inhibited using FUDR. Half medium was replaced with fresh medium every week until use.

Solutions, media and reagents

- **Dissection Solution**: 18.8g NaCl, 0.74g KCl, 0.26g $MgSO_4$, 0.86g $CaCl_2$, 2.4g Hepes, 2.0g Glucose, 0.004g Phenol Red.
- **Enzymatic Solution** was prepared from 10mL of dissection solution containing papain (100 units), 2mg L-Cysteine, 100µL EDTA (50mM, pH 8.0), 100µL $CaCl_2$ (100mM), 30µL NaOH (1N), 100µL DNAse I (300 - 450 Kunitz / mL of DNAse I in 10 mL of solution).
- **Inactivation Solution** was prepared supplementing 10mL of serum media with 25mg bovine albumin and 100µL DNAse I.

- **Serum Media**: 500mL Minimum Essential Medium w/ Earle's salts w/o L-glutamine supplemented with 25mL Fetal Bovine Serum (Thermofisher), 1,9 gr glucose and 1mL Mito+ Serum Extender*** (BD Bioscience – Fisher)
- Plates were pretreated with sterile 0.01mg/mL **Poly-D-Lysine** in 0.1M Sodium Borate buffer (pH 8.4) (Both from Sigma) for at least 2 hours, next plates were washed 3 times with Phosphate-Buffered Saline (PBS 1X) before cells seeding.
- **Phosphate-buffered saline** (PBS): 136.87 mM NaCl, 2.5 mM KCl, 0.8 mM NaH_4PO_4, 1.47 mM K_2HPO_4, pH 7.4.
- **Neurobasal-A Media:** (GIBCO) supplemented with B-27 Supplement (10mL) (GIBCO) and Glutamax-I Supplement (5mL) (GIBCO).
- **FUDR**: 100mg 5-Fluoro-2'-Deoxyuridine (1 bottle) (Sigma), 250mg Uridine in 50mL Minimum Essential Medium w/ Earle's salts w/o L-glutamine.

Cell lines

Human embryonic kidney HEK293T cells were cultured in Dulbecco's Modified Eagle Medium (DMEM) (Sigma) containing 10% FBS (Thermofisher), 25 U/mL penicillin, and 25 µg/mL streptomycin. Cells were maintained in a humidified incubator at 37ºC with 5% CO_2. Culture medium was changed every 2-3 days and cell passages were performed once a week after tripsinization.

3. Cell treatments

OAβ oligomerization

$A\beta_{1\text{-}42}$ oligomers were prepared as previously described[255–257]. Briefly, lyophilized peptide from Bachem (Bachem,United Kingdom) was dissolved in hexafluor-2-propanol (HFIP), homogenized and then evaporated in a speed-vac at 800g <25ºC 15-20 min. The precipitate could be stored at -80ºC until used or be diluted to a 5mM concentration in 100% DMSO. Finally, DMEM-F12 phenol red-free media was

added to obtain a 100µM concentration and incubated 24h at 4ºC to allow oligomerization. Before use, oligomers were centrifuged for 10 min at 14000 x g and supernatant was used for cell treatments.

Oligomerization protocol was previously standardized in Dr. José Rodríguez lab. After preparation oligomers were resolved in 12%. Bis-Tris Bicine gel without urea to checked its composition (Figure 8).

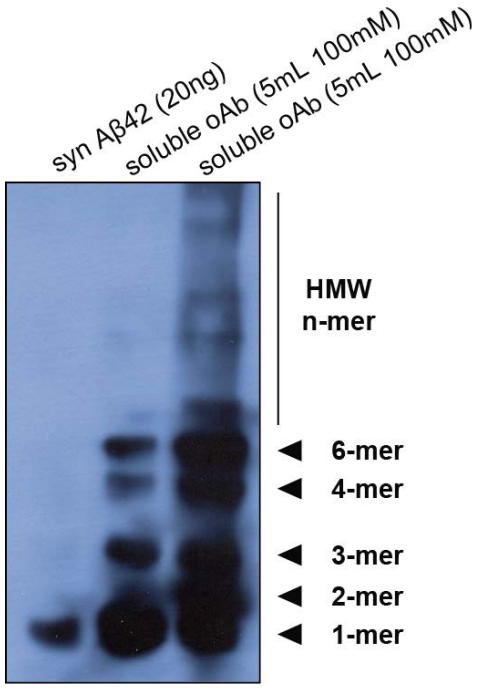

Figure 8: Presence of monomers, dimers and oligomers was confirmed by resolving oligomer preparation in 12%. Bis-Tris Bicine gel without urea. (Image courtesy of Dr. Alfredo J. Miñano).

17-19 DIV hippocampal neurons were treated adding oligomers 100 µM solution directly to the culture media to obtain a 5µM final concentration and left until lysis.

Chemical stimulation of hippocampal neurons

Before stimulation, cells were incubated in ACSF buffer (125 mM NaCl; 2.5 mM KCl; 1 mM $MgCl_{2;}$ 2 mM$CaCl_{2;}$ 33 mM D-Glucose and 25 mM HEPES; pH 7.3) for 30 min at 37°C .

For chemical LTD induction (cLTD), neurons were stimulated for 5 min with 50 µM NMDA in the ACSF with no $MgCl_2$. After 5 min, buffer was removed and replaced by complete supplemented ACSF and cell were lysated after 2 hours.

In the same way, chemical LTP (cLTP) was induced with Forskolin (50 µM) / Rolipram (0.1 µM) treatment for 10 min and cells were lysate after 2.

50 µM bicuculline was also used to induce neuronal activity in miRNA expression experiments. In this case, bicuculline was directly added to the culture media and left until miRNA extraction point times.

4. Biochemical methods

Tissue and cell lysis and protein quantification

Hippocampal cultures were lysed in ice with cold NP-40 lysis buffer (for miRVana Paris protocol see Methods 4.1 miRNA extraction) (150µl per 35 mm diameter dishes). Cells were collected in a fresh Eppendorf tube with a plastic scrapper and sonicated for 3 seconds before protein concentration determination according to Bradford method[258]. Samples were stored at -20°C until use.

Human brain tissue was lysed in ice with cold RIPA buffer (100 µl for each 100 mg of tissue) and homogenate using a pestle mixer and solubilized in ice for 1 hour. Next, lysates were sonicated 3 times for 5 sec each and placed on ice in between sonication to prevent samples from heating. After 15 minutes centrifugation (10,000 rpm, 4°C) supernatant was recovered and concentration was determined by BCA assay. Samples were stored at -80°C until use.

Solutions:

NP-40 lysis buffer: 20 mM Tris-Base, pH 7.4, 150 mM NaCl, 5 mM EDTA, 1% NP-40, 1 mM Na_3VO_4, 1 mM PMSF, 1/100 protease inhibitors and 1/100 phosphatases inhibitors cocktail.

RIPA lysis buffer: 50 mM Tris base pH 7.4, 150 mM NaCl, 2 mM EDTA, 1% NP40, 0.5% Triton X-100, 0.1% SDS, 1 mM Na_3VO_4, 25 mM NaF, 1 mM PMSF, 1/100 protease inhibitors and 1/100 phosphatases inhibitors cocktail.

SDS-PAGE and Western Blotting

Proteins were diluted with sample loading buffer and heated at 95°C for 5 min before being loaded an equal amount of protein in 10-12% polyacrylamide gels. Protein separation was performed by electrophoresis under denaturing conditions (Poly Acrilamide Gel Electrophoresis-Sodium Dodecyl Sulfate; PAGE-SDS). Precision Plus Protein™ Standard All Blue (Bio-Rad) was used to determine proteins molecular weight. Proteins were then transferred (60 min at 80 V) to nitrocellulose membrane (GE Healthcare) and stained with 0.1% Ponceau S solution (Sigma) to verify correct transference. Membranes were further incubated with blocking solution for 1 hour and washed with phosphate buffer saline-Tween (PBT-T) or Tris-buffered saline-Tween (TBS-T) (2 x 5 min + 2 x 10 min) and following incubated with primary antibody (Table 4) diluted in antibody buffer overnight at 4°C. Membranes were washed with PBT-T or TBS-T (2x5 + 2x10 min) and incubated at room temperature for 1h with secondary peroxidase-coupled antibodies (mouse or rabbit as needed) prepared in blocking solution. After repeating washes, proteins were detected by chemoluminescence reaction using ECL Western Blotting reagent (GE Healthcare).

Buffers and reagents:

- Sample loading buffer (4X Laemmli-SDS): 250 mM Tris HCl pH 6.8, 2.5% glycerol, 5% SDS, 1.4M β-mercaptoethanol (βME) and 0.01% bromophenol blue.
- Electrophoresis running buffer: 25 mM Tris buffer, 192 mM Glycine, 1% SDS.Transfer buffer: 25 mM Tris base and 192 mM glycine, 20% methanol.
- TBS-T: 20 mM Tris base, 150 mM NaCl, 0.1% Tween-20, pH 7.6
- PBS-T: 136.87 mM NaCl, 2.5 mM KCl, 0.8 mM NaH_4PO_4, 1.47 mM K_2HPO_4, , 0,1% Tween-20, pH 7.4.

- Blocking solution: 0.1% bovine serum albumin (BSA),10% nonfat dried milk in TBS-T or PBS-T, pH 7.5.
- Primary antibody buffer: 0.1% BSA, 0.02% thimerosal in TBS-T or PBS-T, pH7.4.

Antibody	Host	Source	Ref	Dilution
NP1	Mouse	BD	610370	1:1000
NPR	Mouse	Santa Cruz	sc-390081	1:500
Bcl-2	Mouse	Santa Cruz	610538	1:500
BDNF	Rabbit	Santa Cruz	546	1:500
GAPDH	Mouse	Ambion	AM4300	1:20000
Actin-β	Mouse	Sigma	A-1978	1:5000
AKAP79	Rabbit	Millipore	ABS-102	1:1000
GluA1	Rabbit	Millipore	AB1504	1:1000

Table 4: Antibodies used for protein detection in human brain an in hippocampal cultures.

5. Molecular biology methods

Samples processing and miRNA extraction

Blood samples were collected by venipuncture, by a trained phlebotomist, in EDTA-containing tubes, as recommended[259]. After a 20 minutes centrifugation (2500xg), plasma was separated, aliquoted and stored at -80 ◦C until use. Plasma samples were thawed in ice for RNA extraction and hemolysis of each sample was analyzed at the time measuring absorbance at 414/375 nm (414/375 ratio >1.4 were considered hemolysed)[204] and excluded from further analysis. RNA from plasma samples was isolated using the miRNeasy RNA isolation kit (Qiagen) improved for purification of cell-free miRNA from small volumes of serum and plasma. Following the manufacturer's indications, 200 μl of plasma were mixed with 1ml of QIAzol Lysis Reagent and kept at room temperature for 5 min. 200 μl of chloroform were added to each tube and then vigorously shaken for 15" and kept at room temperature for 3 min. Samples were centrifuged 15 min at 12.000 x g at 4°C. The upper aqueous phase was transferred to a new tube and 1.5 volumes of absolute ethanol were added to each tube and mixed thoroughly. Samples were loaded into

an RNeasy MinElute spin column and centrifuged at 8.000 x g for 15” at room temperature. Flow-through was discarded and columns were washed with supplied RWT and RPE buffers as indicated, and finally with 500 μl of 80% ethanol. Before elution, columns were dried with 5 min full speed centrifugation. 12 μl of RNAse-free water were used for elution.

miRNA from postmortem human brains and mice brain tissue was isolated from 20 to 100 mg of tissue using *miR*Vana miRNA Isolation Kit (Thermo Fisher Scientific). Frozen tissue was kept in dry ice to prevent thawing, then transferred to a 1.5 ml RNAse-free tube (Eppendorf) and quickly homogenized in ice. Manufacturer’s indications were followed, adapting the reagents volume according to the initial weight of the tissue in each case. Briefly, for 50 mg of tissue, 500 μl of ice-cold denaturing lysis buffer were added and a mechanic homogenizer was used to disrupt the samples. Once homogenized, 50 μl of homogenate additive were added to each tube and kept on ice for 10 min. 300 μl of Acid-Phenol:Chloroform were added to the tubes and samples were gently mixed for 30” before being centrifuged at 10.000 x g for 5 min at room temperature. The upper aqueous phase was transferred to a new tube. 1.25 volumes of absolute ethanol were added to each tube and passed through a clean Filter Cartridge containing a glass-fiber filter which immobilizes the RNA. Samples were centrifuged at 10.000 x g for 15” at room temperature and eluate was discarded. The filter column was washed 3 times as indicated and the columns were centrifuged empty for 1 min to dry before elution. Finally the RNA was eluted with preheated water (95°C).

miRNA from cultured neurons was isolated using *miR*Vana miRNA Isolation Kit (Thermo Fisher Scientific) following the same protocol as for tissue samples, or with the *mir*Vana™ PARIS™ Kit that allows the isolation of both protein and RNA from the same experimental sample. In both cases, the protocol begins with the washing of the plates with PBS, before addition of ice-cold lysis or cell disruption buffer was added to the culture plates. Then the lysates were collected with a scrapper and transferred to a RNAse-free tube. For *miR*Vana miRNA Isolation Kit, the protocol follows as for tissue samples. For *mir*Vana™ PARIS™ Kit the lysates were vigorously mixed and 1/3 of the volume was separated and kept on ice for 10 min before storage at -20°C until protein analysis. The remaining volume (300 μl) was

processed for miRNA extraction immediately following manufacturer instructions. Briefly, lysates were mixed thoroughly with an equal volume of 2X Denaturing solution containing high concentration of guanidinium thiocyanate that prevents RNA degradation by cellular ribonucleases. After 5 min incubation on ice, 600 μl of Acid-Phenol:Chloroform were added to each tube, gently vortexed for 30" and centrifuged at 10.000 x g for 5 min at room temperature. From here the protocol is identical to the *miR*Vana miRNA Isolation Kit.

RNA quality was evaluated using the agilent 2100 byoanalyzer. For human brains, samples with RNA integrity number (RIN) under 4 were excluded [260], for mice tissue and cultures, samples with RIN under 8 were excluded.

Reverse transcription

For tissue and cultures samples, 10 ng of RNA were reverse-transcribed to cDNA using TaqMan™ MicroRNA Reverse Transcription Kit (Thermo Fisher Scientific) following manufacturer indications. Briefly, reverse transcription (RT) mix containing dNTPs, 10X RT buffer, RNAse inhibitor (20 U/μl) and MultiScribe™ Reverse Transcriptase (50 U/μL) was mixed on a with 10 ng of RNA and 3 μL 5X RT primer (Taqman probes used in this study are listed in table 5). PCR was performed in a thermal cycler using the following program: 30 min at 16°C, 30 min at 42°C and 5 min at 85°C. Subsequently PCR amplification was performed or samples were stored at -20°C until use.

For plasma samples, 2 μl of miRNA were reverse-transcribed to cDNA using TaqMan™ Advanced miRNA cDNA Synthesis Kit (Thermo Fisher Scientific). This protocol, in opposite as the previous one that requires a specific probe for each miRNA RT, is adapted for detecting desired miRNAs from the same orginal cDNA. This is especially important in samples with low miRNA expression or little starting material, as plasma samples case. For cDNA template obtaining, first a poly(A) tailing reaction to extend the 3' end of the mature transcript is needed, then, the adaptor ligation reaction extends the 5' end. Finally, this modified miRNAs undergo universal RT as described and cDNA is uniformly amplified for all miRNAs.

miRNA	TaqMan Advanced reference (plasma)	TaqMan Assay reference (Tissue and cultures)
hsa-miR-92a-3p	477827_mir	000430
hsa-miR-181c-5p	477934_mir	000482
hsa-miR-210-3p	477970_mir	000512
hsa-miR-584-5p	-	001624
hsa-miR-143-5p	-	002146
hsa-miR-373	-	000561
hsa-miR-642a-3p	-	474715_mat
hsa-miR-3120	-	242355_mat
hsa-miR-1306-5p	-	242734_mat
hsa-miR-7151-3p	-	466506_mat
hsa-miR-132	-	000457
hsa-miR-137	-	001129
hsa-miR-484	478308_mir	-
hsa-miR-191-5p	477952_mir	-
hsa-miR-423-5p	478090_mir	-
RNU44	-	001094
RNU48	-	001006
RNU6b	-	001093
sno202	-	001232
sno234	-	001234
U18	-	001204
U6 snRNA	-	001973

Table 5. miRNAs included in qPCR analysis. Notice TaqMan assays for plasma detection are Advanced technology.

For poly(A) reaction, 3 µL of mix containing 10X poly(A) buffer, ATP and poly(A) enzyme is mixed with 2 µL of RNA. Reaction was done in a thermal cycler 45 min at 37°C for polyadenylation and 10 min at 65°C to stop the reaction. Immediately, adaptor ligation reaction must be performed mixing 5 µL of poly(A) reaction product with 10µL ligation mix (5X DNA ligase buffer, 50% PEG 8000, 25X ligation adaptor and RNA ligase). Ligation reaction was completed after 60 min at 16°C. 15 µL of this product were reverse transcribed with 15 µL of RT mix containing 5X RT buffer, 25mM dNTPs, 20X universal RT primer and 10X RT enzyme mix. After vortex thoroughly, samples were reverse transcribed in a thermal cycler during 15 min at 42°C and reaction was stopped with 5 min step at 85°C. Finally, the miR-Amp reaction uniformly amplified all miRNAs by mixing 5 µL of RT product with 45 µL of

miR-Amp mix (2X miR-Amp Master mix and 20X miR-Amp primer mix). Thermal cycler program was the following:

Step	Temperature	Time	Cycles
Enzyme activation	95°C	5 min	1
Denature	95°C	3 sec	14
Anneal/Extend	60°C	30 sec	
Stop reaction	99°C	10 min	1

The cDNA template product was diluted 1:10 in TE buffer and used for RTqPCR.

For mRNA analysis or 500 ng RNA was reverse trancribed was performed in 20 µl of total volume, using Oligo(dT) primers (1 µM; Life technologies), random hexamers (1 µM; Life technologies), dNTPs (0.5 mM; Life technologies), DTT (0.45 mM; Life technologies), RNAseOut (10 units; Life technologies), reaction buffer (1x, Life Technologies) and SuperScriptTM II reverse transcriptase (200 units; Life technologies). First, a mix containing the RNA, dNTPs, Oligo(dT) primers and random hexamers, in 12 µl of volume, was incubated at 65 ºC for 5 min, in order to avoid secondary RNA structures and allow appropriate binding of the primers. Immediately after this time, reactions were incubated on ice while 8 µl of a mix containing DTT, RNAseOut and reaction buffer was added to each tube. After 2 min incubation at 42°C, and 2 at room temperature, SuperScriptTM II was added to each tube, and incubated at 42ºC for 50 min and 70ºC for 15 min. The product cDNA was stored at -20ºC.

Quantitative real-time PCR

Quantitative real-time PCR (qPCR) was performed in compliance with The Minimum Information for Publication of Quantitative Real-Time PCR Experiments (MIQE) guidelines [261].

From 5µl of 1/10 diluted cDNA (plasma samples) using TaqMan Fast Advanced Master Mix and TaqMan Advanced miRNA Assays (Thermo Fisher Scientific) or from 1.33 µl of cDNA (tissue and cultures samples) using TaqMan™ Universal Master Mix II, with UNG. Amplification was performed using the Applied Biosystems 7500 Fast instrument (see table 6 for conditions). Samples were run in duplicate and internal control samples were repeated in every plate to avoid batch effects.

Raw Ct data acquired using the 7500 Software v2.0.6 (Applied Biosystems) was exported to LinRegPCR software[262] to calculate the amplification efficiency for each reaction. Reactions with amplification efficiency below 1.6 were discarded. Ct values and average efficiencies obtained from LinRegPCR were used to analyze miRNA levels by the comparative ΔΔCt method [263].

Step	Temperature	Time (Plasma program)	Time (Tissue and cultures program)	Cycles
Enzyme activation	95°C	20 sec	10 min	1
Denature	95°C	3 sec	15 sec	40
Anneal/Extend	60°C	30 sec	60 sec	

Table 6: qPCR was perfrmed using Applied Biosystems 7500 Fast instrument under described conditions.

To date, there is no consensus on the use of particular reference genes for miRNA levels normalization in AD studies. Therefore, in this study, the stability of some described reference genes was evaluated using the NormFinder algorithm. hsa-miR-191-5p and hsa-miR-484 were identified as the most stable reference genes along all plasma samples. In addition, hsa-miR-191-5p and hsa-miR-484 showed higher correlation than other candidates (Spearman's correlation coefficient r=0.89; p<0,0001).

The stability of four small-nucleolar RNAs (snoRNAs), commonly used for miRNA normalization was test. U18 and RNU48 were selected for tissue normalization using Normfinder algorithm[264] (Figure 9). miRNA levels were normalized versus the geometric mean of selected reference genes, to compensate abundance differences between miRNAs and prevent statistical outliers [265].

Cell culture miRNA levels were normalized versus U6 RNA.

Gene name	Stability value
U6b	0.130
U18	0.104
U44	0.118
U48	0.075

Intragroup variation

Group identifier	Control	ADI-II	ADIII-IV	ADV-VI
U6b	0.206	0.218	0.488	0.194
U18	0.295	0.120	0.149	0.104
U44	0.352	0.119	0.344	0.090
U48	0.034	0.090	0.193	0.086

Intergroup variation

Group identifier	Control	ADI-II	ADIII-IV	ADV-VI
U6b	-0.093	0.037	0.038	0.018
U18	-0.017	-0.066	0.105	-0.023
U44	0.129	-0.054	-0.028	-0.047
U48	-0.019	0.082	-0.114	0.051

Best gene	**U48**
Stability value	**0.075**
Best combination of two genes	**U18 and U48**
Stability value for best combination of two genes	**0.066**

Figure 9: Example of reference genes selection. Stability was assessed using Normfinder algorithm. Furthermore, stability was confirmed by a comprehensive ranking between different methods (Delta Ct[266], BestKeeper[267], GeNorm[265] and Normfinder[264]) available online[268].

Droplet digital PCR

Droplet Digital PCR (ddPCR) technology is based on the use of a water-oil emulsion droplet system to the partitions that separate the template DNA molecules. In this way, each droplet undergoes an individual PCR reaction allowing massive sample partitioning (assessing thousands of independent amplification events from a single sample), key feature of the ddPCR technique.

Briefly, DNA and probes (same TaqMan Assays as for RTqPCR) were combined with the Bio-Rad ddPCR supermix and placed into the QX200 Droplet Generator that generated an emulsion of about 20,000 droplets. The emulsion is then transferred to a 96-well PCR plate and PCR was performed in a thermal cycler. The

amplified product is placed in the QX200 Droplet Reader that performed individually droplet reading. Finally, QuantaSoft™ software was used to count PCR-positive and PCR-negative droplets and an absolute quantification in copies per µL was obtained.

ddPCR set-up require testing different reaction temperatures, probes concentration and DNA optimal amount to generate the adequate number of droplets and to achieve a good differentiation between fluorescence levels of negative and positive events. Considering the time required for reaching optimal conditions for each miRNA detection, we finally decided to use TaqMan Advanced RTqPCR method. However, we do not rule out using this technique in the future, especially to attempt the detection of those candidates that we have not been able to detect with the chosen technique.

Generation of lentiviral vectors

pLVTHM-shmiRNA generation

Oligonucleotids containing each miRNA target sequence (Table 7) and the BglII and HindIII restriction enzymes sites needed for insertion in the pSUPER vector (pSUPER.retro.puro from OligoEngine Inc (Figure 10) were designed using Serial Cloner software (Serialbasics.com)

Insert name	Oligonucleotids sequences 5'-3'
Anti-miR92a-3p	Fw gatcccc**TATTGCACTTGTCCCGGCCTGT**tcaagagaCAGGCCGGGACAAGTGCAATAttttttg Rv agctcaaaaa**TATTGCACTTGTCCCGGCCTGT**ctcttgaaCAGGCCGGGACAAGTGCAATAggg
Anti-miR181c-5p	Fw gatcccc**AACATTCAACCTGTCGGTGAGT**ttcaagagaACTCACCGACAGGTTGAATGTTttttttg Rv agctcaaaaa**AACATTCAACCTGTCGGTGAGT**tctcttgaaACTCACCGACAGGTTGAATGTTggg
Anti-miR-210-3p	Fw gatcccc**CTGTGCGTGTGACAGCGGCTGA**ttcaagagaTCAGCCGCTGTCACACGCACAGttttttg Rv agctcaaaaa**CTGTGCGTGTGACAGCGGCTGA**tctcttgaaTCAGCCGCTGTCACACGCACAGggg

Table 7: Oligonucleotide sequences used for shmiRNA lentiviral vectors generation. In bold 22 nucleotids of sense mature miRNA sequences.

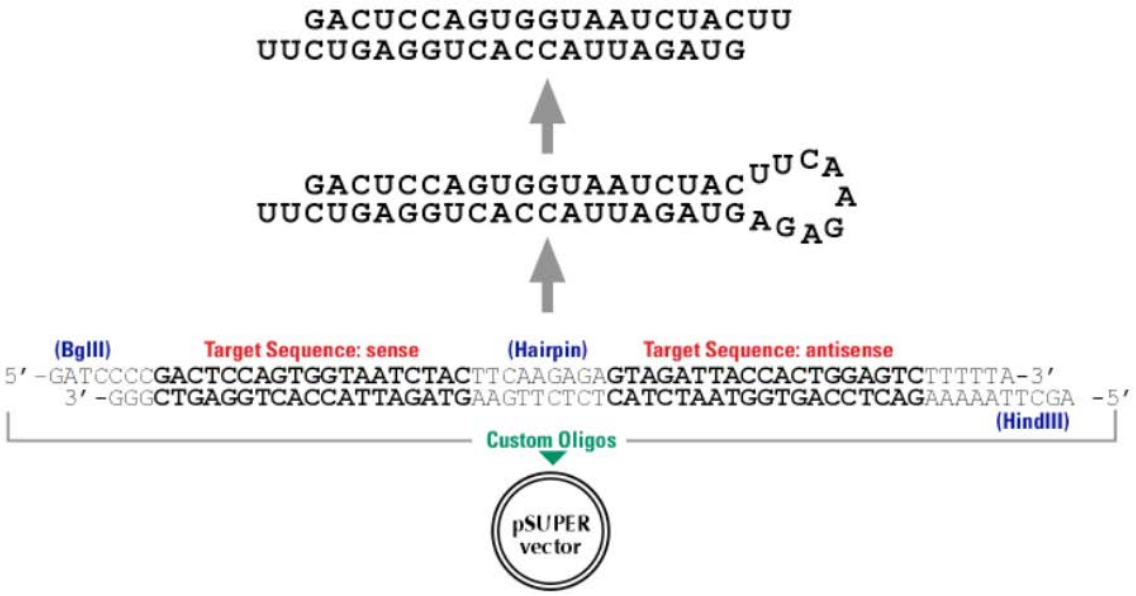

Figure 10: shRNA subcloning in a pSUPER vector. We followed an shRNA approach to clon a miRNA coplementary sequence in pSUPER vector to as a middle step to generate pLVTHM-shmiRNA vector for miRNA silencing.

Oligonucleotids (Invitrogen) were diluted to a final concentration of 100 µM, and phosphorylated by T4 polynucleotide kinase (NEB) before complementary strands were annealed in a 50mM Hepes pH 7.4, 100 mM NaCl buffer overnight with gradually decreasing temperature from 95°C to room temperature.

Moreover, 1 µg of the pSUPER plasmid was sequentially digested with HindIII for 1 h and then with BglII for 2 h. Both incubations were done at 37°C with 10 units of each enzyme (Genecraft). Once linearized, the product was resolved in a 1% agarose gel run at 80 V and selected bands were purified using NucleoSpin gel and PCR clean-up kit (Macherey-Nagel).

Annealing products for each miRNA were diluted to 1µM (2µl) and ligated with 200ng of linearized pSUPER (2µl) using 1µl of T4 ligase enzyme (NEB) in 20µl reaction volume. Negative controls were included. Ligation reaction was performed in a thermocycler at 16°C overnight, with a final step of 15 min at 65°C.

Ligation product was used to transform competent *E. coli* DH5α through heat shock (1 min at 42°C and immediately 2 min on ice) that were then seeded in LB-agar ampicillin plates. Isolated colonies ampicillin resistant were selected and growth in

LB medium overnight at 37°C in shaking conditions. Plasmids were purified using Nucleo Spin plasmid DNA/RNA purification kit (Macherey-Nagel) and following manufacturer's indications.

5 µg of each plasmid and 1.5 µg of empty pLVTHM were sequentially digested first with EcoRI (Sigma) for 2 h and then with ClaI (NEB) for other 2 h. Both reactions were done at 37°C with 10 units of each enzyme in 30 µl final reaction volume. Digested products were loaded in 2% agarose gel and band corresponding to H1 promoter-shmiRNA fragments and linearized pLVTHM were purified as before. 1 µl of pLVTHM (25ng aprox) was ligated with 2 µl (120ng aprox) of each H1-shmiRNA fragment, *E. coli* DH5α were transformed and colonies were selected and growth as described. Plasmids were purified, digested with EcoRI and ClaI and loaded in 2% agarose gel to detect colonies which has inserted the H1-shmiRNA fragment. Confirmation was further obtained by sequencing. pLVTHM plasmids with shmiRNAs inserted were amplified using Nucleo Bond Xtra Maxi EF (Macherey-Nagel) and used for lentiviruses production.

Overexpressing miRNA plenti vector

Overexpressing miRNA vector pLenti-III-mico-GFP (Figure 11) with miR-181c-5p sequence inserted for miRNA overexpression was purchased from Applied Biological Materials (**abm**) and used for lentiviruses production.

Figure 11: pLenti-III-mico-GFP lentiviral vector (abm) map. This vector allows overexpression of inserted miRNA and contains a GFP reporter for monitoring transfection efficiency.

pmirGLO Dual-Luciferase miRNA Target Expression Vector

Oligonucleotides (Integrated DNA technologies) were designed containing selected miRNA target region (Table 8) and XbI and SacI restriction sites. An internal NotI restriction site was added to oligonucleotides sequences for further clone confirmation. Oligonucleotides were annealed and ligated into the previously linearized pmirGLO Vector (Promega) as before. pmiRGLO-miRNA vectors were obtained after *E. coli* DH5α transformation, colonies selection in LB-agar ampicillin plaques and plasmid purification as describe before.

Insert name	Oligonucleotides sequences 5'-3'
miR92a-3p target sequence	Fw tagcggccgctagt**CAGGCCGGGACAAGTCCAATA** Rv ctagTATTGCACTTGTCCCGGCCTGactagcggccgctaagct
miR181c-5p target sequence	Fw tagcggccgctagt**ACTCACCGACAGGTTGAATGTT** Rv ctagAACATTCAACCTGTCGGTGAGTactagcggccgctaagct
miR-210-3p target sequence	Fw tagcggccgctagt**TCAGCCGCTGTCACACGCACAG** Rv ctagCTGTGCGTGTGACAGCGGCTGAactagcggccgctaagct

Table 8: Oligonucleotide sequences used for pmiRGLO luciferase vectors generation.

Lentiviruses production

Lentiviral particles were obtained by co-transfection in HEK 293T cells with plasmid of interest (pLVTH-shmiRNAs or plenti-miRNAs as needed), together with psPAX2 (packaging plasmid) and pMD2G (envelope plasmid) by calcium phosphate method (Clontech).

Briefly, HEK 293T seeded in 10mm diameter plates in DMEM medium supplemented with 10% FBS should be 70-80% confluent before transfection. Medium was changed for the same medium plus chloroquine 25 μM to increase transfection efficiency. Transfection solutions were composed of 10 μg of psPAX2 and pMD2G and 30 μg of pLVTH plasmid, 2,5 mM $CaCl_2$, and sterile H_2O mixed drop wise with HBS 2X (237mM NaCl; 10.2mM KCl; 1.4mM Na_2HPO_4; 42mM Hepes; 10mM glucose; pH 7.05). After 20 min at RT DNA mixture solution is added

to each plate drop wise and incubated for 6-8 hours at 37°C. Then, medium was completely replaced with fresh DMEM.

Medium containing the lentiviral particles was collected at 24, 36 and 48 hours after transfection and concentrated by ultracentrifugation (25000 rpm for 2 hours at 4°C). The viral pellet was resuspended in 100 μL cold sterile PBS1X by slow shaking at 4°C for 24 hours, then aliquoted and stored at -80°C.

In order to use the same amount of viral particles each time, lentiviral particles were titrated through GFP-positive detection (infected HEK 293T cells) in a flow cytometer (Cytomics FC 500, Beckam Coulter) 72 hours after infection. Hippocampal cell were infected with 1 infective particle per cell when needed.

Luciferase assay

The pmirGLO Dual-Luciferase miRNA Target Expression Vector allow miRNA activity evaluation by inserting miRNA target sites in the 3'UTR region of the firefly luciferase gene (luc2) (Figure 12).

17-19 DIV hippocampal neurons were transfected by calcium phosphate method with pmiRGLO dual vectors containing our selected miRNA target sequences.

Transfection solutions were composed of 1 μg pmiRGLO plasmid (wich is a dual plasmid containing its own renilla control in the same plasmid), $CaCl_2$, and sterile H_2O following manufacturer indications, mixed drop wise with HBS 2X (237mM NaCl; 10.2mM KCl; 1.4mM Na_2HPO_4; 42mM Hepes; 10mM glucose; pH 7.05).

Before transfection, half culture medium is removed from each well and mixed with the same amount of fresh medium and kept at 37°C for following steps. In addition, fresh medium is incubated at 10% CO_2 for further use.

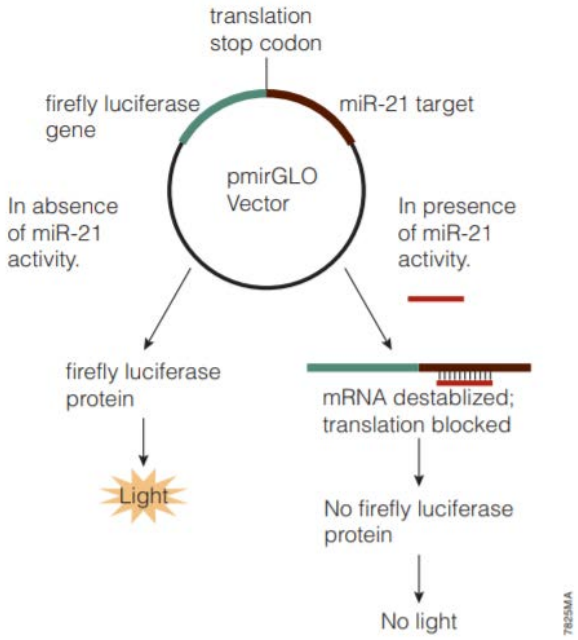

Figure 12: pmirGLO Vector (Promega) mechanism of action. Our selected miRNAs target sequences were inserted in pmiRGLO vector for luciferase assay experiments.When endogenous miRNA bind to the target sequence in the pmiRGLO, luciferase translation is blocked and decrease in luciferase levels are detected.

The transfection solution was incubated for 20 min at RT, and then 50µl of DNA mixture solution is added to each well (volume 500 µl) drop wise and incubated for 1 hour at 37°C. Calcium crystals must be formed during this time. Next, medium was aspirated and 1 ml of 10% CO2 pre-warmed (37ºC) medium was added to each well for 5 min to acidify medium facilitating calcium precipitates to dissolve. Finally, 10% CO_2 media was removed and half conditioned medium was added and cells were kept in incubator for 24 hours before lysis.

Luciferase assay was performed following manufacturers indications. Briefly, media was removed from wells and washed with PBS1X. 75 µl of passive lysis buffer were added to each well and after 15 min gentle agitation at RT, each well volume was collected separately. Protocol was optimized so that half volume of LARII and Stop&Glo was used for each reaction. Luciferase and renilla activities were measured with Wallac 1420 Victor 3 Multilabel Counter instrument (Servei de Cultius cel·lulars, producció d'anticossos i citometria de la UAB).

6. Microarray analysis

Three randomly selected tissue samples from each group listed in Table 2 (12 samples for each brain area) were used for microarray analysis Affymetrix® miRNA 4.1. In accordance to miRBase 20, includes 2578 human mature miRNA probe sets, 1996 human snoRNA and scaRNA probe sets and 2025 human pre-miRNA probe sets. First the Affymetrix® Expression Console™ (v 1.4.1.46 by Affymetrix), allow hybridization quality control, identification of outliers, detect differences in samples by QC metrics, view of the distribution and monitoring sample quality. The CEL files' data were extracted, normalized using RMA quantile normalization and converted into log2 notation.Next, the differential miRNA expression analysis, was performed by the Transcritpome Analysis Console 4.0 (TAC) applying a univariate ANOVA analysis and selecting genes with a fold change of over ±1,5 and a p-value <0.05.

In the meantime, we selected a group of 100 synaptic-related genes (Table 9) from a list of 1080 found in available databases (Genes2cognition.org Human orthologues of mouse PSD adapted from Collins et al, 2006. Source G2C. Gene list: L00000009) (Figure 13-A). mRNA-miRNA validated interactions were checked in miRWalk 2.0 database[269,270] and 1302 miRNAs were found to target those 100 genes (Figure 13-B). From those more than 1300 miRNAs, 154 matched with altered miRNAs previously identified by the microarray (Figure 13-C), either in entorhinal cortex (112) or hippocampus (156) (See Figure 17, page 70). Subsequently, we selected 6 miRNAs (let-7b-3p, miR-98-3p, miR-143-5p, miR-584-3p, miR642a-3p and miR-7151-3p) with synaptic-validated targets which were deregulated both in enthorinal cortex and hippocampus at any pathological stage (Figure 13-D). 3 miRNAs were selected from the screening (miR-143-5p, miR-584-5p and miR-7151-3p) prioritizing deregulation in early stages and considering the interest of their potential targets. Fold change and p-values significance were also evaluated.

Moreover, we looked in the bibliography for miRNAs potentially related to synaptic proteins and other interesting candidates showed up (miR-92a-3p, miR-132, miR-137, miR-181c-5p and miR-210-3p) (Figure 13-E). 3 additional candidates from bibliography were included for further study: miR-92a-3p, miR-181c-5p and miR-

210-3p, all related to synaptic function. miR-132 was also incorporated as a control, since this miRNA has been widely described to be downregulated in AD[182,271,272].

ACAT1		*CASKIN1*		*HOMER1*		*PPP1R9A*	*STX7*
AKAP5		*CDK5*		*KCNMA1*		*PPP1R9B*	*STXBP1*
AKAP9		*CDK5R1*		*KCNQ2*		*PPP2CA*	*STXBP5*
APP		*CS*		*MAP2*		*PPP2R1A*	*SYN1*
CACNA1A		*GABARAPL2*		*MAP2K1*		*PPP3CA*	*SYN3*
CACNA1B		*GABBR1*		*MAPK1*		*PRKACB*	*SYNGR1*
CACNA1C		*GABBR2*		*MYO6*		*PRKAR1A*	*SYNGR3*
CACNA1E		*GABRA1*		*NPTX1*		*PRKAR2A*	*SYNJ1*
CACNA2D1		*GRIA1*		*NPTXR*		*PRKAR2B*	*SYNJ2*
CACNA2D2		*GRIA2*		*NRXN1*		*PRKG2*	*SYNPO*
CACNA2D3		*GRIA3*		*NRXN3*		*SHANK1*	*SYP*
CACNB1		*GRIA4*		*NSF*		*SHANK2*	*SYT1*
CACNB3		*GRIN2A*		*PDE10A*		*SHC1*	*SYT2*
CACNG2		*GRIN2B*		*PDE11A*		*SNAP25*	*SYT5*
CACNG3		*GRIN2D*		*PDE2A*		*SNAP47*	*SYT7*
CAMK2A		*GRM1*		*PDE4B*		*SNAP91*	*UBE2V1*
CAMK2B		*GRM3*		*PDE4D*		*SNCA*	*UCHL1*
CAMK2D		*GRM5*		*PPP1CA*		*STX12*	*VAMP2*
CAMK2G		*GRM7*		*PPP1CB*		*STX1A*	*VAPA*
CAMKV		*GSK3B*		*PPP1CC*		*STX1B*	*VAPB*

Table 9: 100 synaptic genes were selected from Genes2cognition.org database. Original list gene were of 1080 genes.

Selected miRNAs for study are presented highlighted in red in Figure 13-D/E. Their validated targets are listed at the results (Table 10, page 74).

In addition, miR-137, miR-373, miR-642a-3p and miR-1306-5p were analyzed in selected areas. The analysis of this second group could be found in Annex page 164.

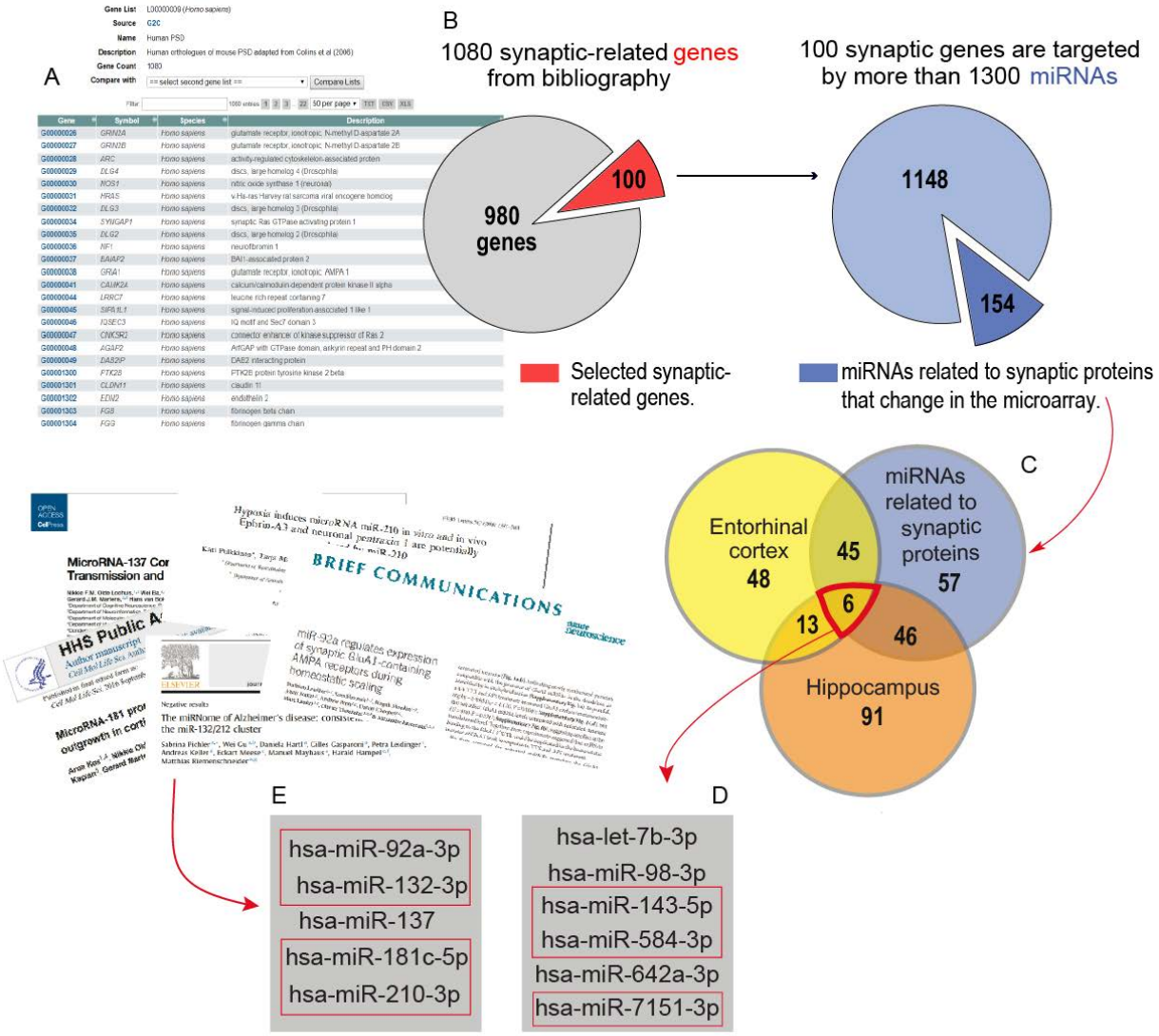

Figure 13: miRNAs selection process workflow. 100 synaptic-related genes were selected from bibliography (Genes2cognition.org) (A). mRNA-miRNA validated interactions were checked in available databases (MirWalk 2.0) and data were crossed with microarray results (B). Changes in the levels of 154 miRNAs with synaptic genes validated interactions were found in the microarray (C). Changes in 6 miRNAs related to synaptic proteins were observed in human hippocampus and entorhinal cortex (C-D). Synaptic-related miRNAs described in the bibliography were also selected for further study (E).

7. Statistical analysis

Statistical analysis was performed using GraphPad Prism software v6.01 (GraphPad Software Inc., California, USA) and MedCalc (v17.9.7). Statistical outliers (≥2 SD from the mean) were removed from the analyses. Normality (D'Agostino & Pearson and Shapiro-Wilk tests) and homoscedasticity were tested in each data set before further analysis by one-way or two-way analysis of variance (ANOVA) followed by Bonferroni post hoc test or two-sided nonparametric Mann-Whitney according to each case requirement. If not otherwise specified, data is shown as the mean ± standard error of the mean (SEM) or standard deviation (SD). Receiver operating characteristic (ROC) curve analysis under a nonparametric approach was used to obtain the area under de curve (AUC) to evaluate sensitivity and specificity of each miRNA as a predictive biomarker. Logistic regression was applied to evaluate biomarker combination by ROC curve analysis. Differences with p value < 0.05 were considered significant.

RESULTS

1. miRNA levels deregulation during AD progression in different brain areas: Microarray results

Microarrays have demonstrated its usefulness as a first approach to study deregulation of miRNAs during AD development. From the screening in experimental animal models[273] to massive analysis in human brain and circulating fluids, microarray analysis could provide a huge amount of information by testing several pathological aspects. Major reviews on the role of miRNAs in AD pathology[274] highlight the importance of studying miRNAs expression in different conditions related to AD, using experimental animal models, human tissue and circulating biofluids in order to obtain an overview of the role that miRNAs may play during the development of the disease. We consider that using this tool to obtain a global view of miRNAs alteration during disease progression, analyzing thousands of miRNAs in samples from different brain areas at different pathological stages, could provide enormously valuable information.

For assessing miRNA levels during AD progression, human brain tissue of entorhinal cortex, hippocampus, prefrontal cortex and cerebellum at different Braak stages were analyzed by Affymetrix® miRNA 4.1 array. Comparison of each pathological group with control subjects was performed and graphed as a volcano plot, where fold changes are plotted versus ANOVA p-values. All expressed miRNAs are represented, though only significant downregulated (blue) and upregulated (red) miRNAs for the settled parameters (1.5> FCh < -1.5 and p-value <0.05) are highlighted.

Considering AD pathogenic progression pattern, entorhinal cortex (Figure 14) and hippocampus (Figure 15) plots are shown for its particular interest in this study.

According to Braak classification[69,71], while patients in stages I-II do not present visible symptoms, in stages III-IV cognitive deficits starts to be detectable and can be considered as an MCI state. For this reason the transition between these stages could be an interesting point to study miRNAs deregulation. Therefore, ADIII-IV stage was compared to ADI-II in entorhinal cortex and hippocampus (Figure 16).

A total of 112 miRNAs were significantly disregulated in AD entorhinal cortex, comparing each pathological stage to control subjects, of which 63 were upregulated and 49 downregulated (Figure 17 upper panel). Next, changes in miRNAs leves were classified considering the first stage of affection and the progression in later stages. From 49 miRNAs altered in early stage ADI-II in entorhinal cortex, 11 continue changed in ADIII-IV and 6 in ADV-VI. In addition, 29 miRNAs were detected to be altered in ADIII-IV from which 5 remain altered in ADV-VI. Additional 34 miRNAs showed no significant changes until late stages (ADV-VI). Hippocampus analysis showed 156 diferentially expressed miRNAs; 70 upregulated and 86 downregulated (Figure 17 bottom panel). Levels of 24 miRNAs were significantly different from control level at early stages (ADI-II), of which 4 remain altered in ADIII-IV and 4 until ADV-VI. 16 of the 66 miRNAs affected from ADIII-IV were still altered at late stages. Finaly, 66 miRNAs showed levels singificantly different in ADV-VI compared to control subjects.

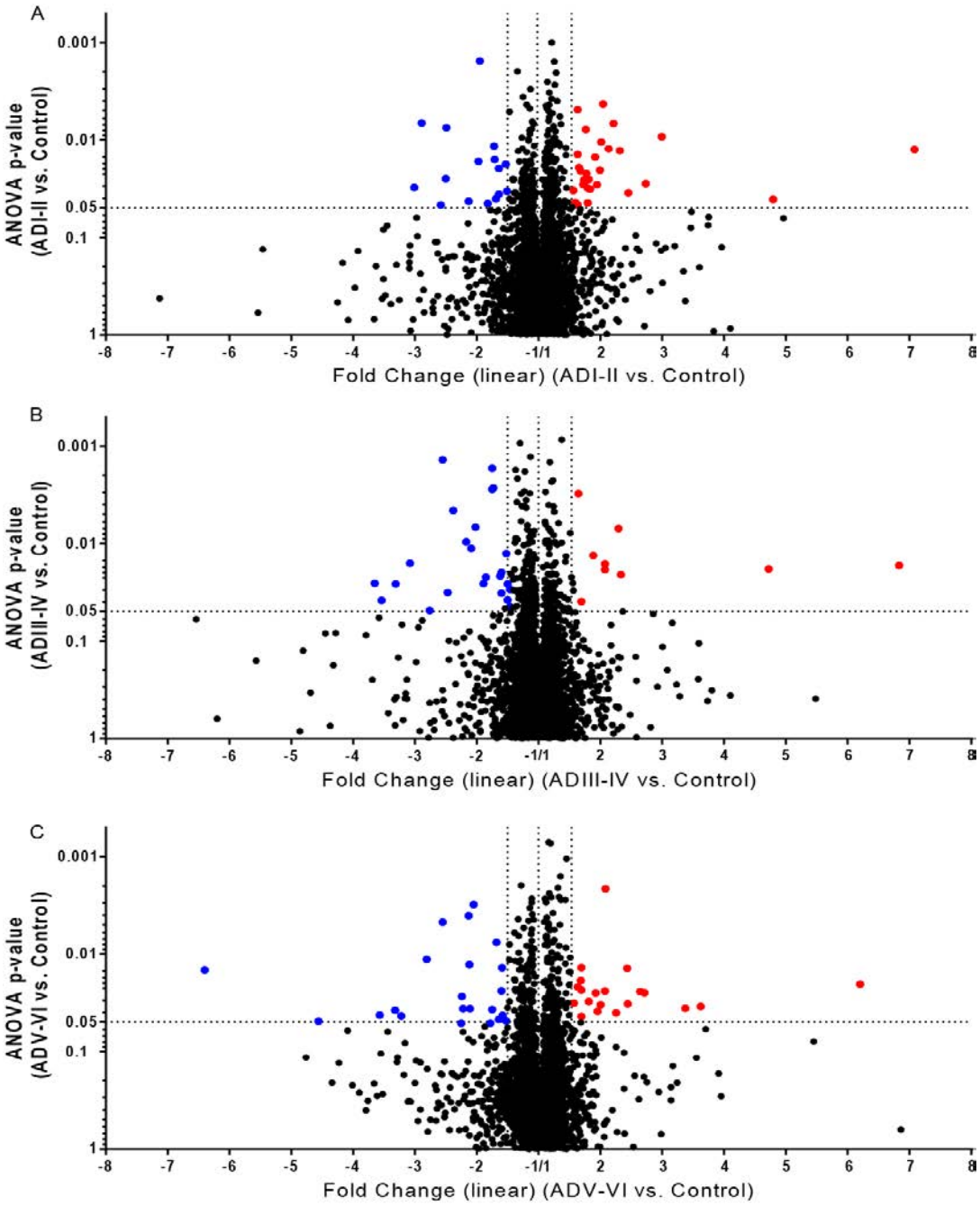

Figure 14: miRNAs levels in human enthorinal cortex: microarray results. Volcano plot representing fold change and p-value for each miRNA evaluated in Affimetrix miRNA 4.1 array. Patients in stages ADI-II (A), ADIII-IV (B) and ADV-VI (C) of AD pathology were compared to control subjects. Downregulated (blue) and upregulated (red) miRNAs are shown. Fold change > 1.5 and p-value < 0.05 were considered significant.

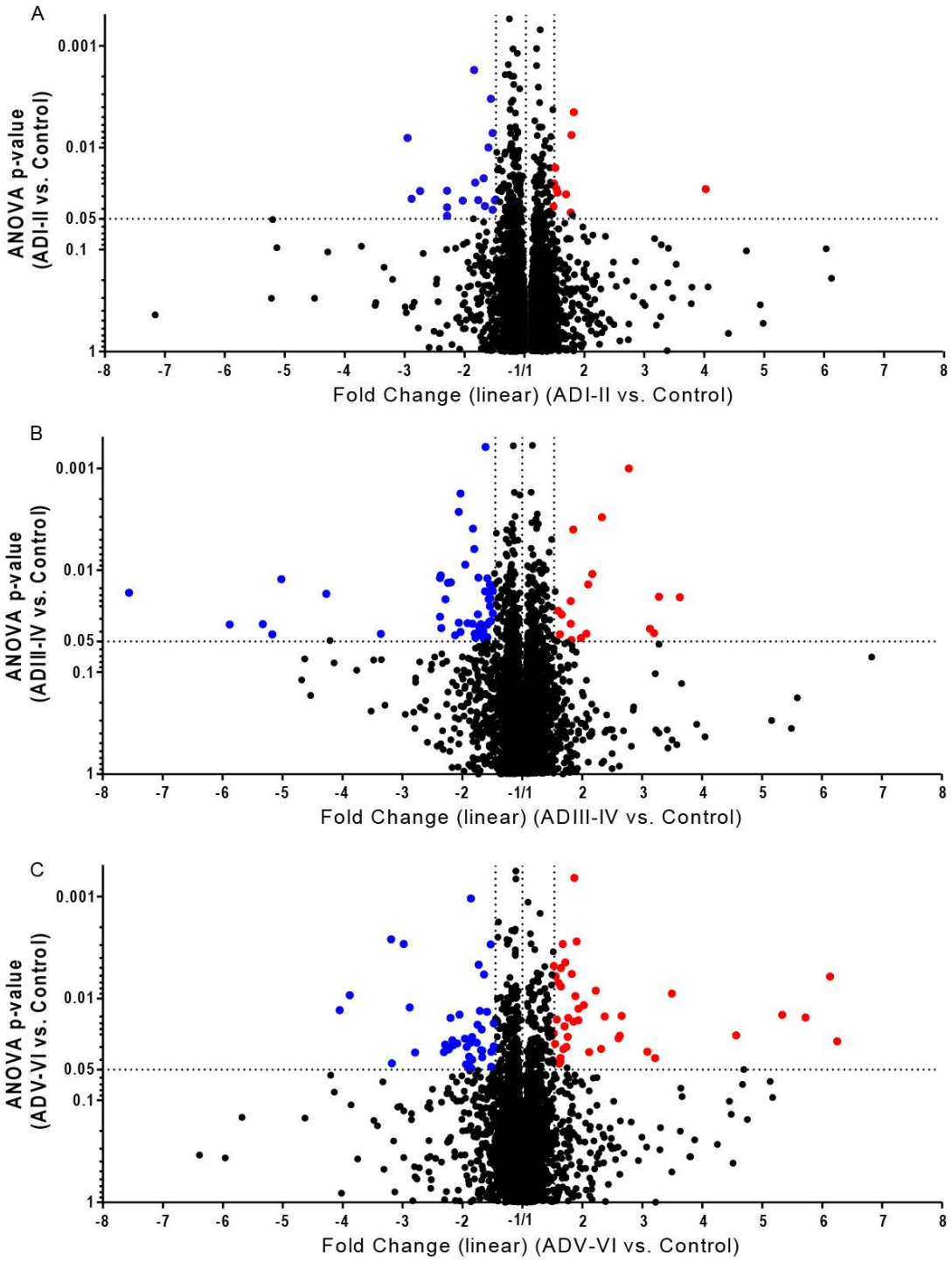

Figure 15: miRNAs levels in human hippocampus: microarray results. Volcano plot representing fold change and p-value for each miRNA evaluated in Affimetrix miRNA 4.1 array. Patients in stages ADI-II (A), ADIII-IV (B) and ADV-VI (C) of AD pathology were compared to control subjects. Downregulated (blue) and upregulated (red) miRNAs are shown. Fold change > 1.5 and p-value < 0.05 were considered significant.

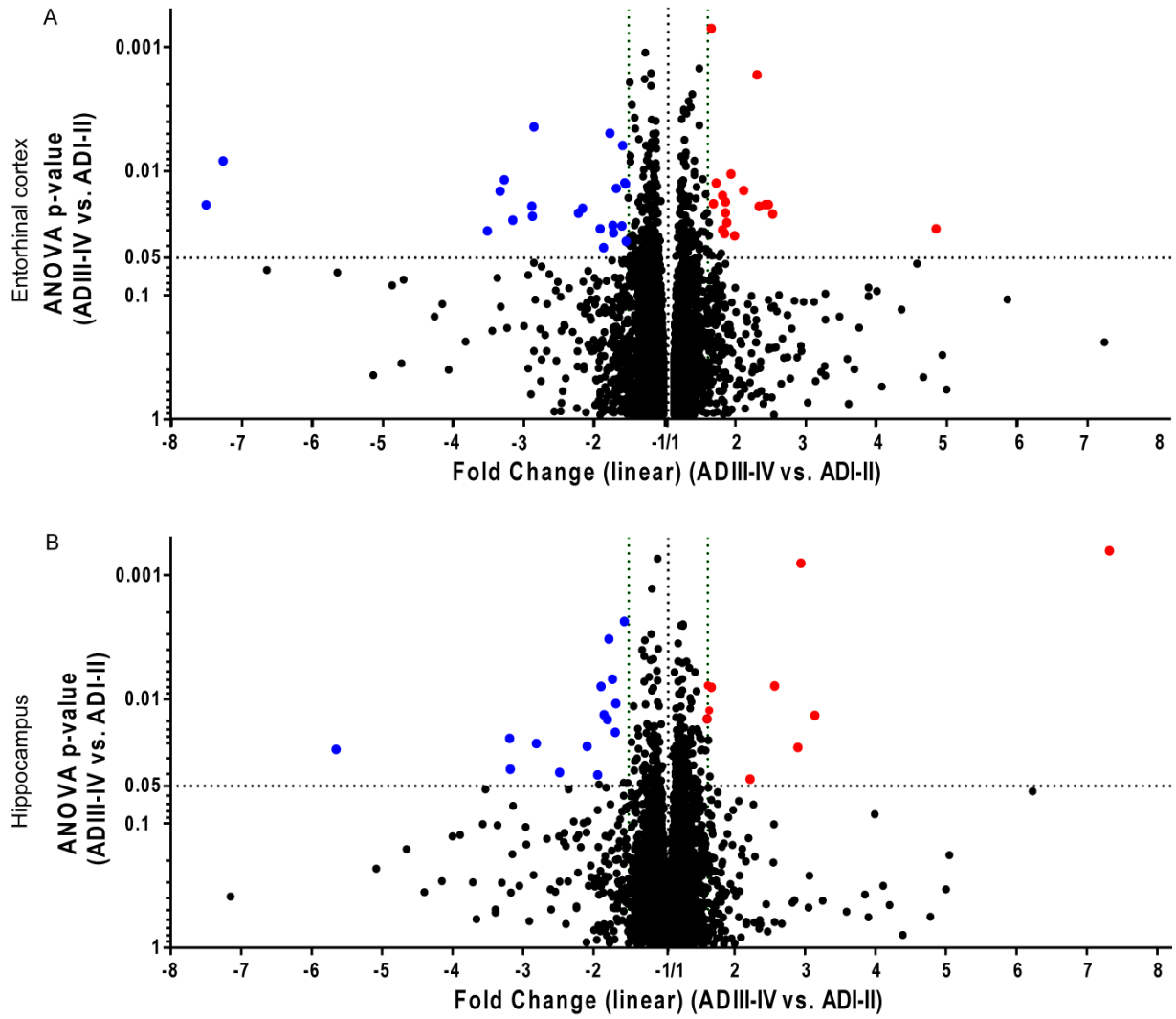

Figure 16: miRNAs levels in human enthorinal cortex (A) and hippocampus (B): microarray results. Volcano plot representing fold change and p-value for each miRNA evaluated in Affimetrix miRNA 4.1 array. Patients in stages ADIII-IV were compared to ADI-II subjects. Downregulated (blue) and upregulated (red) miRNAs are shown. Fold change > 1.5 and p-value < 0.05 were considered significant.

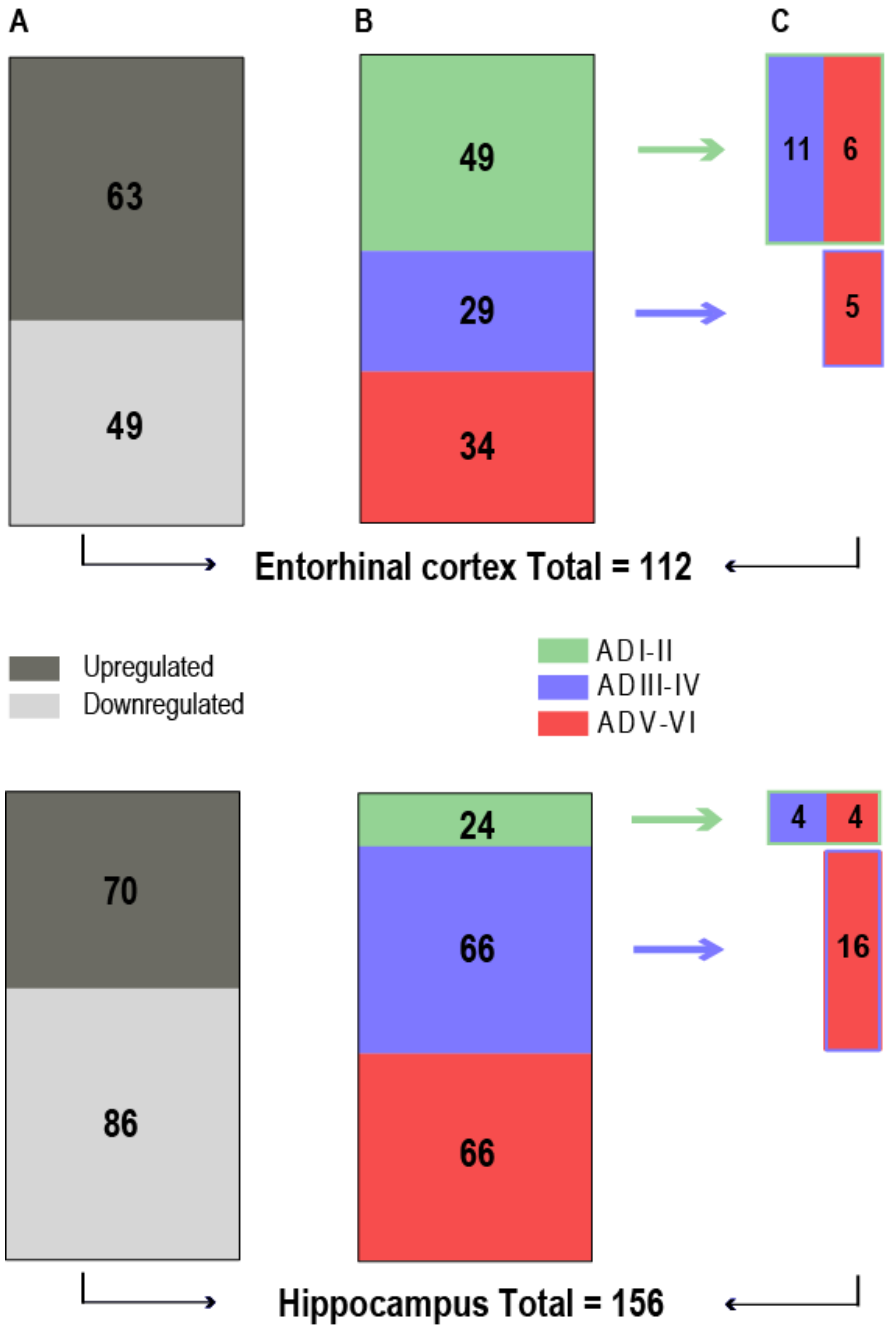

Figure 17: Microarray summary. miRNAs signiticantly affected in AD human entorhinal cortex (upper panel) and hippocampus (bottom panel) compared to healthy subjects. The number of miRNAs shown refers to the total number of miRNAs with increased or decreased leveles in any stage of the pathology (A), the first Braak&Braak stage where those miRNAs are affected (B), and the number of miRNAs that remains affected in later stages (C).

As expressed previously, of the 4 areas that we had available for study, we focused our analysis in entorhinal cortex and hippocampus, the first areas affected during AD progress. Early pathological stages, where cognitive deficits are not present (ADI-II) or only in a mild form (ADIII-IV), might be considered as synaptic phases, thus, is where our interest relies. In addition, maintained alterations over time could be important from the biomarker point of view, since a marker that is affected from initial phases of the pathology and that remains stable during its progress, would facilitate the detection of the pathology in any of its stages. This is why we filter the data obtained in the microarray and focused on those miRNAs altered in entorhinal cortex and hippocampus in early stages of AD, that remain affected until final stages of the disease.

Compared to control subjects, in entorhinal cortex (Figure 18), 5 miRNAs were downregulated and 1 upregulated in ADI-II and maintained until final stages. 5 additionally miRNAs were affected in stages III-IV and remained changed until stages V-VI (3 downregulated and 2 upregulated). For detailed information Annex page 162.

In hippocampus (Figure 19), 4 miRNAs were downregulated in ADI-II and maintained until ADV-VI. Moreover, 16 miRNAs were altered from stages III-IV up to stages V-VI (9 downregulated and 7 upregulated). Full data can be found Annex page 163.

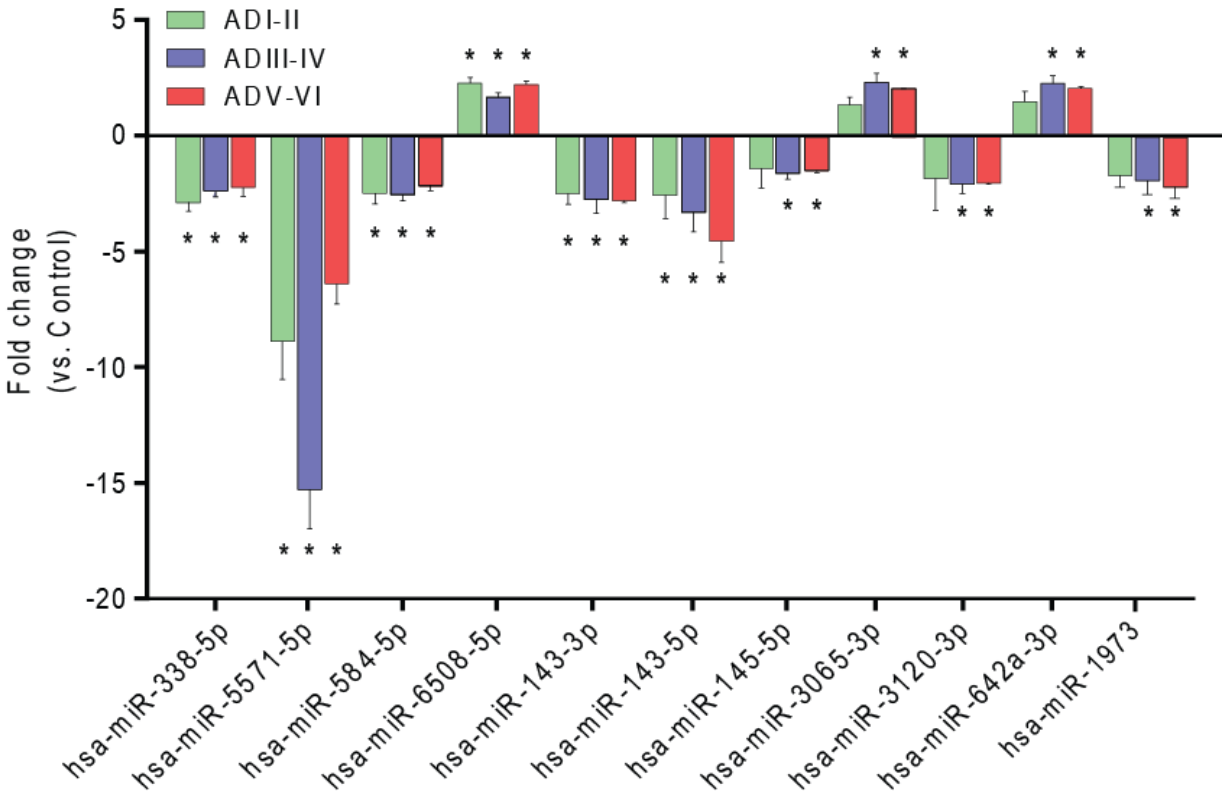

Figure 18: Early entorhinal cortex changes maintained until late pathological stages. Fch ≥ 1.5 in ADI-II and mantained in later stages compared to healthy subjects, and changes starting in ADIII-IV maintained until ADV-VI are shown. P-value < 0.05 was considered significant.

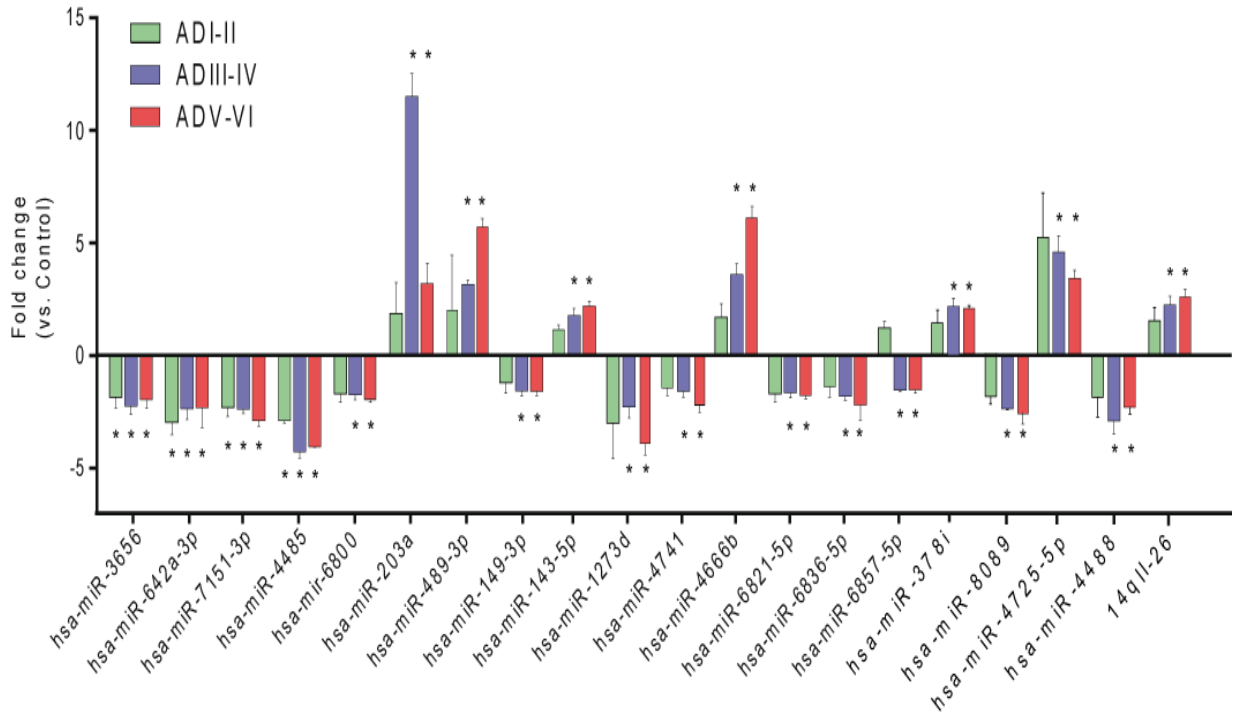

Figure 19: Early hippocampus changes maintained until late pathological stages. Fch ≥ 1.5 in ADI-II and mantained in later stages compared to healthy subjects, and changes starting in ADIII-IV maintained until ADV-VI are shown. P-value < 0.05 was considered significant.

This initial screening allowed us to identify a group of deregulated miRNAs in the brain areas of greatest interest for the development of the disease. As explained in the methods (Figure 13, page 60) miR-143-5p, miR-584-5p and miR-7151-3p were selected from the microarray as remarkably potential candidates for further study, since they have synaptic-validated targets and are deregulated in entorhinal cortex or hippocampus at early pathological stages. Additionally, 3 candidates from bibliography (miR-92a-3p, miR-181c-5p and miR-210-3p) were included for their potential role in synaptic function regulation. miR-132-3p was also incorporated as a control, since it has been widely described to be downregulated in AD[182,271,272]. Selected miRNAs and some of their validated targets are listed in Table 10.

Selected miRNAs	Validated targets
hsa-miR-92a-3p	CAMPKV, GluA1, CASKIN1, CDK5R1, GSK3B, MYO6, NR '1CC, PPP2R1A.
hsa-miR-132-3p	SIRT1, p250GAP, MeCP2, CRTC1 Control
hsa-miR-143-5p	AKAP9, PPP2CA, SYT1, MAPK1
hsa-miR-181c-5p	CAMK2D, GRM5, MAP2K1, NPR, GABRA1, GRM1, NRXN1, STXBP5
hsa-miR-210-3p	NP, CAMKV, KCNAB2, NRXN1, STXBP5, NPR
hsa-miR-584-5p	MAPK1, PPP2CA, UBE2V1
hsa-miR-7151-3p	NPR, SNAP47, STX7

Table 10: Candidates miRNAs selected both from microarray screening and from literature. Validated mRNA-miRNA interactions for candidate miRNAs based on miRWalk2.0 database are listed.

2. Microarray validation: human brain

snoRNAs RNU18 and RNU48 were selected for miRNA levels normalization in brain samples

As indicated in the methods, RNU18 and RNU48 were identified as the most stable genes through all tissue samples (Figure 20) and their geometric mean was used to normalize miRNA levels in all tissue samples.

Figure 20: snoRNAs RNU18 and RNU48 were selected for miRNAs levels normalization in all tissue samples. Four snoRNAs usually used for miRNAs normalization were evaluated using available algorithms.

Determination of the control group

Almost of the brain samples received for miRNAs levels analysis that were classified as controls, belonged to ischemic patients. Cerebrovascular diseases are frequently related to AD hence, variation between ischemic and not ischemic subjects could affect further analysis. Although these subjects will be represented in the subsequent figures, they have been excluded from the analysis since we do not consider them suitable controls for this study.

Instead, expression levels of selected miRNAs in tissue samples from early AD (ADIII-IV) and late AD (ADV-VI) subjects were analyzed by RT-qPCR and compared with cognitively normal controls (ADI-II). as reported[275]. Even though its classification indicates the beginning of pathological signs in the brain, these are reduced, and intellectual function is still preserved. In addition, we consider that using this stage as a control will allow us to relate tissue results with plasma results, since control subjects for plasma analysis include asymptomatic early AD patients, and MCI could correlate with ADIII-IV Braak stages.

miR-132-3p levels decrease during AD progression in all studied brain areas

As it is well established that miR-132-3p is downregulated in AD brains[209], we selected it as positive control to provide more confidence in the results obtained for other miRNAs. miR-132-3p levels were evaluated in entorhinal cortex, hippocampus, prefrontal cortex and cerebellum (Figure 21). As expected, its levels significantly decrease during AD progression, and remarkably, in all evaluated areas. Interestingly, miR-132-3p levels were not significantly altered in the microarray analysis, indicating that although the microarray provides valuable preliminary information, validation in a larger number of samples is crucial.

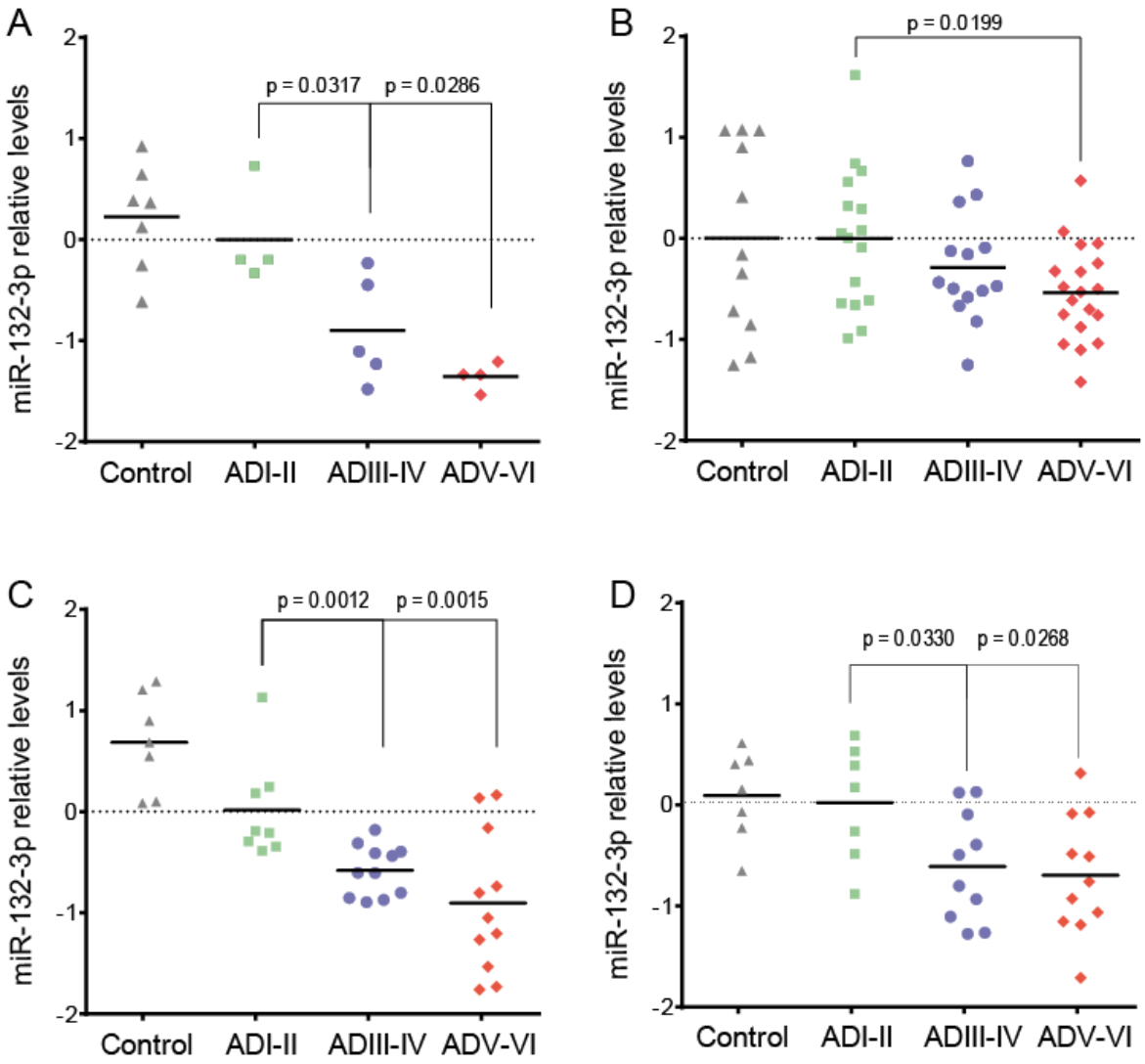

Figure 21: miR-132-3p levels decrease during AD progression in different brain areas. Selected miRNAs levels were analyzed in enthorinal cortex (A), hippocampus (B), prefrontal cortex (C) and cerebellum (D) at different Braak stages of AD pathology and were compared with cognitively normal ADI-II subjects. Log2 transformed data were normalized versus the geometric mean of U18 and U48 levels. p-value <0.05 was considered significant.

miR-92a-3p and miR-181c-5p levels increase in AD entorhinal cortex

Levels of selected miRNAs were first evaluated in entorhinal cortex (Figure 22). A significant increase was found in miR-92a-3p (p = 0.0159, log2 fold change = 0.6435) and miR-181c-5p (p = 0.0286, log2 fold change = 0.5882) levels at late stages compared to normal cognitive subjects. In addition, an increasing trend was observed from ADIII-IV stage. Probably due to the low number of samples analyzed in this area, although miR-143-5p (p = 0.200, log2 fold change 0.9247) and miR-

210-3p (p = 0.1143, log2 fold change 0.5761) levels trend to increase in ADV-VI stages, they do not reach significance. Additionally, a negative trend was observed in miR-7151-3p levels (p = 0.1111, log2 fold change -0.6599) in stages III-IV.

miR-92a-3p, miR-143-5p and miR-7151-3p levels increase in early AD hippocampus

We found that 3 miRNAs (*miR-92a-3p, miR-143-5p and miR-7151-3p)* were significantly increased in hippocampus in ADIII-IV compared to ADI-II cognitively normal subjects (Figure 23; miR-92a-3p: *p* = 0.0329, log2 fold change = 0.5375; miR-143-5p: *p* = 0.0396, log2 fold change = 0.5375; miR-7151-3p: *p* = 0.0266, log2 fold change = 0.3813). Moreover, miR-181c-5p levels show an increasing trend in ADIII-IV (p = 0.0851, log2 fold change 0.5081). No changes in hippocampal miR-210-3p neither miR-584-5p levels were observed at any stage. This area is especially interesting not only for its implication in the disease, but also because of the number of samples analyzed (n=61), that gives more confidence to the obtained results.

miR-181c-5p levels are increased in prefrontal cortex in late AD stages

RT-qPCR analysis revealed an increase in miR-181c-5p levels in prefrontal cortex in stages V-VI compared to cognitively normal subjects (Figure 24; miR-181c-5p: *p* = 0.0406, log2 fold change = 0.4946). The increase in miR-181c-5p levels in late stages in this area, together with its increase in entorhinal cortex and an increasing trend in hippocampus, is interesting, especially when the pathology spread pattern is considered. Moreover, miR-143-5p and miR-584-5p levels show a decreasing and increasing trend, respectively (miR-143-5p: *p* = 0.1084, log2 fold change = -0.2976; miR-584-5p: p = 0.0613, log2 fold change = 0.6402). Levels of miR-92-3p, miR-210-3p and miR-7151-3p remain stable at prefrontal cortex during AD progression.

miR-92a-3p and miR-584-5p levels are altered in cerebelum of AD patients

The cerebellum has been considered for many years as a control area not affected in AD. However, in recent years its involvement in certain aspects of the pathology has been described. Including cerebellum in the analysis allows a more comprehensive view of potential miRNAs alterations and their distribution pattern during disease progress.

miR-92a-3p levels increased in cerebellum at late stages of the disease while miR-584-5p levels decrease with AD progression (Figure 25; miR-92a-3p: p = 0.0266, log2 fold change = 0.5271; miR-584-5p: p = 0.0431, log2 fold change = -0.2715). In addition, miR-584-5p levels are still affected in ADV-VI stages (p = 0.0204, log2 fold change = 0.7168). No changes were observed in this area in miR-143-5p, miR-181c-5p, miR-210-3p, miR-584-5p nor miR-7151-3p levels at any pathological stage.

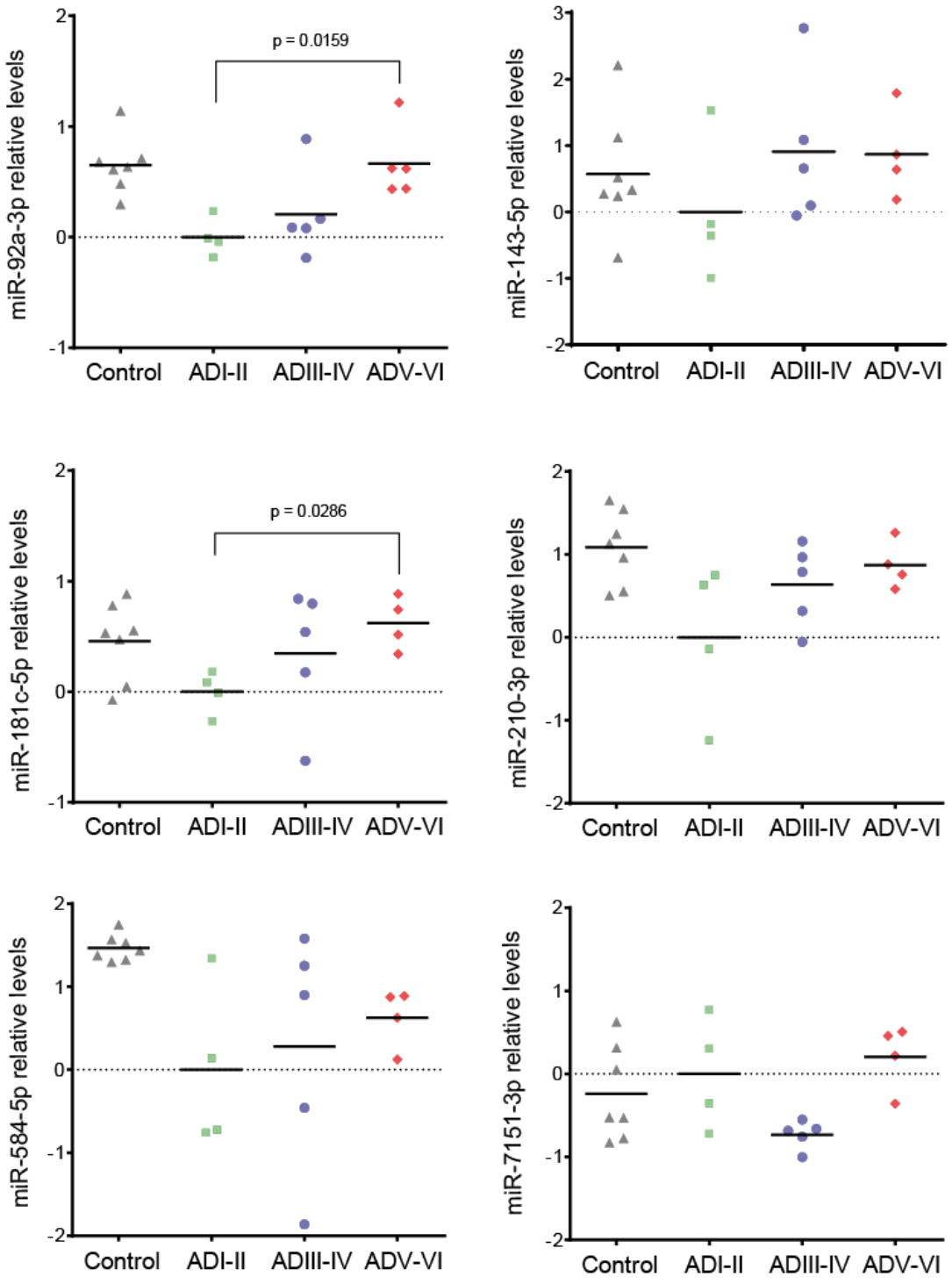

Figure 22: Human entorhinal cortex miRNAs levels. Selected miRNAs levels were analyzed at different Braak stages of AD pathology and were compared with cognitively normal subjects. Log2 transformed data were normalized versus the geometric mean of U18 and U48 levels. p-value <0.05 was considered significant.

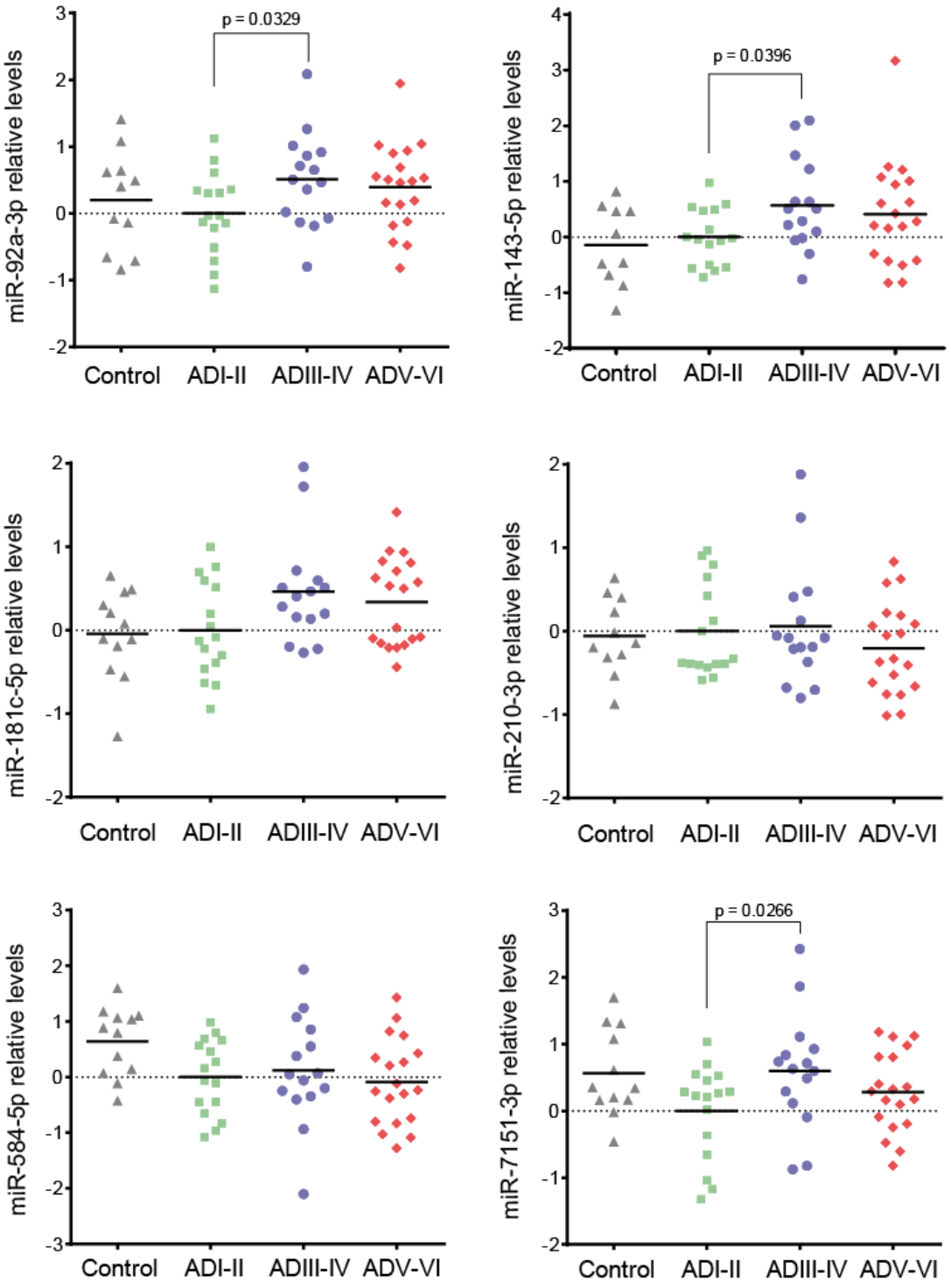

Figure 23: Human hippocampus miRNAs levels. Selected miRNAs levels were analyzed at different Braak stages of AD pathology and were compared with cognitively normal subjects. Log2 transformed data were normalized versus the geometric mean of U18 and U48 levels. p-value <0.05 was considered significant.

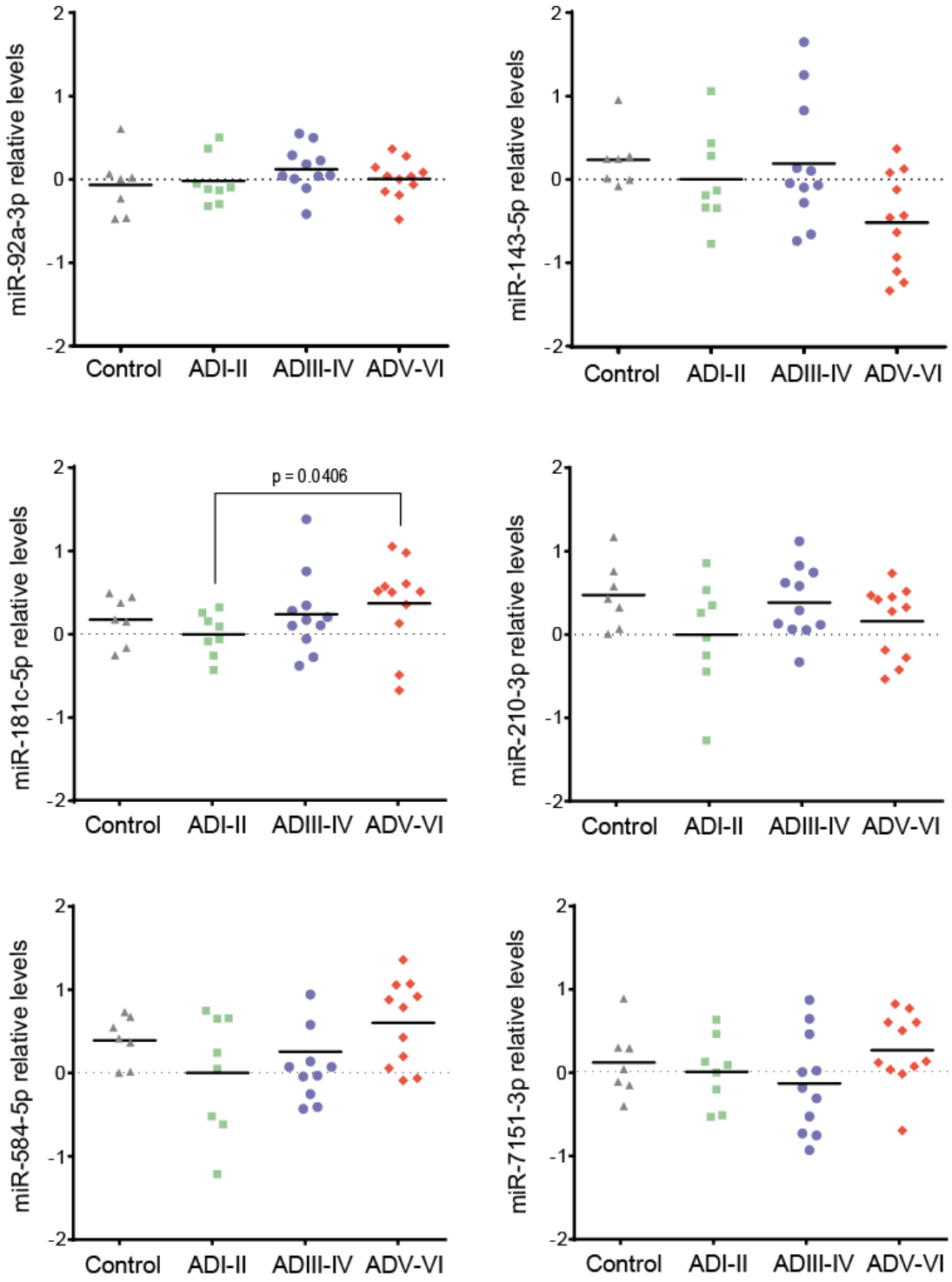

Figure 24: Human prefrontal cortex miRNAs levels. Selected miRNAs levels were analyzed at different Braak stages of AD pathology and were compared with cognitively normal subjects. Log2 transformed data were normalized versus the geometric mean of U18 and U48 levels. p-value <0.05 was considered significant.

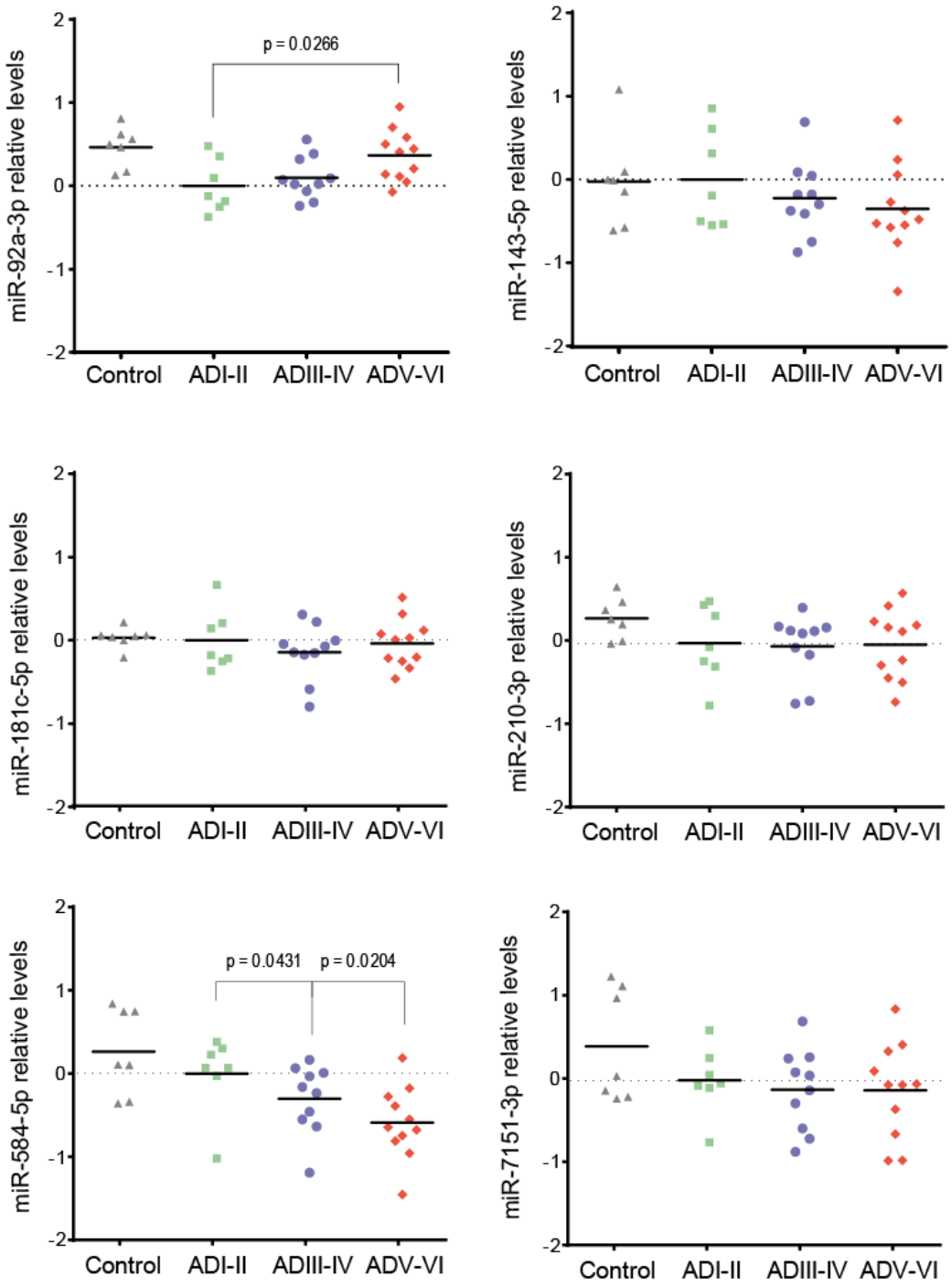

Figure 25: Human cerebellum miRNAs levels. Selected miRNAs levels were analyzed at different Braak stages of AD pathology and were compared with cognitively normal subjects. Log2 transformed data were normalized versus the geometric mean of U18 and U48 levels. p-value <0.05 was considered significant.

3. Microarray validation: human plasma

The analysis of different brain areas can give us valuable information on the alteration of miRNAs during the pathology. However, from a more clinical point of view, it is of vital importance the identification of deregulated miRNAs in circulating fluids as possible biomarkers of the disease. In this regard, we evaluate the levels of the previously selected miRNAs in plasma samples from MCI and AD subjects.

miR-191 and miR-484 were selected for miRNA levels normalization in plasma

As indicated in the methods (page 50), miR-191 and miR-484 were identified as the most stable genes through all plasma samples (Figure 26) and their geometric mean was used to normalize miRNA levels of all plasma samples analyzed.

Figure 26: miR-191 and miR-484 were selected for miRNAs levels normalization in all plasma samples according to NormFinder algorithm results.

miR-92a-3p, miR-181c-5p and miR-210-3p are increased in plasma levels from MCI and AD patients.

To assess the levels of circulating miRNAs during AD progression, plasma samples from 14 controls, 26 MCI/probable early AD and 56 sporadic AD subjects (see

Methods, Table1, page 37) were analyzed. From the 6 miRNAs selected, only 4 were successfully detected. RT-qPCR analysis revealed an increase in miR-92a-3p, miR-181c-5p and miR-210-3p levels in AD subjects (Figure 27-A to C; miR-92a-3p: $p = 0.0221$, log2 fold change = 0.5218; miR-181c-5p: $p = 0.0012$, log2 fold change = 0.6656; miR-210-3p: $p = 0.0003$, log2 fold change = 0.6036). Significant increase in the levels of miR-181c-5p ($P = 0.0002$, log2 fold change = 0.8036) and miR-210-3p ($p = 0.0138$, log2 fold change = 0.4936) were also observed in MCI plasma samples whereas an increasing trend was detected for miR-92a-3p (p = 0.0798, log2 fold change = 0.5485). By contrast no changes were observed in miR-584-5p levels in MCI or AD subjects (Figure 27-D).

miRNAs changes in plasma together with results obtained from the analysis of AD brains are complementary and promising: recapitulating, miR-92a-3p levels show an increasing trend in entorhinal cortex, which becomes significant in hippocampus and also in cerebellum at late AD stages. In plasma samples, miR-92a-3p levels trend to increase in MCI subjects, but reach significance in AD patients. On the other hand, miR-181c-5p levels were found significantly increased in entorhinal cortex, while an increasing trend was found in hippocampus. Increase in plasma levels of miR-181c-5p from MCI and maintained in AD patients, strengthens data obtained from tissue analysis. In the case of miR-210-3p, brain results did not indicate big affection, despite a not significant increase in entorhinal cortex. However, a clear increase from early MCI stages, and its raising with AD progression, also brings miR-210-3p to the spotlight.

In the case of miR-584-5p, neither tissue results were consistent (since a no significant increase was detected in prefrontal cortex levels while a significant decrease was observed in cerebellum) nor were plasma alterations observed.

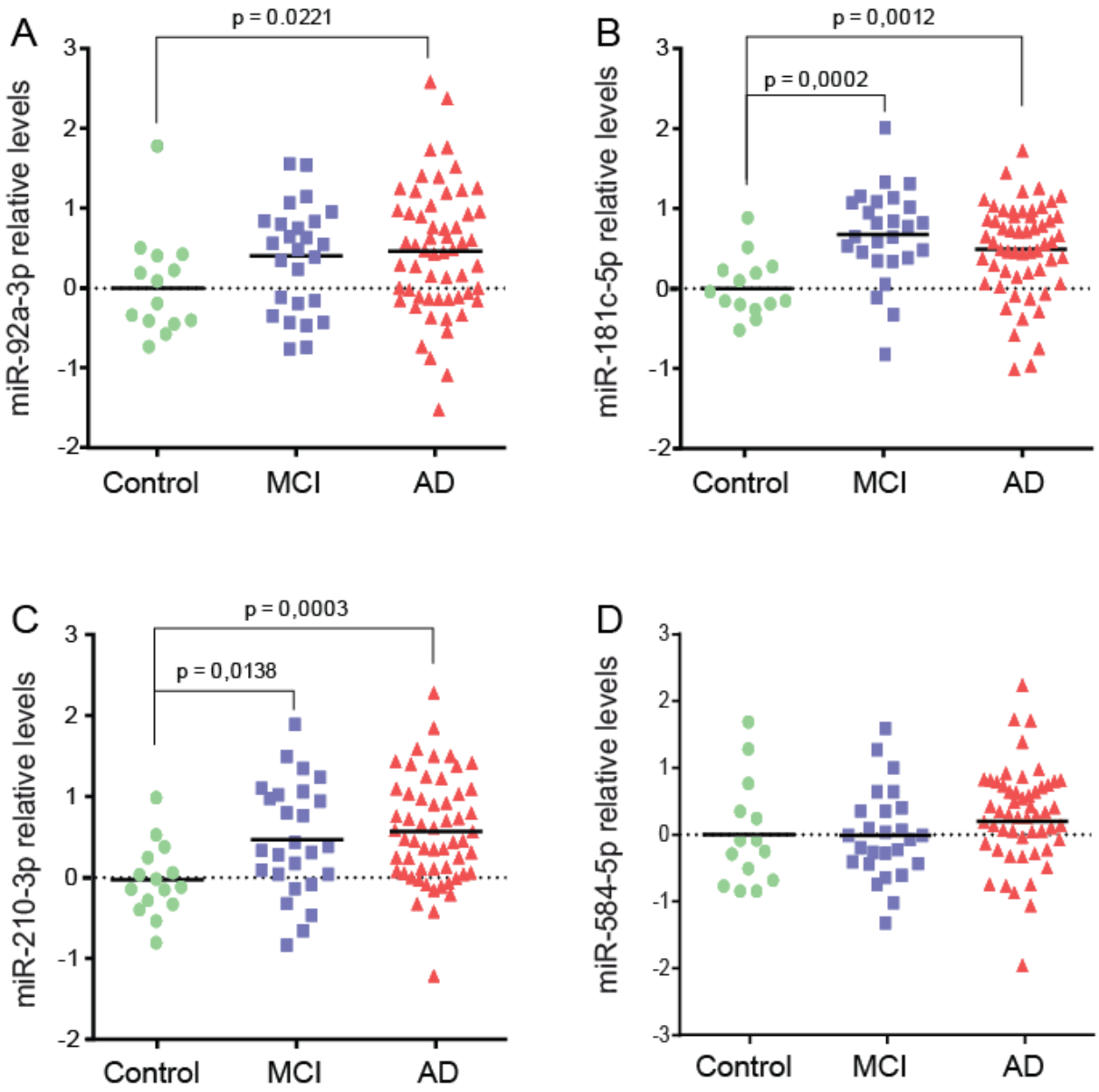

Figure 27: Circulating miRNA levels at different stages of AD pathology compared with cognitively normal subjects. Log2 transformed data were normalized versus the geometric mean of miR-191-5p and miR-484 levels. p-value <0.05 was considered significant.

Subsequently, we decided to continue the analysis on circulating miRNAs with the 3 candidates that we have detected deregulated in MCI and AD cases: miR-92a-3p, miR-181c-5p and miR-210-3p.

In order to determine the diagnostic potential of these miRNAs in differentiating early and late pathological stages of AD from healthy controls, a ROC curve analysis was performed to obtain the area under the curve (AUC). AUC is a value of accuracy of a classifier in distinguishing between two groups (healthy/ diseased).

Sensitivity (probability of detecting a diseased subject correctly) and specificity (probability of identifying correctly a negative case) are inherent characteristics of the curve, so that, each point of the ROC curve is a sensitivity/specificity pair corresponding to a particular threshold or cut-off[276,277].

As a result of the analysis, we obtained the AUC for comparing miR-92a-3p, miR-181c-5p and miR-210-3p levels between control and MCI subjects were: 0.673, 0.843 and 0.736 respectively (Figure 28). Sensitivity, specificity, p-values and cut-off values are shown in Table 11. On the other hand, when healthy controls were compared to AD subjects, AUC values were 0.697 for miR-92-3p, 0.773 for miR-181c-5p and 0.799 for miR-210-3p. Sensitivity, specificity, p-values and cut-off values for are shown in Table 12.

Since it is difficult that a single miRNA could differentiate pathological stages across a variable population, the identification of a molecular signature composed of several miRNAs that, as a whole, could be able to distinguish pathological stages is a more accurate approximation. Thereby, identified miRNAs could be used as a molecular signature combining their predictive power to provide a better diagnostic value for both, MCI and AD differentiation. When MCI cases are compared to control subjects, an AUC value of 0.893, 84.6% of sensitivity and 85.71% of specificity were obtained (Figure 29-A, Table 11). This molecular miRNA signature provide an AUC value of 0.855, a 92.86% of sensitivity and a 71.43% of specificity when AD was compared to controls (Figure 29-B, Table 12).

Several evidence suggest that AD may be more prevalent in females than in males[278,279], therefore, eventual sex-dependent differences in the diagnostic potential of the examined miRNAs were also evaluated (Figure 29 C to F). We found slightly better diagnostic values for males when distinguishing MCI from healthy controls (Table 11): a) the AUC values were 0.821 and 0.957; b) 87.5% and 100% sensitivity; c) 71.43% and 85.71% specificity for female and male, respectively. On the other hand, the values obtained when comparing AD with control subjects also indicated a better diagnostic specificity and a lower sensitivity for males: a) the AUC values for females and males are 0.815 and 0.938; b) 90.24% and 75% sensitivity; c) 71.43 % and 100 % specificity for females and males, respectively. All AUC,

sensitivity, specificity, significance and cut-off values for individual and signature miRNAs, are listed in table 11 for MCI and in table 12 for AD cases.

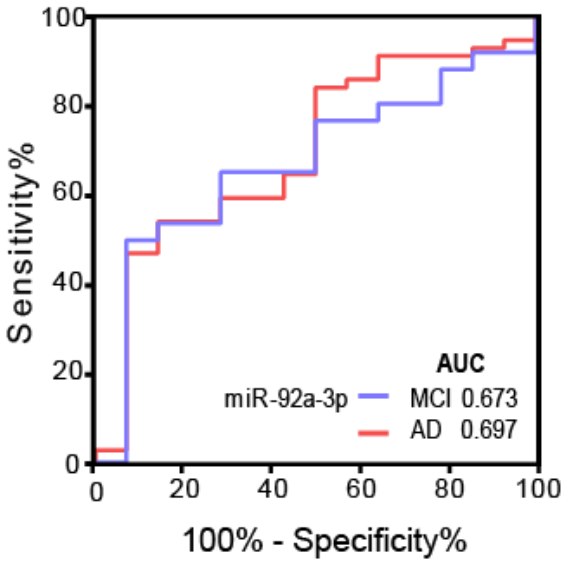

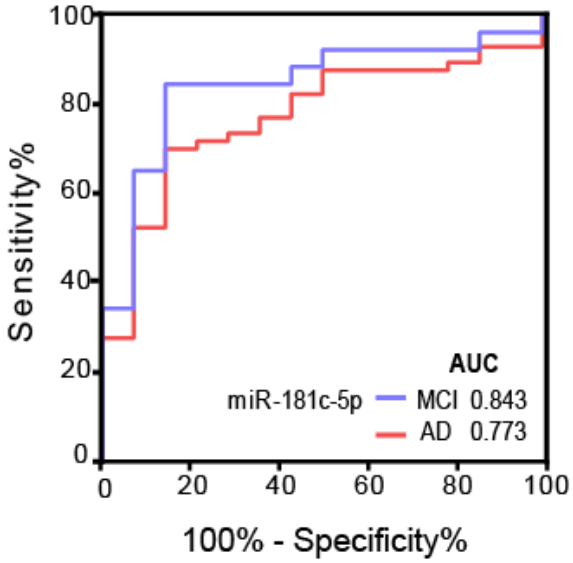

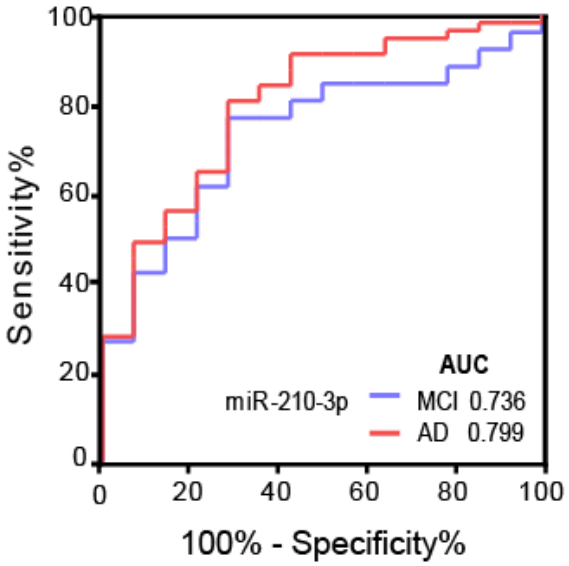

Figure 28. Receiver operating characteristic (ROC) curve analysis for circulating miRNA levels was performed to distinguish MCI (blue) and AD (red) cases from healthy controls. Area under the curve (AUC) is shown for each miRNA and stage. For detailed information on ROC curve analysis results go to table x.

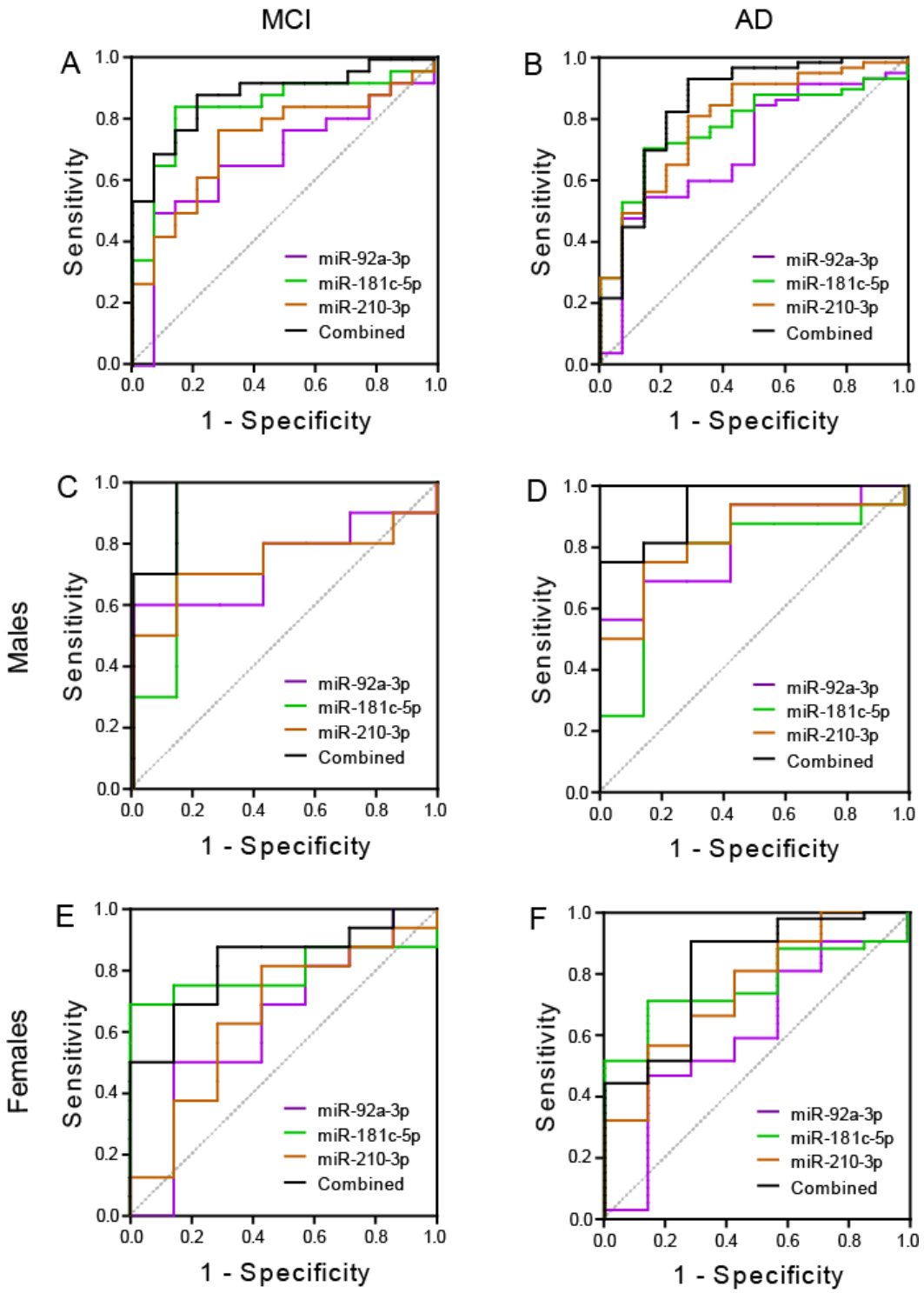

Figure 29: miRNAs were combined to reach the best predictive value. ROC curve analysis for MCI (A) and AD cases (B) are shown. Values for males (C-D) and femlaes (E-F) are represented separately.

miRNA/signature	AUC	Sensitivity	Specificity	Youden index J	P-value
miR-92-3p	0.673	50.00%	92.86%	0.4286	0.0563
miR-181c-5p	0.843	84.62%	85.71%	0.7033	<0.0001
miR-210-3p	0.736	76.92%	71.43%	0.4835	0.0038
miR-92-3p/miR-210-3p	0.731	73.08%	71.43%	0.4451	0.0050
miR-92-3p/miR-181c-5p	0.838	84.62%	78.57%	0.6319	<0.0001
miR-181c-5p/miR-210-3p	0.865	88.46%	78.57%	0.6703	<0.0001
miR-92-3p/miR-181c-5p/miR-210-3p	0.893	84.62%	85.71%	0.7033	<0.0001
Females	0.821	87.50%	71.43%	0.5893	0.0005
Males	0.957	100.00%	85.71%	0.8571	<0.0001

Table 11: Individual and signature miRNAs performance characteristics in predicting MCI stage. Signature miRNAs performance characteristics in females and males. AUC: area under the curve.

miRNA/signature	AUC	Sensitivity	Specificity	Youden index J	P-value
miR-92-3p	0.697	47.37%	92.86%	0.4023	0.0124
miR-181c-5p	0.773	70,18%	85.71%	0.5589	<0.0001
miR-210-3p	0.799	80.70%	71.43%	0.5213	<0.0001
miR-92-3p/miR-210-3p	0.807	87.72%	64.29%	0.5201	<0.0001
miR-92-3p/miR-181c-5p	0.787	84.21%	71.43%	0.5564	0.0001
miR-181c-5p/miR-210-3p	0.853	84.21%	78.57%	0.6278	<0.0001
miR-92-3p/miR-181c-5p/miR-210-3p	0.855	92.86%	71.43%	0.6441	<0.0001
Females	0.815	90.24%	71.43%	0.6167	0.0009
Males	0.938	75.00%	100.0%	0.7500	<0.0001

Table 12: Individual and signature miRNAs performance characteristics in predicting AD stage. Signature miRNAs performance characteristics in females and males. AUC: area under the curve.

Majority of evaluated MCI patients progress to AD

Since it is expected that a large number of MCI cases developed AD over time[280], an up-dated diagnosis of MCI cases included in this study was requested to evaluate disease progression (Table 13). From 26 cases first diagnosed as MCI, 82% progressed to some kind of dementia, 12% remained stable with some cognitive affection, and a 6% were finally diagnosed as cognitively normal subjects. Among those patients who progress to dementia, 85% of cases did it to AD, 7% of cases to frontotemporal dementia (FTD) and other 7% of cases progressed to vascular dementia (VD) (Figure 30).

Patients	First diagnosis	Date	Last diagnosis	Date
P1	MCI	2006	AD	2017
P2	MCI	2007	AD	2011
P3	MCI	2006	AD	2017
P4	MCI	2006	NCI	2007
P5	MCI	2005	AD	2008
P6	MCI	2007	NFU	
P7	MCI	2006	FTD	2011
P8	MCI	2006	NCI	2010
P9	MCI	2006	AD	2017
P10	MCI	2005	NFU	
P11	MCI	2007	VD	2014
P12	MCI	2006	NFU	
P13	MCI	2007	AD	2017
P14	MCI	2006	MCI	2017
P15	MCI	2006	AD	2013
P16	MCI	2006	NFU	
P17	MCI	2005	NFU	
P18	MCI	2005	MCI	2008
P19	MCI	2005	AD	2017
P20	MCI	2005	NFU	
P21	MCI	2005	AD	2006
P22	MCI	2006	NCI	2007
P23	MCI	2005	NFU	
P24	MCI	2006	AD	2017
P25	MCI	2006	AD	2007
P26	MCI	2006	AD	2006

Table 13: Follow-up of MCI patients. P: patient. MCI: mild cognitive impairment. AD: Alzheimer's disease. FTD: frontotemporal dementia. VD: vascular dementia. NCI: no cognitive impairment. NFU: no follow-up available.

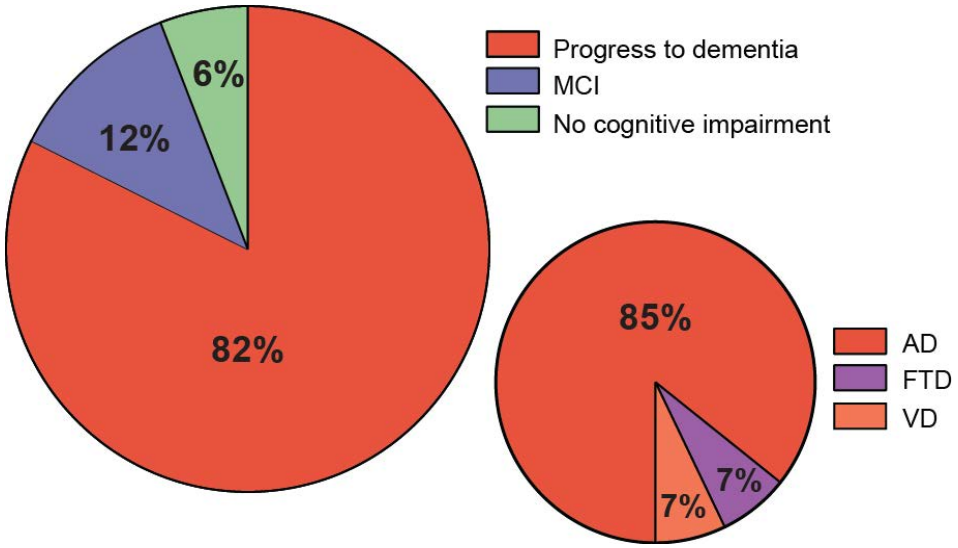

Figure 30: Follow-up of MCI patients. 82% of patients diagnosed as MCI, progressed to some kind of dementia (85% progress to AD, 7% to FTD and other 7% to VD). MCI: mild cognitive impairment. AD: Alzheimer's disease. FTD: frontotemporal dementia. VD: vascular dementia.

Expression levels of miR-92a-3p, miR-181c-5p and miR-210-3p are not affected in FTD patients

In order to determine if the changes observed miR-92a-3p, miR-181c-5p and miR-210-3p were specific of MCI and AD subjects, we decided to analyze plasma samples from a cohort of FTD patients (n = 51; Methods, Table 1, page 37). The results (Figure 31) indicate that the expression levels of none of the above mentioned miRNAs changed in FTD, confirming that the deregulation detected in MCI and AD patients is not present in other dementia related subjects.

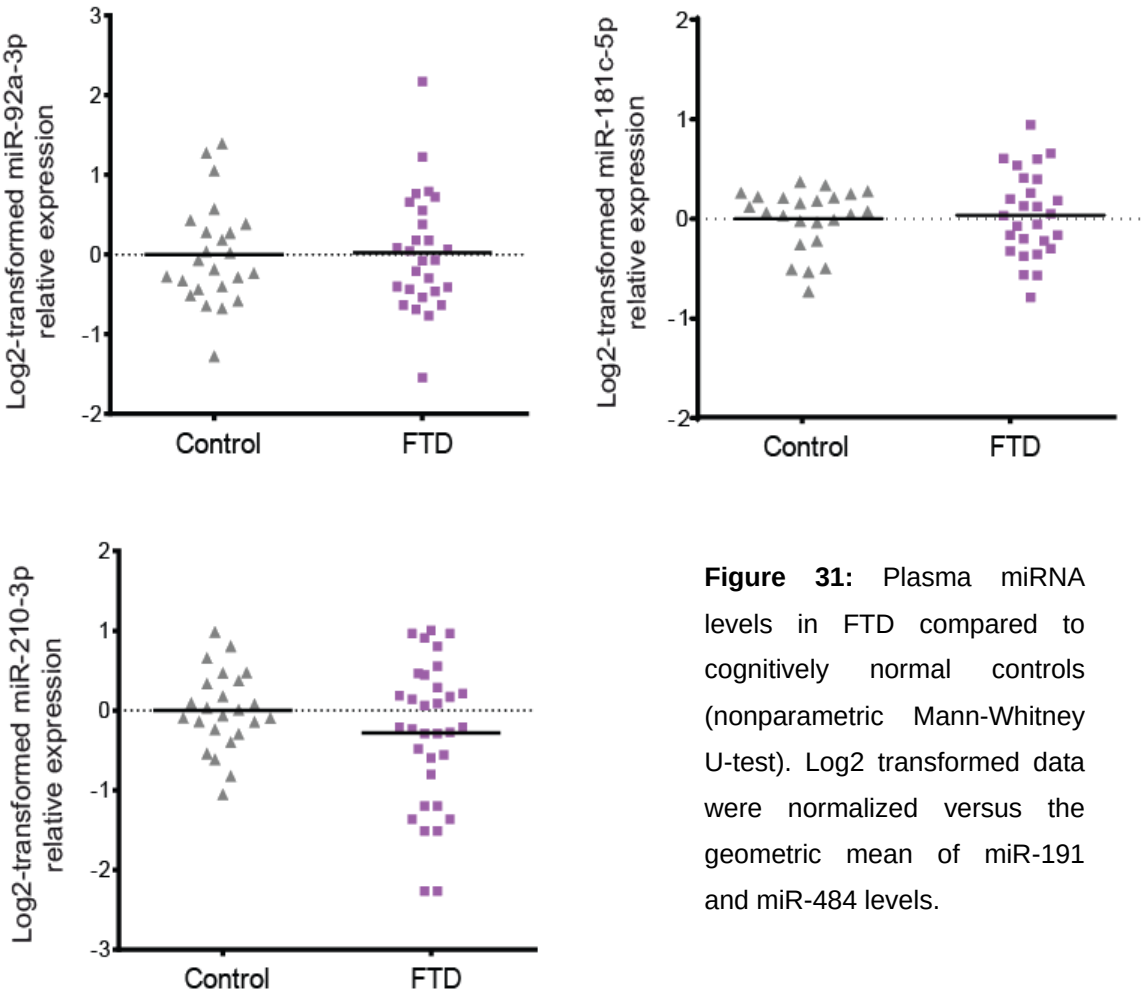

Figure 31: Plasma miRNA levels in FTD compared to cognitively normal controls (nonparametric Mann-Whitney U-test). Log2 transformed data were normalized versus the geometric mean of miR-191 and miR-484 levels.

4. Study of selected-miRNAs protein target levels during AD progression

Synaptic dysfunction is an early event on AD development that is due, in part, to the alteration of glutamatergic transmission. In this regard, changes in AMPA receptors levels and alteration of its trafficking and anchoring in the cell surface are of great importance to understand the synaptic phase of the pathology. In order to evaluate the possible role of selected miRNAs regulating synaptic proteins related to AD development, several of its potential targets levels were assessed by western blot. Among the list of synaptic-validated targets shown in Table 10, we selected GluA1, neuronal pentraxin 1 (NP1) and neuronal pentraxin receptor (NPR), as validated targets of miR-92a-3p, miR-181c-5p and miR-210-3p. In addition, although BDNF and Bcl-2 were no predicted by miRWalk database, they were experimentally validated as miR-181c-5p and miR-210-3p targets and included in western blot analysis.

Bcl-2 levels increase in entorhinal cortex during AD progression

Western blot analysis revealed a significant increase in Bcl-2 levels in late AD stages (Figure 32; $p = 0.0159$). Additionally, NP1 and NPR exhibited a decreasing trend ($p = 0.063$ and 0.111, respectively) although statistical significance was no reached. GluA1, AKAP and BDNF levels were no altered in early nor late AD compared no cognitively normal subjects.

Total GluA1 levels decrease in hippocampus during AD progression

Total GluA1 levels decreased in ADIII-IV hippocampus compared to cognitively normal subjects (Figure 33; $p = 0.0059$). Other tested targets did not show changes, despite a slight no significant decrease in ADIII-IV in NPR, NP1 and BDNF levels ($p = 0.178$, 0.228 and 0.187, respectively). AKAP and Bcl-2 levels remain stable across compared groups.

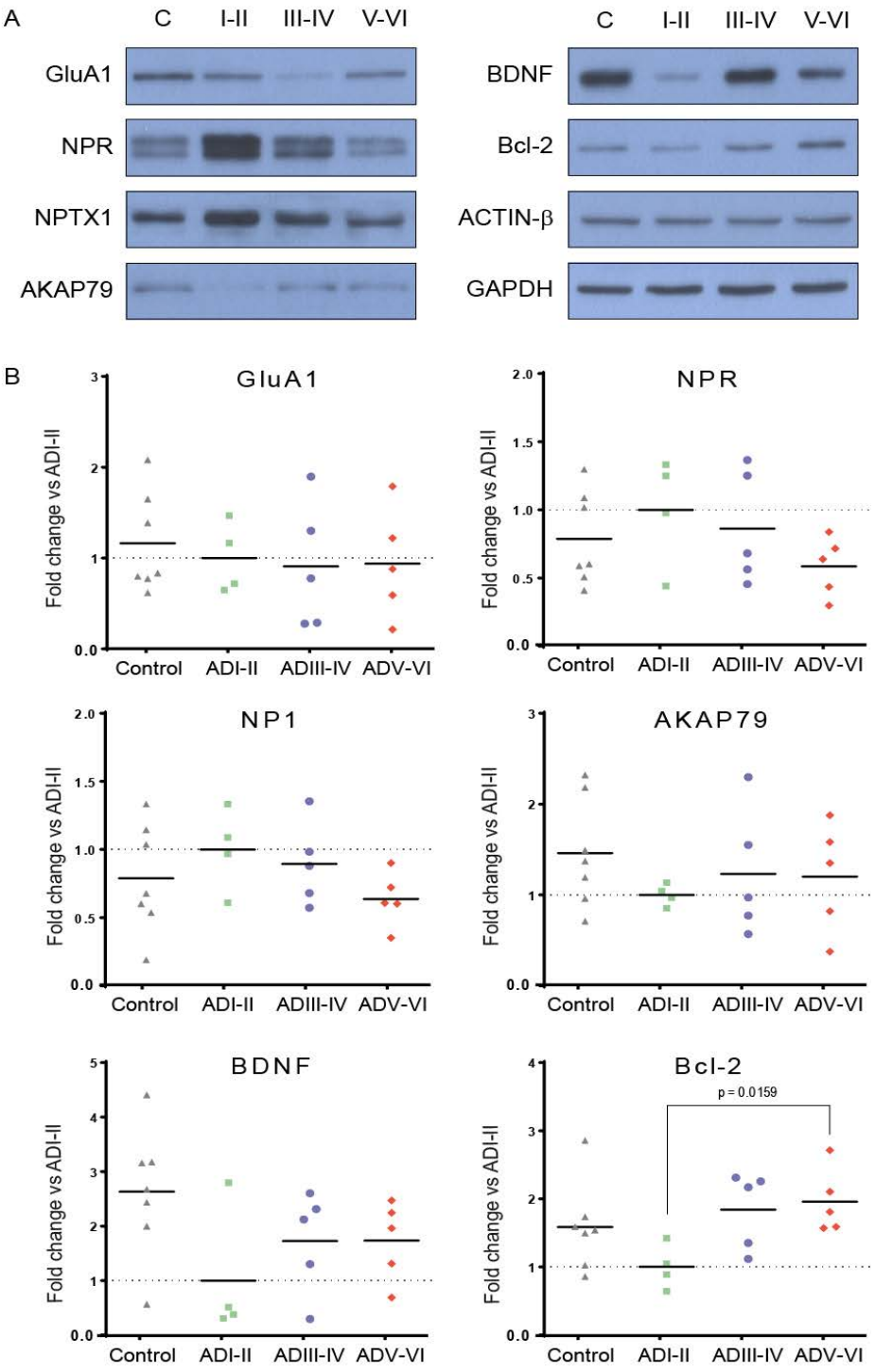

Figure 32: Human entorhinal cortex target proteins levels. Representative western blot analysis for each AD stage (A). Densitometry values for all samples analyzed (B). Protein levels were normalized vs GAPDH or ACTIN-β levels and fold change expressed is compared to ADI-II normal cognitively group.

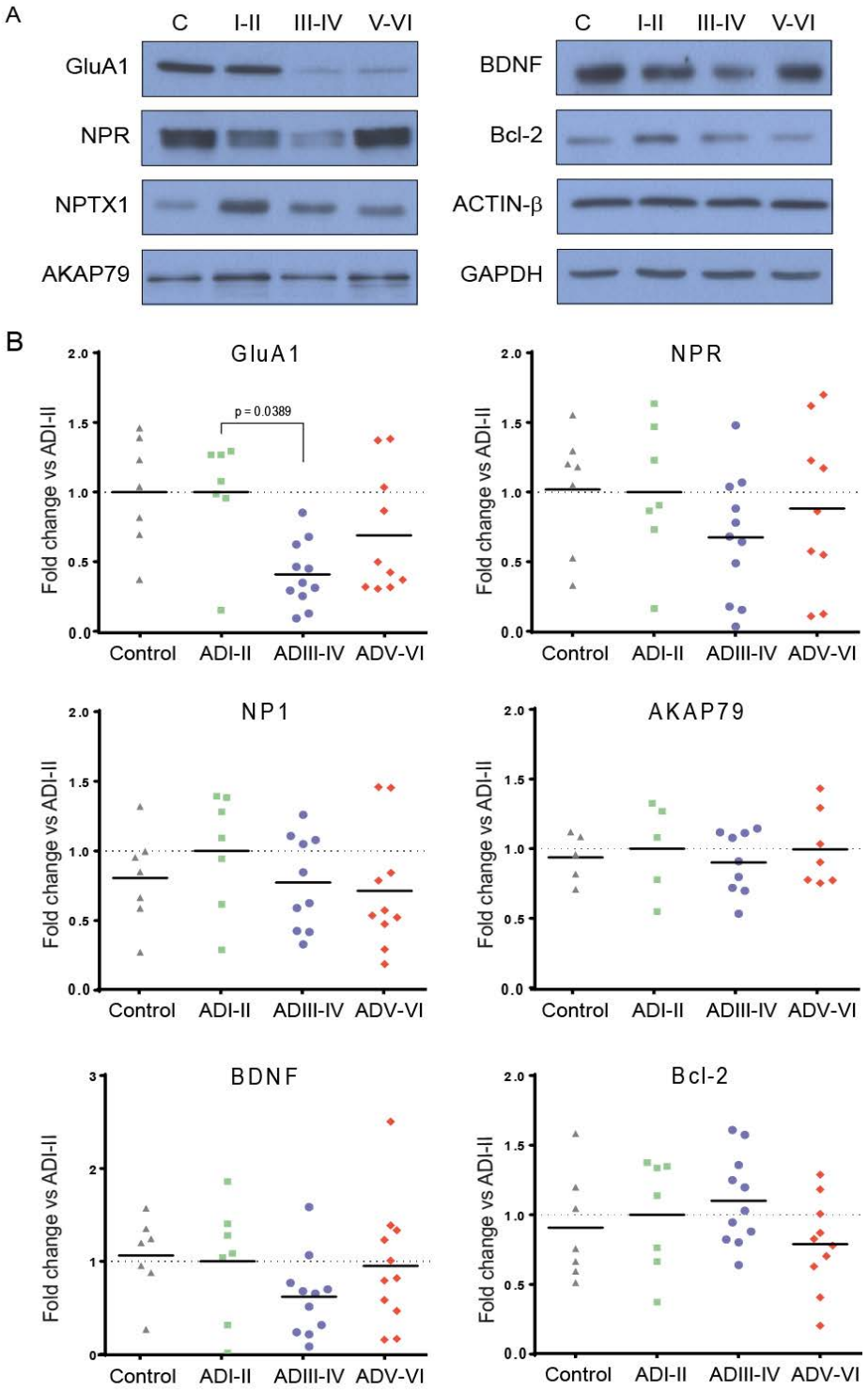

Figure 33: Human hippocampus target proteins levels. Representative western blot analysis for each AD stage (A). Densitometry values for all samples analyzed (B). Protein levels were normalized vs GAPDH or ACTIN-β levels and fold change expressed is compared to ADI-II normal cognitively group.

5. Study of selected miRNA levels *in vitro*

In order to gain knowledge in the eventual role that the described changes in these miRNAs could have during early phases of AD, we decided to test if the observed changes in human samples were also present in experimental models. Experimental models may allow us to unravel some of the molecular mechanisms implicated and the key players involved, which could hopefully lead to the identification of possible therapeutic targets.

oAβ exposure increase miR-181c-5p and miR-210-3p levels

In order to mimic *in vitro* described early oAβ effect on synaptic transmission, and to assess if alterations in selected miRNA are observed in this conditions, hippocampal neurons (17-19 DIV) were treated with 5 μM oAβ at different incubation times. miR-92a-3p, miR-181c-5p and miR-210-3p levels were evaluated. After 3 hours exposure to oAβ, we observed a significant increase in miR-181c-5p and miR-210-3p levels (Figure 34; p = 0.038, fold change: 1.47 and p = 0.002, fold change: 2.26, respectively). Although miRNA levels remain over the basal at longer exposure time, these differences are not significant and are gradually recovered. miR-92a-3p levels were no affected by the treatment.

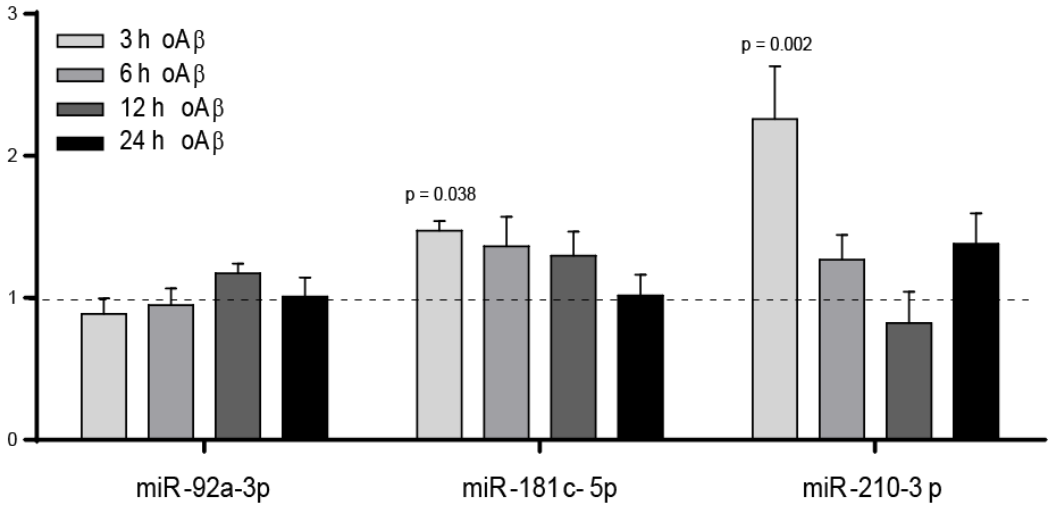

Figure 34: oAβ exposure increase miR-181c-5p and miR-210-3p levels. miRNA levels were increase after 3 hours 5μM oAβ treatment in hippocampal neurons. Levels were compared to basal condition control and normalized to U6 snRNA. ANOVA p = value is shown for significant changes.

miR-92a-3p levels are no significantly affected by neuronal activity induction with bicuculline

As activity-dependent miRNA regulation has been described for several groups[281–283], we wanted to assess if some of our candidates response to neuronal activity induction. Therefore, hippocampal cultured neurons were treated with 50 µM bicuculline (a GABAA receptor antagonist used to increase neuronal activity in vitro[284]) and miRNA levels were evaluated by qPCR. No significant changes were observed after treatment, however a decreasing trend was observed for miR-92a-3p levels (Figure 35-A). GriA1 (Figure 35-B) mRNA levels were increased after 2 hours bicuculline exposure, however no changes were observed in GluA1 protein levels (Figure 35-C).

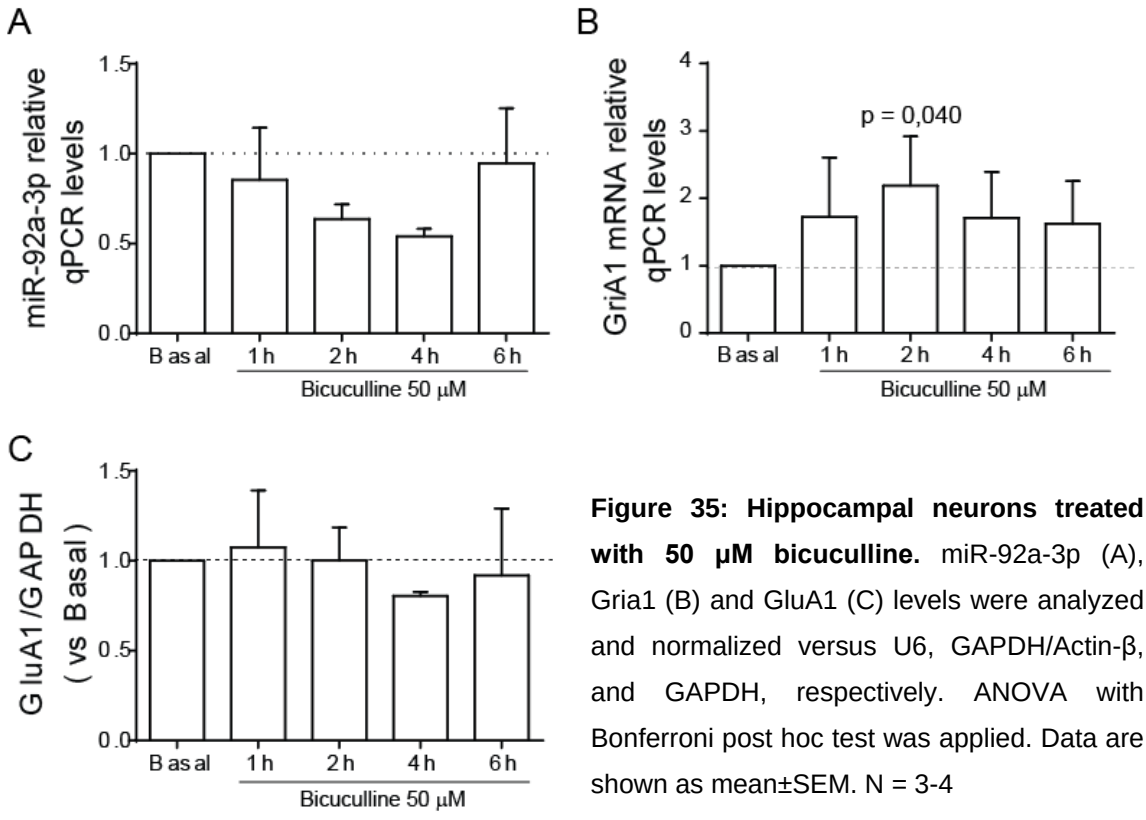

Figure 35: Hippocampal neurons treated with 50 µM bicuculline. miR-92a-3p (A), Gria1 (B) and GluA1 (C) levels were analyzed and normalized versus U6, GAPDH/Actin-β, and GAPDH, respectively. ANOVA with Bonferroni post hoc test was applied. Data are shown as mean±SEM. N = 3-4

While an increase in GluA1 protein levels would be more consistent with a decrease in miR-92a-3p levels, the results are not clear, and above all it is not possible to relate both elements yet.

miRNAs silencing and overexpression

In order to assess if miRNA levels regulate the expression of target proteins in our experimental model, we designed the tools to overexpress and downregulate them, so that allow us to collect more solid data on the mechanisms that could be altered due to miRNA levels changes.

RTqPCR is not an adequate mechanism to evaluate success of shmiRNA generation, even a false overexpression could be detected as is unlikely that miRNA degradation occurs. Consequently, we used a pmiRGLO vector (for details see methods, page 52) where we inserted miRNA target sequences to check shmiRNA activity. This approach permits testing miRNA binding through luciferase activity determination. Plasmids were tested in HEK 293T cells, as neurons were visible negatively affected by transfection (pmiRGLO vector) plus infection (pLVTHM-shmiRNAs). After HEK 293T cells infection with pLVTHM-shmiR, luciferase assay revealed a slight non-significant decrease in miRNA binding to target sequence, observed as an increase in luciferase activity for sh-miR210 (Figure 36).

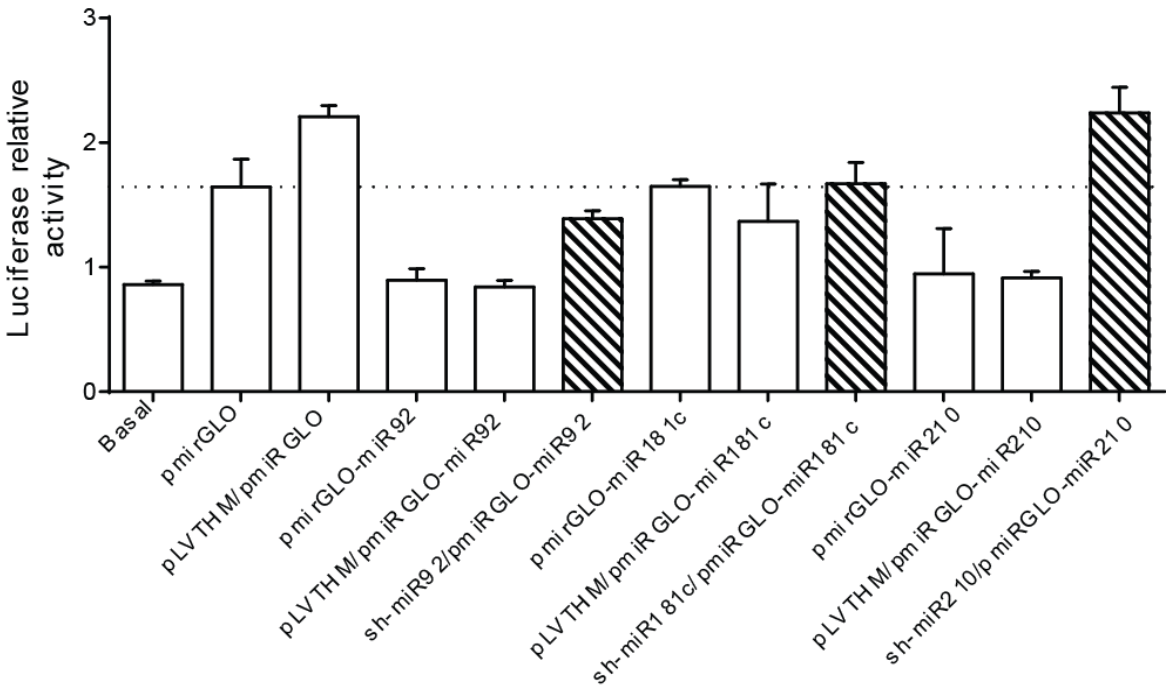

Figure 36: Luciferase assay was used to determine sh-miRNA efficiency. HEK 293T cells were infected with pLVTHM-miRs and transfected 48 hours later with pmiRGLO vector and infected with shmiRNA sequences. Luciferase activity normalized versus renilla levels and represented versus pmiRGLO empty vector.

On the other hand, lentiviral particles overexpressing selected miRNAs were also generated (see methods, page 49). miRNA overexpression was confirmed by qPCR in HEK cells and hippocampal neurons (Figure 37).

Figure 37: plenti-miR-181c vector was tested in hippocampal cultures and HEK 293T cells. Overexpression of miR-181c-5p was confirmed by RTqPCR. N = 2.

Although luciferase assay results suggest no efficient silencing, we wanted to evaluate miRNA target protein levels in hippocampal cultures after miRNA silencing an also after overexpressing selected miRNAs through lentiviral infection.

GluA1 protein levels were evaluated by western blot after shmiRNA (Figure 38-A) and plenti-overexpressing plasmids (Figure 38-B) were transduced into hippocampal primary neurons. No significant changes were observed in any case, and high variability between experiments was detected.

GluA1 after overexpressing miR-181c was also checked under cLTP conditions, induced by Forskolin/rolipram (see methods page 42). As commented before, miRNA differential activity-dependent regulation has been described in several occasions, thus, although results did not reach significance, the opposite effect suggested in GluA1 levels under LTP conditions could to be remarked (Figure 38-B).

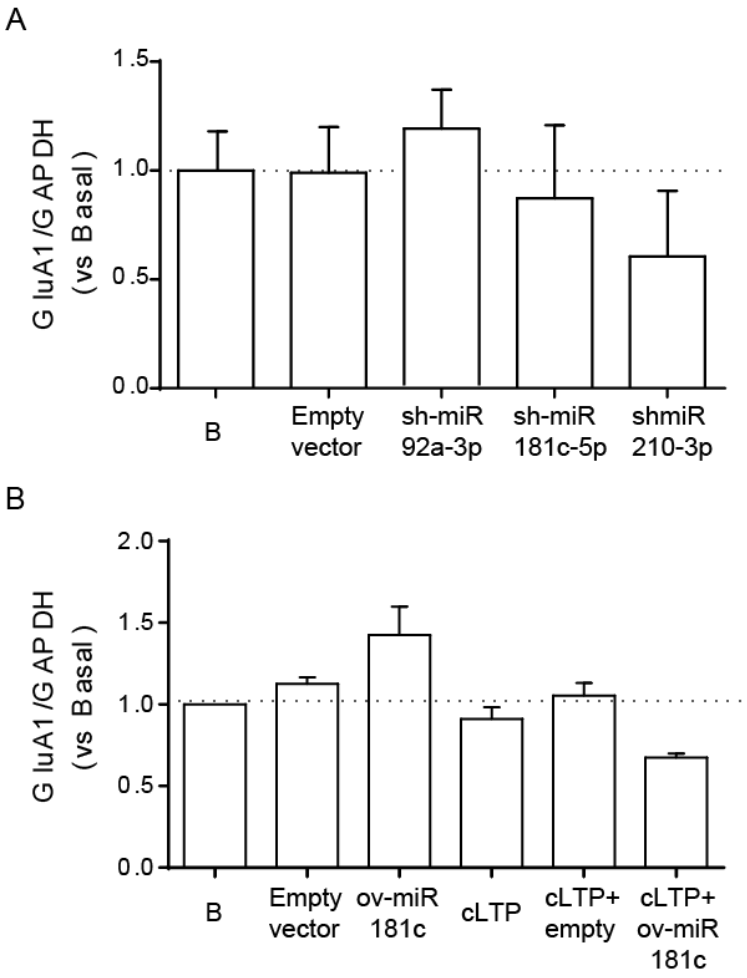

Figure 38: Possible effect of miR-92a-3p, miR-181c-5p and miR-210-3p silencing (A) and miR-181c overexpression (B) under basal and cLTP conditions was tested on GluA1 protein levels. Results from 2-3 independet experiments were normalized to GAPDH levels. Data is shown as mean ± SEM.

Although we did not observed any change in GluA1 levels after shmiRNA nor plenti-miRNA infection we wanted to assess the effect of silencing miRNAs in presence of oAβ. As a regulation dependent on neuronal activity has been reported for several miRNAs, we consider interesting to test if blocking oAβ-dependent increase of miR-181c-5p and miR-210-3p (see previous results, page 96, Figure 34), target proteins levels could be affected. To test this, and considering that shmiRNA silencing efficiency could not be successfully confirmed, we tried another silencing method using miRCURY *LNA*™ power inhibitors (Exiqon). These are antisense oligonucleotides that bind with perfect

sequence complementary to the selected miRNA, preventing it from hybridizing with its normal cellular target. Silencing our selected miRNAs with a more efficient system may allow us to observed protein miRNA target alterations as reporterted[187].

Potential targets are not affected by oAβ nor LNA miRNA inhibitors

In order to reduce miRNA levels for next experiments, miRCURY LNA™ specific miRNA inhibitors were added to the culture media. To evaluate the possible miRNAs regulation on target protein levels, permeable inhibitors were added to hippocampal cultures media at 15 DIV and left for 72 hours. In addition, to assess the relation between the oAβ-dependent increase in the levels of miR-181c-5p and miR-210-3p, with possible changes in their targets levels, neurons were next exposed to oAβ for 3 hours as previously. Protein levels were evaluated by western blot (Figure 39).

Neither LNA inhibitors nor oAβ treatment affected tested protein levels, at least at the evaluated time.

Although target levels were no affected by oAβ treatment nor by LNA inhibitors in basal conditions, it is interesting to remark that NP1 levels seem to be affected by LNA inhibitor for miR-210-3p in the presence of oAβ. The same trend is observed in GluA1 and NPR levels, although in these cases decrease in protein levels did not reach significance. More experiments are needed but a role of miR-210-3p-3p in specific neuronal activity conditions, such as when oAβ is present in the media, could be suggested.

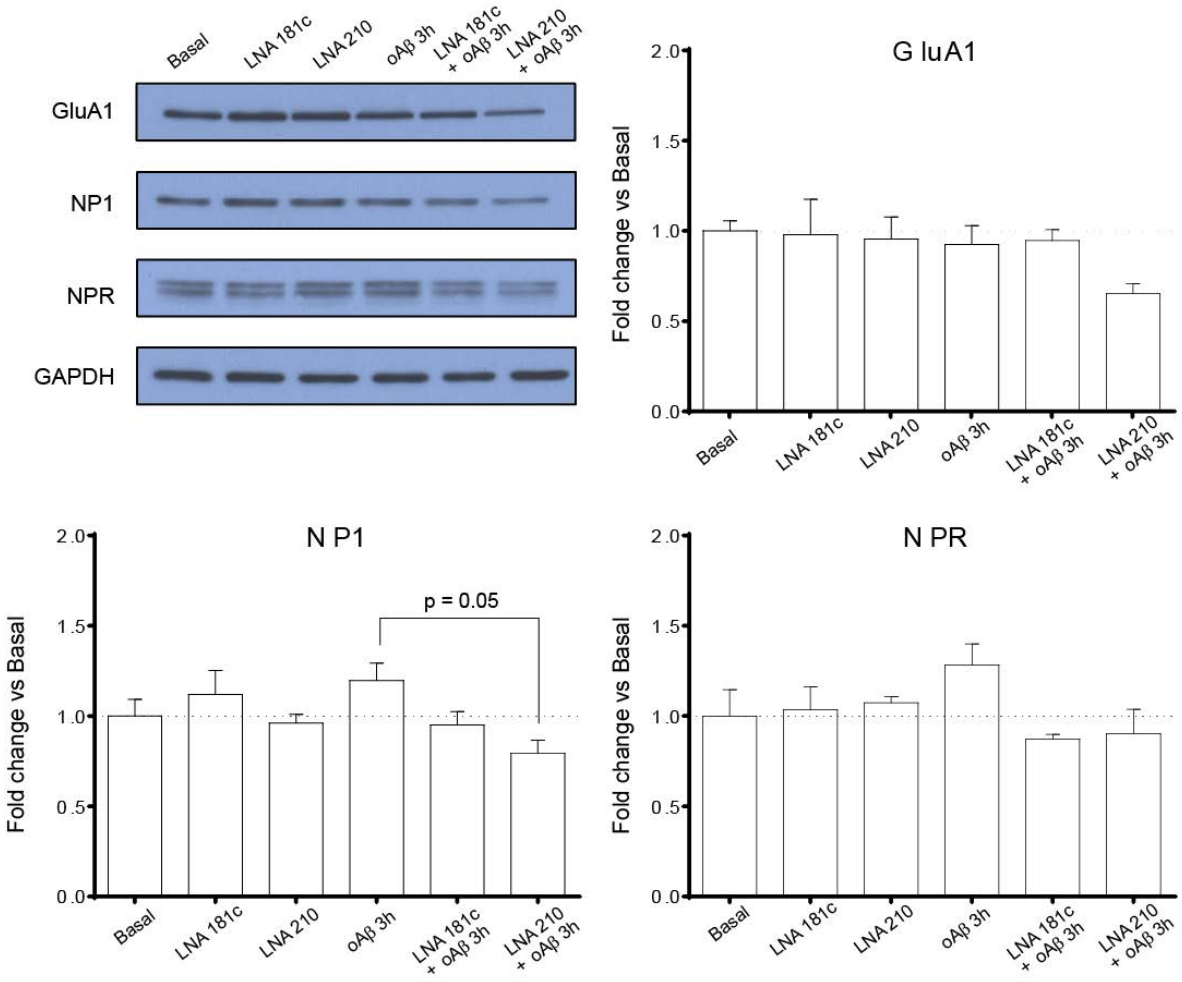

Figure 39: oAβ exposure nor LNA inhibitors affect miRNA target protein levels. Hippocampal neurons were exposed for 3 hours to 5μM oAβ treatment or/and LNA inhibitors for specific miRNAs were added to culture media. Levels were compared to basal condition control and normalized to GAPDH levels. Data are shown as mean ± SEM of 3-4 independent experiments. ANOVA p-value is shown for significant changes.

LNA miRNA inhibitors efficiency in not clear

Since the effect of LNA inhibitors was not the expected, we decided to confirm its function using a luciferase assay where miR-181c-5p and miR-210-3p target sequences were inserted in the 3'-UTR region after the coding sequence for firefly luciferase gene (*luc2*). As expected, increased firefly luciferase expression was observed when LNA-210 was added to the culture media. This increase is explained by the release of endogenous miR-210-3p-mRNA binding due to miRNA sequestration into miRNA-LNA stable duplexes (Figure 40). However, luciferase

assay must be fine-tune to obtain clearer results on LNA effect, since expected decreased in luciferase activity after the pmiRGLO-miRNA sequence transfection (without LNA addition) when compared to pmiRGLO empty vector, was not observed. This would be the confirmation that endogenous miR-210-3p is binding to the cloned miRNA target sequence.

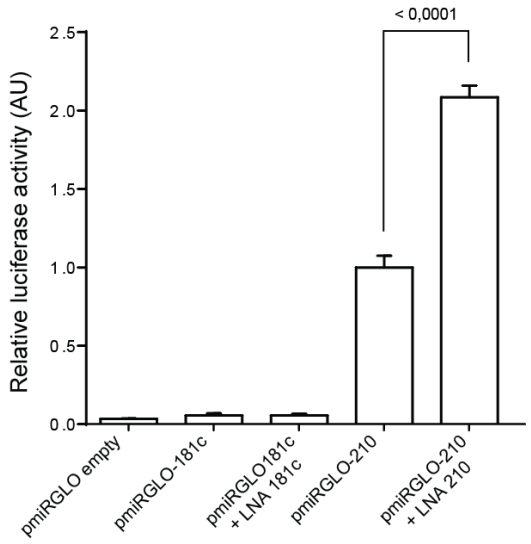

Figure 40: Luciferase assay for LNA efficiency testing. Although the expected increase when LNA-210 is added to the culture media was observed; miR-210-3p-dependent luciferase activity decrease was not observed.

6. Study of selected miRNA levels in the hippocampus of $APP_{Sw,Ind}$ transgenic mice

We considered interesting to find an animal model of AD with which it would be possible to correlate the changes previously observed in human samples. An animal model that allow us to study and monitor how those miRNs are affected by the progress of the pathology would be a valuable tool both, from the point of view of the search for biomarkers and, specially, for the study of the molecular mechanisms in which the deregulation of those miRNAs may be involved. In this context, and taking into account our interest in the initial stages of the pathology, where synaptic dysfunction starts to be evident, we used $APP_{Sw,Ind}$ mice. This model is characterized by early synaptic deficits associated with increased accumulation of oAβ. Interestingly, spatial learning deficits in Morris water maze (MWM) at 6 month of age were described in correlation with a decrease in surface GluA1[127,253].

APPSw,Ind mice MWM

Animals were subjected to the MWM spatial learning memory test as described[285]. A significant increase in the latency time to reach the platform was found in 9 month $APP_{Sw,Ind}$ mice, and a trend in the same way was observed in 6 month $APP_{Sw,Ind}$ animals after 2 days of training. Both groups recovered normal levels of lantecy after 5 days of training, indicating that the deficit exhibit at 2 days is some way compensated. Moreover, the time in the platform quadrant trend to decrease in 9 month $APP_{Sw,Ind}$ animals, suggesting a worse memory retention associated to disease progression (Figure 40).

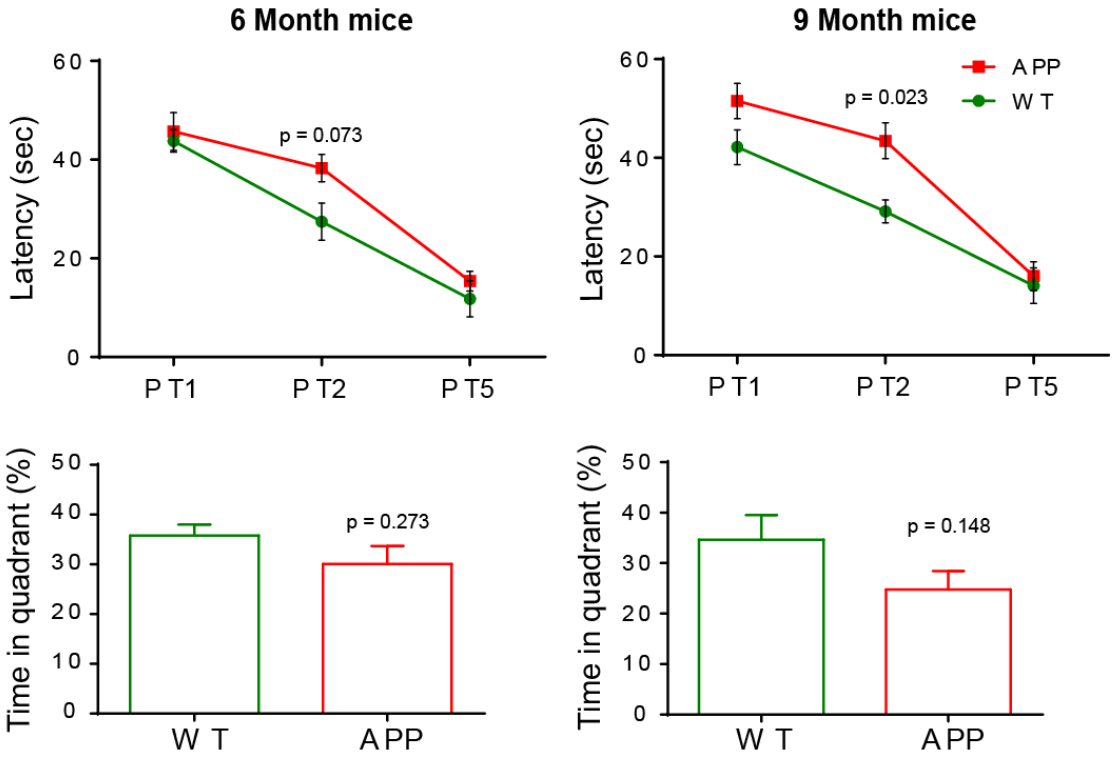

Figure 41: WT and $APP_{Sw,Ind}$ mice were training in the spatial learning MWM. Latency time to reach the platform was increased in APP animals after 2 days of training, and recovered after 5 days. Time in quadrant exhbit a decreasing tren in 9 month animals.

miRNA levels were no affected by genotype in hippocampus of APP mice

To assess a possible relation between candidate miRNAs levels and early deficits observed in $APP_{Sw,Ind}$ mice, we analyzed the levels of miR-92a-3p, miR-181c-5p and miR-210-3p in mice hippocampus.

Levels of selected miRNAs were evaluated in hippocampus of $APP_{Sw,Ind}$ mice and compared to WT naïve mice. Animals were euthanized at 2 an 5 days after MWM training to evaluate short memory acquisition. Learning effect on miRNA levels were checked after 2 days and 5 days of MWM training in WT and $APP_{Sw,Ind}$ mice. Two-way ANOVA revealed neither genotype effect nor interaction between genotype and training. On the other hand significant decrease of miR-92a-3p, miR-181c-5p and miR-210-3p levels after 2 days of training were found in 6 month mice (Figure 42; p-values for WT trained mice compared to WT naïve: miR-92a-39; p = 0.08, log2 fold

change = -0.62, miR-181c-5p; p = 0.012, log2 fold change = -0.91 and miR-210-3p; p = 0.027, log2 fold change = -0.92). In addition, a significant increase was found in miR-181c-5p levels in WT 9 month mice after 5 days of training (p = 0.0081)

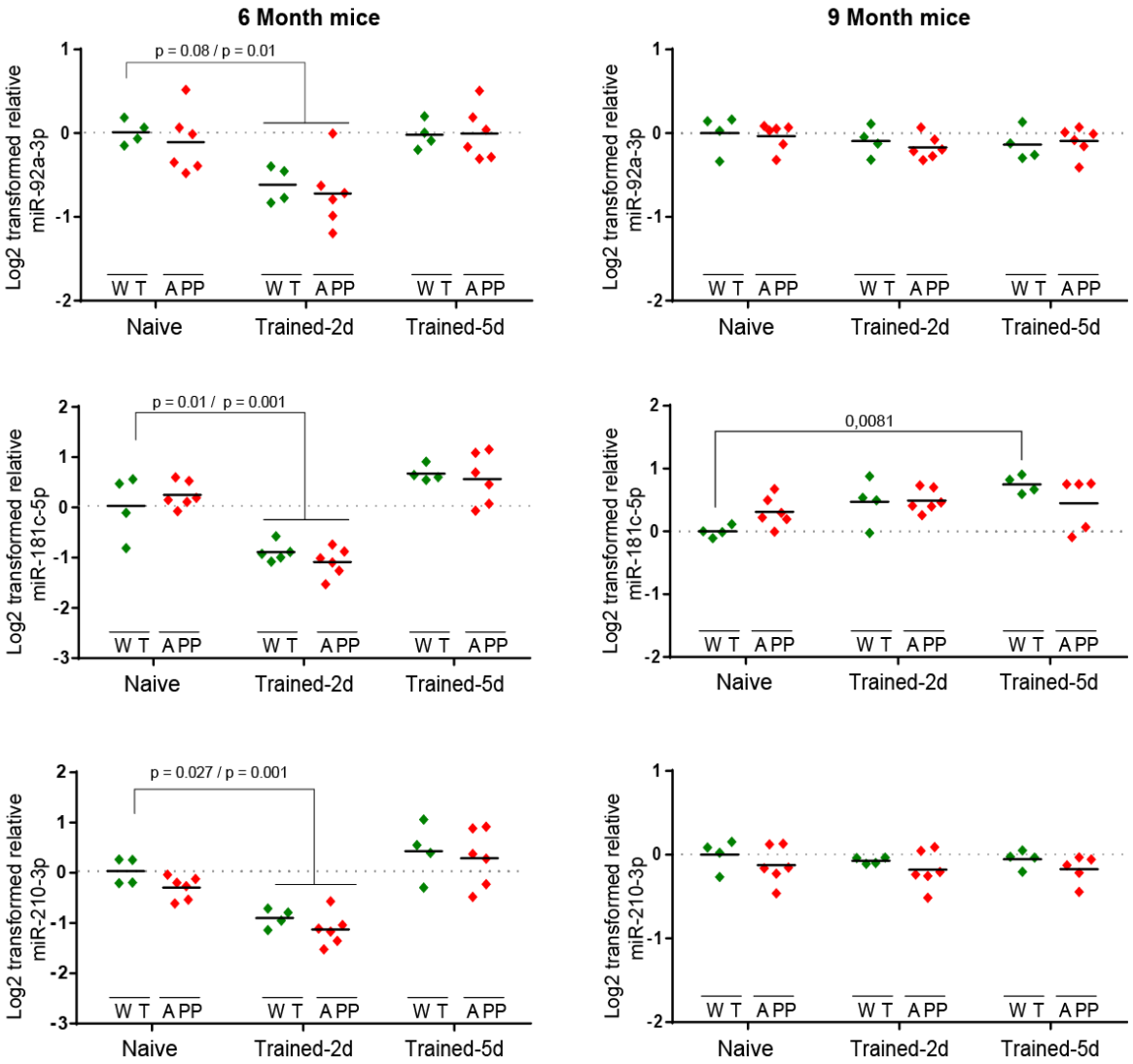

Figure 42: Hippocampus miRNA levels in WT and APP mice at different ages with or without being tested at the MWM. Two-way ANOVA showed no differences in miRNA levels due to genotype. All groups were compared to WT naïve mice. miRNA levels were normalized to sno234 levels and log2 transformed.

Once discarded an effect of genotype on miRNA levels regulation, we evaluated the effect of age and training on miRNA levels. Two-way ANOVA showed an effect of both, training and age, and also an interaction between factors. As shown before

significant decrease of miR-92a-3p, miR-181c-5p and miR-210-3p levels after 2 days of training is exhibited in the hippocampus of 6 month WT mice. Moreover, 9-month mice miRNA levels are significantly different from 6-month mice after 2 days of training ($p < 0.0001$ in the three cases).

DISCUSSION

On the urgent need of AD early diagnosis

The early detection of Alzheimer's disease is an urgent need in order to improve currently available therapies. Many efforts are made every day to expand the knowledge of the mechanisms that underlie the disease, especially in its early stages, to improve potential therapies, to find new therapeutic targets and to identify biomarkers that allow an early and affordable diagnosis.

Many therapies against AD have failed[286] and one of the causes could that when dementia is evident, the disease has been developing silently for 10 to 20 years. Neuronal death present in advanced stages of the disease could make the success of any therapy unlikely[287].

Increasing the chances of potential therapies of being effective is a compelling reason to accelerate the development of tools that allow the identification of patients in asymptomatic and early AD stages. In this regard, miRNAs are promising molecules to be used as biomarkers of the disease[288,289] not only because they could be detected in biological samples, such as plasma and CSF, but also because they are regulatory molecules directly related to disease progression mechanisms.

While miRNA research in other diseases, such as cancer[199,202,203,290], has been active for several years, miRNAs is a relatively new area for research in AD. However, the urgency of developing new methods for early AD detection, which meet the requirements of being non-invasive, affordable and that allow screening analysis, places miRNAs in an important place in biomarker research field. This need is highlighted by the appearance of research grants programs specifically aimed at for the identification of biomarkers that could be detectable in biological fluids, such as the peripheral biomarkers program of the Alzheimer's drug discovery foundation (ADDF)[291].

Our approach, aims an limitations

In this thesis we wanted to address the knowledge of miRNAs as biomarkers and also as regulatory molecules that can exert a local role on the synaptic dysfunction observed during the first stages of the disease. We were interested in including several approaches with the purpose of achieving a complete view of the role of the

selected miRNAs during AD pathology. Consequently, we include miRNAs analysis of different brain areas and plasma of subjects at different AD stages, and also animal experimental models that could allow us to mimic early stages of the disease, were synaptic dysfunction starts to be evident.

Human brain samples were used to identify altered miRNAs during the first stages of the disease starting from a microarray analysis of postmortem brain tissue of different AD stages. We have also included several candidates reported in the literature to target synaptic-related proteins, although they had not been identified in the initial screening.

It is worth considering that the variability in the microarray analysis could be high due to the number of samples analyzed (3 per area per pathological group) thus differences in validation step after screening could be expected[292]. It is also important to contemplate that the number of selected miRNAs for validation was small, and in the same way that some miRNAs did not come up validated; other interesting candidates could have been ignored. For instance, some miRNAs that were downregulated in the microarray analysis showed no significant changes (such as miR-584-5p) or were upregulated (miR-7151-3p) in the RTqPCR validation step. On the other hand, miR-143-5p levels were found increased in hippocampus, in agreement with microarray results and also with other studies performed in temporal cortex[271].

Our approach also included the detection of these candidates in plasma, which has been complicated at some points, since the best methods of detection in circulating fluids are not well stablished yet. Moreover, miRNA expression could be different between brain and circulating fluids, so that miRNAs enriched in brain could be hardly detectable in circulating fluids. We tested different protocols for the detection of miRNAs in plasma, as the detection is more difficult due to lower expression and less amount of sample available compared to detection in tissue. In this regard, we tried including an extra pre-amplification step[293] to improve RTqPCR, however no significant improvement was achieved. We also test droplet digital PCR (ddPCR) technology, especially attractive since requires lower sample volume (very limited in plasma miRNA extraction) and provides an absolute quantificaction (copies/µl) that bypass reference genes and normalization issues. However, the set-up for this

technique required a lot of time and was discarded in favor of the optimization of the available time. Finally, we chose TaqMan™ Advanced method, that allow all miRNAs amplification from a unique cDNA template, permitting sample volume optimization (see methods, page 47). Even so we could not successfully detect some miRNAs in plasma, as miR-143-5p, which seemed a promising candidate after tissue analysis.

The identification of a synaptic-related miRNA deregulated in early AD an its first validation as a potential biomarker for early AD diagnosis, is the major and more exciting goal of this thesis, however, our scientific interest and the possible description of new therapeutic targets make also valuable the understanding of the mechanisms that relate these miRNAs to AD pathology. Consequently, experimental models were also included to evaluate selected miRNAs changes at the molecular level, trying to elucidate their role during early stages of AD, specifically through regulation of synaptic-targets.

About the difficulties to compare studies and the need for standardization

Our data point out certain differences with results reported by other groups, but this is not unexpected. Since miRNAs research is a relatively new field, standardization of protocols is still needed. Methodological issues, such as selected methods for RNA isolation, amplification, quantification, normalization and statistical analysis[231,259,271,288]**,** can largely explain the differences found in literature on the expression of miRNAs in AD. In the case of circulating fluids analysis, even the anticoagulant used could produce differential expression of miRNAs**.**

Moreover, data that a priori may seem contradictory, when analyzed more carefully could be explained by samples variability affected by the geographic origin, age, sex, ethnic and social differences of the patients; the source of miRNAs obtaining (tissue, CSF, plasma or serum); postmortem delay until the sample is obtained or the pathological stage and composition of compared groups (sometimes AD refers only to late stages, other studies put early and late stages together, while other studies, as ours, compare stages separately).

A delicate and controversial issue that deserves a special mention is the selection of endogenous controls. Since their levels can affect the entire analysis, introducing variability between studies, is important to test potential reference genes every time across analyzed samples. Remarkably, endogenous controls that are useful for some pathological condition, are not for others, and also can be different between tissue and circulating fluids. Interestingly, miR-16, quite used as a reference gene in plasma, has been shown to be affected during AD pathology[292]. Using more than one reference gene is a more accurate method of miRNA normalization.

Nevertheless, many factors affect the variability between studies, as we can deduct from a study that using miR-191 as a control (one of which we have used to normalize plasma data), find a downregulation of miR-181c in MCI and AD patients, opposite to our results. To consider, they isolated miRNAs from serum and each group analyzed included seven subjects [245,275].

The aforementioned issues are supported by a large amount of bibliography, [259,271,288,294–296] which calls for a standardization of protocols without further delay. Protocols standardization will allow not only a reduction of variability and a better interpretation of obtained results, but also will enable the possibility of data comparison across time and studies**.**

On the tested experimental models

To establish the relationship of the selected miRNAs with the pathology development, and particularly with the regulatory role on synaptic targets during early stages of the disease, we used two experimental models that resulted in different observations.

On the one hand, the in vitro model testing the effect of oAβ on hippocampal mature neurons (17-19 DIV) yielded results that seem to correspond better with what we see in human brain and plasma, showing an increase on miR-181c-5p and miR-210-3p levels after 3 hours of oAβ treatment (Results; page 89, Figure 34) Rapid changes in miRNA levels in response to Aβ peptides were also observed by Schonrock and collaborators[273,297], although they observed a decrease in miR-181c

levels, among others. In other study, 7PA2 cell-secreted human soluble Aβ induced miR-210 upregulation, while no changes were observed neither with synthetic soluble Aβ nor with synthetic fibrilar insoluble forms[298].The rapid regulation of miRNA levels in presence of oAβ might support a role of these miRNAs during early stages of the pathology, regulating expression of proteins related to early events of the amyloid cascade. On the other hand it is known that increased calcium signaling produces neuronal hyperactivity in the first place and a depression of neuronal activity next, thus, it is possible that rapid miRNA alteration could play a role in these processes.

On the other hand, the $APP_{Sw,Ind}$ mouse model did not show any kind of variation in selected miRNAs linked to genotype (Figure 42) , raising interrogations about the validity of this model for the study of alterations on miRNAs levels during early AD development. However, other groups have reported successful results in experimental AD mice models. For instance, miR-181c decrease has been reported in seven month APP23 mouse[273,297] (initial plaque deposition and cognitive deficits), while no significant changes were found in 2 (no plaques and asymptomatic) and 13 month mice (established AD pathology)[299]. Interestingly, differences between males and females were also described in WT mice, with significant lower miR-181c levels in females[275].

Since we did not detect significant changes in the levels of the selected miRNAs related to genotype, it is plausible to think that $APP_{Sw,Ind}$ mice could not be the better animal model for studying miRNA expression in early AD. It could be interesting to test miRNA levels in animals with earlier affection, to compare with the results obtained with short oAβ treatments in hippocampal cultures. Unfortunately, as changes in miRNA levels related to genotype were not detected, we could not link miRNA result with the changes observed in the latency to reach the platform after two days of training in the $APP_{Sw,Ind}$ mice. This impairment correspond to the changes described in AMPA receptor phosphorylation, known to be linked to cognitive processes[127,253]. .

As genotype did not affect the levels of miRNAs in this model, we put it aside to focus on the in vitro model, where we observed changes in miRNA levels due to oAβ presence.

Although the animal model used has proven to be of great value in other types of studies[127,253,300], it might be necessary to think about other models when looking for answers in the field of miRNAs. For instance, studies performed using transgenic mouse models overexpressing[301] or downregulating[209] specific miRNAs, have demonstrated to be useful tools to assess miRNA effects on particular target proteins, behavior or phenotype. On the other hand, well stablished changes in human AD brains, such as miR-132 downregulation[205,209], could not be replicated by some tested AD animal models, including Tg2576, TgCRND8, PSAPP, 3xTg-AD and 5xFAD[302]. These data suggest that although AD animal models have been used successfully in several studies, there is a need to develop new animal models that allow a better understanding of miRNA roles in pathology and also the progress of preclinical and pharmacological studies directed to miRNAs as therapeutic targets.

Tools for target validation as an approach to potential miRNA based-therapies

The use of miRNAs as therapeutic targets is a promising field but is also a challenge. miRNA-based therapies result attractive considering the capacity of miRNAs to target multiple genes involved in different pathways, but this feature is also a handicap since the same miRNA could regulate protein expression levels with opposite function or targets involved in other pathologies[290].

Some miRNAs-based therapeutics are at preclinical stages for cancer, glioblastoma and vascular disease, among others[199,303], indicating the route that research in AD must follow to get effective therapies based on miRNAs. These therapeutic approaches include modulation of miRNA activity, restoring or inhibition of miRNA function (through miRNA mimics or sponges and antisense oligonucleotides, respectively)[304]. For instance, miR-34 could be the first miRNA mimics to reach the clinic targeting cancer related pathways[305].

In our hands, target validation was not a trivial issue. Our first approximation to miRNA silencing with a designed short hairpin (sh) complementary molecule, did not achieve the expected miRNA levels deregulation. Now, we can consider this failed

as knowledge on miRNA biogenesis and function. An efficient sh-miRNA design requires multiple binding sites for the targeted miRNA to achieve silencing [158,159]. Moreover, miRNA processing could follow several pathways making it difficult to predict the final result of the sh-miRNA produced. For these reasons several groups choose LNA inhibitors as a mechanism to decrease miRNA levels. However, set-up for LNA silencing should be done for each miRNA separately, testing different concentrations, selecting the most appropriate in vitro day for its application and the time that each LNA must act to produce an effect. All this testing requires a large amount of material that was unfortunately limited in our case, and therefore we have not been able to fine-tune it in the best possible way.

Consequently, although a discreet deregulation of NP1 levels is observed in presence of oAβ together with LNA210 inhibitor, we cannot come to a conclusion on the effect of our selected miRNAs on predicted targets related to AMPA receptor function and trafficking. It would be interesting to attempt again the application of LNA technology in order to evaluate the direct effect of our candidate miRNAs on different targets involved in synaptic plasticity processes.

AD brain analysis and possible miRNA-targets deregulation

The study of four different brain areas during AD progression give us a global vision of selected miRNAs levels during pathology progression. As the number of included miRNAs had to be limited, we decided to focus on those which could also be directly involved in the synaptic stage of the pathology. Some interesting results were obtained, although some were contradictory with previous reports. For instance, we detected an increase in miR-181c-5p levels in entorhinal cortex, prefrontal cortex and an increasing trend in hippocampus, whereas other groups have reported its downregulation in frontal cortices and hippocampus of sporadic AD patients[273,275,306]. Differences could be due to many causes that have been already commented, including the studied brain areas or the number of samples analyzed.

Moreover, we found a significant decrease in hippocampal GluA1 levels in early AD subjects (ADIII-IV) that goes in line with human gene expression reported data[307,308]

and with AD mice model results[253]. However, it should also be considered that although in mid-late stages of AD, GluA1 and other synaptic genes were described to be downregulated, it has been also described that during initial asymptomatic stages, there is greater neuronal excitability, increased calcium signaling and upregulation of genes linked to synaptic plasticity[309]. In this way, when using ADI-II subjects as controls, even if these are cognitively normal, it cannot be overlooked the fact that possibly early pathological processes are already taking place. The reduction that we observed in GluA1 and the decreasing trend observed in NPR, NP1 and BDNF levels in hippocampus of early ADIII-IV could also be related to a compensation of those early events, where a large number of deregulated proteins eventually lead to synaptic dysfunction.

The challenge of finding clear data in such a complex disorder is especially bigger in initial stages, where the line between health and disease is so difficult to draw. For instance, while BDNF has been reported to decrease during AD[310] in accordance with our results (Results, page 94); a significant increase of NP1 levels in brain and plasma of AD subjects have been reported [112,117] in opposition to what we observed. Interestingly, it has been also described that knockdown of NPR suppressed GluA1 surface levels, impairing excitatory synaptic transmission[113,311], which is interesting in relation with our results, where NPR levels and GluA1 trend to decrease at ADIII-IV stages. Although we found a weak correlation between GluA1 and NPR levels in samples analyzed ($r = 0.41$, $p = 0.018$) it could be noteworthy further investigate it in a larger samples size, together with a possible connection between protein and selected miRNAs levels.

In the specific group of samples that we analyzed, this decreasing trend makes sense, according with the increase of the selected miRNAs. Obviously, we must not lose sight of the fact that we can probably not expect large changes derived from the alteration of a single miRNA, since these proteins, closely involved in synaptic plasticity, are finely regulated by many different mechanisms beside possible miRNA-dependent translational repression. Although we cannot discard a role of these miRNAs on studied targets regulation, it would be necessary to increase the number of samples analyzed and also to establish *in vitro* a direct relationship between the levels of these miRNAs and the proteins of study.

Circulating miRNAs and their usefulness

The detection of miRNAs in blood is a valuable tool as is not invasive when compared to other sources such as CSF, is affordable for screening studies and it allows patient follow-up over time. The value of miRNAs as biomarkers has been largely probed in other diseases, such as cancer, where miRNA research is more advanced[199,202,203,290].

Analysis of near 100 plasma samples allowed us to detect 3 miRNAs differentially express in plasma from MCI and AD subject, and study of an additionally cohort of FTD patients, permitted to determine the specificity of these changes in AD dementia progression. While other groups have reported observation of miR-181c levels decrease in serum with an AUC value of 0.736 in the ROC curve analysis[312], our results in plasma samples showed a significant increase both in MCI and AD subjects (AUC: 0.843 and 0.773, respectively).

Nevertheless, evidence has shown that thinking of one single miRNA as a biomarker could not be the best approach, considering that each miRNA can regulate the levels of many proteins involved in different processes, even in different pathologies. The identification of a molecular signature deregulated during disease that can be detected in circulating fluids seems a more reliable way to distinguish between early AD and healthy subjects.

Other studies proposed a 12-miRNA signature that distinguish MCI with 0.842 accuracy, 81.1% specificity and 87.7% sensitivity in blood[313], or a 9-miRNAs serum signature with an AUC value of 0.978, 93.4% sensitivity and 98.8% of specificity for AD cases identification, whereas it has not been tested in MCI cases[314]. Our signature composed of 3 miRNAs with an AUC value of 0.893 distinguishing MCI cases and 0.855 for AD cases, could be taken into consideration, since it reaches comparable values with only 3 miRNAs, facilitating its potential application in clinical screenings.

miRNA signature	Source	AUC	Sensitivity (%)	Specificity (%)	Method	Ref.
let-7f-5p, miR-1285-5p, miR-107, miR-103a-3p, miR-26b-5p, miR-26a-5p, miR-532-5p, miR-151a-3p, miR-161, let-7d-3p, miR-112, iR-5010-3p	Blood (MCI vs Control)	0.842*	87.7	81.1	NGS and RTqPCR	313
miR-26a-5p, miR-181c-3p, miR-126-5p, miR-22-3p, miR-148b-5p, miR-106b-3p, miR-6119-5p, miR-1246, miR-660-5p	Serum (AD vs Control)	0.986	93.4	98.8	NGS and RTqPCR	314
miR-92a-3p, miR181c-5p, miR-210-3p	**Plasma (MCI vs Control)**	**0.893**	**84.6**	**85.71**	**RTqPCR**	

Table 14: Comparison of 2 miRNA signatures with ours (highlighted in bold letters). AUC: Area under the curve. (*)They used machine learning procedures (SVM) and accuracy is estimated instead of AUC. NGS: Next generation sequencing.

It is also interesting that our candidates are upregulated both in MCI and AD subjects, facilitating its use as biomarkers of all AD stages. In contrast, other groups reported inconsistent changes between MCI and AD subjects, with candidates being upregulated in MCI and downregulated in AD serum, making it difficult to applied them as a biomarker [315].

A limitation of our study is that all analyzed samples were recruited at the same center with participants of the same nationality. A larger study with a bigger number of samples analyzed and from different locations will be our next step to further validate our miRNA plasma signature.

On the value of these results: achieving something tangible

While our knowledge of the biology and function of miRNAs as regulatory molecules and their use as biomarkers is still limited, their role in pathological processes, including AD, is well-grounded[316]. Many works have been able to identify miRNAs

involved in different processes related to the disease, such as tau hyperphosphorylation or oAβ accumulation.

We believe that the detection of miR-92a-3p, miR-181c-5p and miR-210-3p together can benefit an early diagnosis of the disease, something strongly necessary to deepen the understanding of the pathophysiological basis of the disease and especially to design effective therapeutic strategies.

Interestingly, a high percentage of patients diagnosed as MCI progress to AD (Figure 30), supporting the idea that MCI state is frequently an early phase of AD. To be able to correlate the levels of miR-92a-3p, miR-181c-5p and miR-210-3p in patients progressing to AD and those who do not develop the disease, it is important to increase the number of cases. It would be a great outcome if both groups could be differentiated by the levels of expression of the molecular signature that we propose. In addition, it would be very interesting to analyze current samples from those patients for whom there is updated information, so that we can evaluate the levels of these miRNAs and see if the cases that are now AD behave like those AD analyzed at first.

In table 13 it is shown that the progress of the pathology may be different in patients initially diagnosed the same. Thus, one MCI patient can rapidly evolve to AD while another patient may take years or even never develop the disease, making even more essential early AD diagnosis. The opportunity of a routine monitoring through determination of selected miRNAs levels in plasma of asymptomatic subjects could help in the prediction regarding their vulnerability to develop AD in the future.

As commented previously, several evidences have suggested that women could be more susceptible than men to AD pathology[279]. Sex-differences not only include a higher prevalence of AD in women, but also a more severe progression of the disease. In agreement, we considered important to include a gender perspective in the analysis of samples when possible. The considerable number of plasma samples analyzed allows us to separate groups and to confirm that our 3 miRNAs signature is capable of distinguishing MCI and AD cases both in men and in women. Although the predictive values are slightly better for men (MCI; AUC =0.957 and AD,

AUC= 0.938), high predictive values were also found for women (MCI; AUC =0.821 and AD, AUC= 0.8158).

Even though the mechanisms by which these miRNAs may be involved in the development of AD have not been clarified in this thesis, we believe that the identification of a molecular signature composed of 3 miRNAs capable of distinguishing MCI and AD subjects from healthy control is an important outcome. We achieved the identification of three synaptic-related miRNAs, miR-92a-3p, miR-181c-5p and miR-210-3p, which have been found, increase both, in brain and plasma samples from subjects at different stages of the disease. Moreover, these miRNAs showed a high predictive value distinguishing MCI and AD subjects from healthy controls, suggesting a potential use of this signature in clinic screenings. In addition, this miRNAs are not affected in FTD, demonstrating a specificity needed for distinguishing between different dementias. In this regard, we would like to test our molecular signature in other neurodegenerative diseases, such as Parkinson's disease. Furthermore, in vitro results after oAβ treatment are consistent with that observed in plasma, suggesting that this could be a good model to move forward in the study of the role that miRNA alteration could have on early synaptic dysfunction in AD. We hope that this finding will be the beginning of a deeper understanding on the role of miRNAs in synaptic plasticity processes and especially during AD pathology.

CONCLUSIONS

1. miR-92a-3p, miR-143-5p, miR-181c-5p, miR-7151-3p and miR-584-5p miRNA levels are affected in human brain during AD development.
2. miR-92a-3p, miR-181c-5p and miR-210-3p are increased in plasma from MCI and AD patients while miR-584-5p remain stable during AD pathology in plasma samples.
3. miR-92a-3p, miR-181c-5p and miR-210-3p levels are not affected in FTD samples.
4. ROC curve analysis demonstrates that the combination of these three miRNAs is able to distinguish between MCI and AD patients versus control subjects.
5. Over 80% of MCI patients of this study for which we had updated information, progress to AD in the following years after diagnosis.
6. GluA1 proteins levels are affected in early stages of AD (ADIII-IV) when compared to ADI-II.
7. oAβ treatment increase miR-92a-3p, miR-181c-5p and miR-210-3p levels in primary hippocampal mice neurons.
8. miR-92a-3p, miR-181c-5p and miR-210-3p levels are not affected in $APP_{Sw,Ind}$ cognitive deficient mice.

REFERENCES

1. Ramon y Cajal, S. The structure and connexions of neurons. *Nobel Lect. Physiol. or Med. 1901-1921* 220–253 (1906).

2. Prince, M., Comas-Herrera, A., Knapp, M., Guerchet, M. & Karagiannidou, M. *World Alzheimer Report 2016 Improving healthcare for people living with dementia coverage, Quality and costs now and In the future*. (2016).

3. Braak, H. & Braak, E. Evolution of neuronal changes in the course of Alzheimer's disease. *J. Neural Transm. Suppl.* **53,** 127–40 (1998).

4. Allan, R., Martin, S. & Joshua, K. *Adams and Victor's Principles of Neurology*. (McGraw Hill Professional, 2014).

5. McKhann, G. M. *et al.* The diagnosis of dementia due to Alzheimer's disease: recommendations from the National Institute on Aging-Alzheimer's Association workgroups on diagnostic guidelines for Alzheimer's disease. *Alzheimers. Dement.* **7,** 263–9 (2011).

6. World Health Organization -Dementia Fact Sheet. Available at: http://www.who.int/news-room/fact-sheets/detail/dementia. (Accessed: 8th August 2018)

7. Mendiola-Precoma, J., Berumen, L. C., Padilla, K. & Garcia-Alcocer, G. Therapies for Prevention and Treatment of Alzheimer's Disease. *Biomed Res. Int.* **2016,** 2589276 (2016).

8. Hebert, L. E., Weuve, J., Scherr, P. A. & Evans, D. A. Alzheimer disease in the United States (2010-2050) estimated using the 2010 census. *Neurology* **80,** 1778–83 (2013).

9. Mattsson, N. *et al.* Prevalence of the apolipoprotein E ε4 allele in amyloid β positive subjects across the spectrum of Alzheimer's disease. (2018). doi:10.1016/j.jalz.2018.02.009

10. Isidro Carretero, Víctor; Pérez Muñano, Cynthia; Sánchez-Valladares Jaramillo, Vanesa; Balbás Repila, A. *Guía práctica para familiares de enfermos de Alzheimer. Fundación Reina Sofía.* (2011).

11. Xu, J., Zhang, Y., Qiu, C. & Cheng, F. *Global and regional economic costs of dementia: a systematic review*. *The Lancet* **390,** (2017).

12. Prince, M. *et al. World Alzheimer Report 2015. The Global Impact of Dementia*. (Alzheimer's Disease International, 2015).

13. *2018 ALZHEIMER'S DISEASE FACTS AND FIGURES Includes a Special Report on the Financial and Personal Benefits of Early Diagnosis*.

14. Savonenko, A. V., Melnikova, T., Li, T., Price, D. L. & Wong, P. C. Alzheimer Disease. in *Neurobiology of Brain Disorders* 321–338 (Elsevier, 2015). doi:10.1016/B978-0-12-398270-4.00021-5

15. Ralph A. Nixon. Autophagy, amyloidogenesis and Alzheimer disease. doi:10.1242/jcs.019265

16. Selkoe, D. J. Alzheimer's Disease: Genes, Proteins, and Therapy. *Physiol. Rev.* **81,** (2001).

17. Terry, R. D. *et al.* Physical basis of cognitive alterations in alzheimer's disease: Synapse loss is the major correlate of cognitive impairment. *Ann. Neurol.* **30,** 572–580 (1991).

18. Scheff, S. W., Price, D. A., Schmitt, F. A. & Mufson, E. J. Hippocampal synaptic loss in early Alzheimer's disease and mild cognitive impairment. *Neurobiol. Aging* **27,** 1372–1384 (2006).

19. Goedert, M. & Spillantini, M. G. A Century of Alzheimer's Disease. *Science (80-.).* **314,** 777–81 (2006).

20. Hodges, J. R. Alzheimer's centennial legacy: origins, landmarks and the current status of knowledge concerning cognitive aspects. *Brain* **129,** 2811–22 (2006).

21. O'brien, C. Auguste D. and Alzheimer's Disease. *Science (80-.).* **273,** (1996).

22. Lanoiselé, H. L.-M. *et al. APP, PSEN1, and PSEN2 mutations in early-onset Alzheimer disease: A genetic screening study of familial and sporadic cases*.

(2017). doi:10.1371/journal.pmed.1002270

23. Reitz, C. & Mayeux, R. Alzheimer disease: epidemiology, diagnostic criteria, risk factors and biomarkers. *Biochem. Pharmacol.* **88,** 640–51 (2014).

24. Querfurth, H. W. & LaFerla, F. M. Alzheimer's disease. *N. Engl. J. Med.* **362,** 329–44 (2010).

25. Mutations Search | ALZFORUM. Available at: https://www.alzforum.org/mutations/search?genes%5B%5D=348&genes%5B%5D=493&genes%5B%5D=494&diseases%5B%5D=145&keywords-entry=&keywords=#results. (Accessed: 21st August 2018)

26. AD&FTD Mutation Database. Available at: http://www.molgen.ua.ac.be/ADmutations/default.cfm?MT=1&ML=1&Page=MutByQuery&Query=tblMutations.Phenotype In (%27Alzheimer Disease%27)&Selection=Phenotype In (Alzheimer Disease). (Accessed: 21st August 2018)

27. Bird, T. D. *Early-Onset Familial Alzheimer Disease*. *GeneReviews*® (University of Washington, Seattle, 1993).

28. Yu, J.-T., Tan, L. & Hardy, J. Apolipoprotein e in Alzheimer's disease: an update. *Annu. Rev. Neurosci.* **37,** 79–100 (2014).

29. Bisht, K., Sharma, K. & Tremblay, M.-È. Chronic stress as a risk factor for Alzheimer's disease: Roles of microglia-mediated synaptic remodeling, inflammation, and oxidative stress. (2018). doi:10.1016/j.ynstr.2018.05.003

30. Picard C, Julien C, Frappier J, Miron J, Théroux L, Dea D; Breitner JCS, P. J. Alterations in cholesterol metabolism–related genes in sporadic Alzheimer's disease. *Neurobiol. Aging* **66,** 1–4 (2018).

31. Boyle, K., Notterpek, M. & Anderson, J. Accumulation of Apolipoproteins in the Regenerating Mammalian Peripheral Nerve. *J. Biol. Chem.* **265,** 17805–17815 (1990).

32. E. H. Corder, A. M. Saunders, W. J. Strittmatter, D. E. Schmechel, P. C.

Gaskell, G. W. Small, A. D. R. & J. L. Haines, M. A. P.-V. Gene Dose of Apolipoprotein E Type 4 Allele and the Risk of Alzheimer's Disease in Late Onset Families. *Science (80-.).* **261,** (1993).

33. Karch, C. M., Cruchaga, C. & Goate, A. M. Alzheimer's Disease Genetics: From the Bench to the Clinic. *Neuron* **83,** 11–26 (2014).

34. Karch, C. M. & Goate, A. M. Alzheimer's disease risk genes and mechanisms of disease pathogenesis. *Biol. Psychiatry* **77,** 43–51 (2015).

35. Van Der Flier, W. M. & Scheltens, P. EPIDEMIOLOGY AND RISK FACTORS OF DEMENTIA. *J Neurol Neurosurg Psychiatry* **76,** 2–7 (2005).

36. Lobo, A. *et al.* Prevalence of dementia and major subtypes in Europe: A collaborative study of population-based cohorts. Neurologic Diseases in the Elderly Research Group. *Neurology* **54,** S4-9 (2000).

37. Alzheimer Europe, 2013. The Prevalence of Alzheimer's in Europe. *http//www.alzheimer-Eur. Prevalence-of-dementia-in-Europe* http://www.alzheimer-europe.org/Research/European (2013).

38. Bachman, D. L. *et al.* Incidence of dementia and probable Alzheimer's disease in a general population: the Framingham Study. *Neurology* **43,** 515–9 (1993).

39. Altmann, A., Tian, L., Henderson, V. W. & Greicius, M. D. Sex modifies the APOE-related risk of developing Alzheimer disease. *Ann. Neurol.* **75,** 563–573 (2014).

40. Ungar, L., Altmann, A. & Greicius, M. D. Apolipoprotein E, gender, and Alzheimer's disease: an overlooked, but potent and promising interaction. *Brain Imaging Behav.* **8,** 262–73 (2014).

41. Xing, Y., Tang, Y. & Jia, J. Sex Differences in Neuropsychiatric Symptoms of Alzheimer's Disease: The Modifying Effect of Apolipoprotein E ε4 Status. *Behav. Neurol.* **2015,** 275256 (2015).

42. Riedel, B. C. *et al.* Age, APOE and Sex: Triad of Risk of Alzheimer's Disease

HHS Public Access Author manuscript. *J Steroid Biochem Mol Biol* **160,** 134–147 (2016).

43. Nebel, R. A. *et al.* Understanding the impact of sex and gender in Alzheimer's disease: A call to action. *Alzheimer's Dement.* (2018). doi:10.1016/j.jalz.2018.04.008

44. De Strooper, B. Proteases and proteolysis in Alzheimer disease: a multifactorial view on the disease process. *Physiol. Rev.* **90,** 465–94 (2010).

45. De Strooper, B. & Annaert, W. Proteolytic processing and cell biological functions of the amyloid precursor protein. *J. Cell Sci.* **113,** 1857–1870 (2000).

46. De Strooper, B. Loss-of-function presenilin mutations in Alzheimer disease. Talking Point on the role of presenilin mutations in Alzheimer disease. *EMBO Rep.* **8,** 141–6 (2007).

47. Shen, J. & Kelleher, R. J. The presenilin hypothesis of Alzheimer's disease: evidence for a loss-of-function pathogenic mechanism. *Proc. Natl. Acad. Sci. U. S. A.* **104,** 403–9 (2007).

48. Xia, D. *et al.* Presenilin-1 Knockin Mice Reveal Loss-of-Function Mechanism for Familial Alzheimer's Disease. *Neuron* **85,** 967–981 (2015).

49. Selkoe, D. J. Translating cell biology into therapeutic advances in Alzheimer's disease. *Nature* **399,** A23-31 (1999).

50. Kim, J. *et al.* A 40 Inhibits Amyloid Deposition In Vivo. *J. Neurosci.* **27,** 627–633 (2007).

51. Selkoe, D. J. & Hardy, J. The amyloid hypothesis of Alzheimer's disease at 25 years. *EMBO Mol. Med.* **8,** 595–608 (2016).

52. Nisbet, R. M., Polanco, J.-C., Ittner, L. M. & Götz, J. Tau aggregation and its interplay with amyloid-β. *Acta Neuropathol.* **129,** 207–20 (2015).

53. John A. Hardy and Gerald A. Higgins. Alzheimer's Disease: The Amyloid Cascade Hypothesis. *Science (80-.).* **256,** 184–185 (1992).

54. Walsh, D. M. & Selkoe, D. J. Deciphering the molecular basis of memory failure in Alzheimer's disease. *Neuron* **44,** 181–193 (2004).

55. Spires-Jones, T. L. & Hyman, B. T. The intersection of amyloid beta and tau at synapses in Alzheimer's disease. *Neuron* **82,** 756–771 (2014).

56. Hardy, J. & Selkoe, D. J. The amyloid hypothesis of Alzheimer's disease: progress and problems on the road to therapeutics. *Science* **297,** 353–6 (2002).

57. Selkoe, D. J. Alzheimer's disease is a synaptic failure. *Science* **298,** 789–91 (2002).

58. Perez-Nievas, B. G. *et al.* Dissecting phenotypic traits linked to human resilience to Alzheimer's pathology. *Brain* **136,** 2510–26 (2013).

59. Selkoe, D. J. & Hardy, J. The amyloid hypothesis of Alzheimer's disease at 25 years. *EMBO Mol. Med.* **8,** 595–608 (2016).

60. Ballatore, C., Lee, V. M.-Y. & Trojanowski, J. Q. Tau-mediated neurodegeneration in Alzheimer's disease and related disorders. *Nat. Rev. Neurosci.* **8,** 663–72 (2007).

61. Wang, Y. & Mandelkow, E. Tau in physiology and pathology. *Nat. Rev. Neurosci.* **17,** 22–35 (2016).

62. Iqbal, K. *et al. Molecular basis of tau protein pathology: role of abnormal hyperphosphorylation*. *Neurobiology of Alzheimer's Disease* (Oxford University Press, 2007).

63. Mroczko, B., Groblewska, M., Litman-Zawadzka, A., Kornhuber, J. & Lewczuk, P. Cellular Receptors of Amyloid β Oligomers (AβOs) in Alzheimer's Disease. *Int. J. Mol. Sci.* **19,** 1884 (2018).

64. Roberson, E. D. *et al.* Reducing endogenous tau ameliorates amyloid beta-induced deficits in an Alzheimer's disease mouse model. *Science* **316,** 750–4 (2007).

65. Roberson, E. D. *et al.* Amyloid-β/Fyn-induced synaptic, network, and cognitive impairments depend on tau levels in multiple mouse models of Alzheimer's disease. *J. Neurosci.* **31,** 700–11 (2011).

66. Larson, M. *et al.* The complex PrP(c)-Fyn couples human oligomeric Aβ with pathological tau changes in Alzheimer's disease. *J. Neurosci.* **32,** 16857–71a (2012).

67. Goedert, M., Spillantini, M. G., Jakes, R., Rutherford, D. & Crowther, R. A. Multiple isoforms of human microtubule-associated protein tau: sequences and localization in neurofibrillary tangles of Alzheimer's disease. *Neuron* **3,** 519–526 (1989).

68. Nelson, P. T. *et al.* Correlation of Alzheimer disease neuropathologic changes with cognitive status: a review of the literature. *J. Neuropathol. Exp. Neurol.* **71,** 362–81 (2012).

69. Braak, H. & Braak, E. Neuropathological stageing of Alzheimer-related changes. *Acta Neuropathol.* **82,** 239–259 (1991).

70. Hyman, B. T., Van Hoesen, G. W., Damasio, A. R. & Barnes, C. L. Alzheimer's disease: cell-specific pathology isolates the hippocampal formation. *Science* **225,** 1168–70 (1984).

71. Braak, H., Alafuzoff, I., Arzberger, T., Kretzschmar, H. & Del Tredici, K. Staging of Alzheimer disease-associated neurofibrillary pathology using paraffin sections and immunocytochemistry. *Acta Neuropathol.* **112,** 389–404 (2006).

72. Villemagne, V. L., Fodero-Tavoletti, M. T., Masters, C. L. & Rowe, C. C. Tau imaging: Early progress and future directions. *The Lancet Neurology* **14,** 114–124 (2015).

73. Pooler, A. M. *et al.* Propagation of tau pathology in Alzheimer's disease: identification of novel therapeutic targets. *Alzheimers. Res. Ther.* **5,** 49 (2013).

74. Mondragón-Rodríguez, S. *et al.* Interaction of Endogenous Tau Protein with

Synaptic Proteins Is Regulated by N-Methyl-D-aspartate Receptor-dependent Tau Phosphorylation *. (2012). doi:10.1074/jbc.M112.401240

75. Shankar, G. M. *et al.* Amyloid-beta protein dimers isolated directly from Alzheimer's brains impair synaptic plasticity and memory. *Nat. Med.* **14,** 837–42 (2008).

76. Malenka, R. C. & Bear, M. F. LTP and LTD: An Embarrassment of Riches. *Neuron* **44,** 5–21 (2004).

77. Benarroch, E. E. Glutamatergic synaptic plasticity and dysfunction in Alzheimer disease: Emerging mechanisms. *Neurology* **91,** 125–132 (2018).

78. Malinow, R. & Malenka, R. C. AMPA Receptor Trafficking and Synaptic Plasticity. *Annu. Rev. Neurosci.* **25,** 103–126 (2002).

79. Kandel, E. R., Dudai, Y. & Mayford, M. R. The Molecular and Systems Biology of Memory. *Cell* **157,** 163–186 (2014).

80. Huganir, R. L. & Nicoll, R. A. AMPARs and synaptic plasticity: The last 25 years. *Neuron* **80,** 704–717 (2013).

81. Sanderson, J. L., Gorski, J. A. & Dell'Acqua, M. L. NMDA Receptor-Dependent LTD Requires Transient Synaptic Incorporation of Ca2+-Permeable AMPARs Mediated by AKAP150-Anchored PKA and Calcineurin. *Neuron* **89,** 1000–1015 (2016).

82. Castillo, P. E. Presynaptic LTP and LTD of Excitatory and Inhibitory Synapses. *Cold Spring Harb. Perspect. Biol.* **4,** a005728–a005728 (2012).

83. Abraham, W. C. How long will long-term potentiation last? *Trans. R. Soc. Lond. B* **358,** 735–744 (2003).

84. Sweatt, J. D. *Long-Term Potentiation: A Candidate Cellular Mechanism for Information Storage in the CNS*. *Mechanisms of Memory* (Elsevier Inc., 2010). doi:10.1016/B978-0-12-374951-2.00007-X

85. Park, P. *et al.* NMDA receptor-dependent long-term potentiation comprises a

family of temporally overlapping forms of synaptic plasticity that are induced by different patterns of stimulation. *Philos. Trans. R. Soc. B Biol. Sci.* **369,** 20130131–20130131 (2013).

86. Huang, Y. Y., Nguyen, P. V, Abel, T. & Kandel, E. R. Long-lasting forms of synaptic potentiation in the mammalian hippocampus. *Learn. Mem.* **3,** 74–85 (1996).

87. Bailey, C. H., Kandel, E. R. & Harris, K. M. Structural Components of Synaptic Plasticity and Memory Consolidation. *Cold Spring Harb. Perspect. Biol.* **7,** a021758 (2015).

88. Park, P. *et al.* Calcium-Permeable AMPA Receptors Mediate the Induction of the Protein Kinase A-Dependent Component of Long-Term Potentiation in the Hippocampus. (2016). doi:10.1523/JNEUROSCI.3625-15.2016

89. Zhou, Z., Liu, A., Xia, S. & Leung, C. The C-terminal tails of endogenous GluA1 and GluA2 differentially contribute to hippocampal synaptic plasticity and learning. (2017). doi:10.1038/s41593-017-0030-z

90. Shepherd, J. D. & Huganir, R. L. The Cell Biology of Synaptic Plasticity: AMPA Receptor Trafficking AMPAR: alpha-amino-3-hydroxy-5-methyl-4-isoxazolepropionic acid receptor. (2007). doi:10.1146/annurev.cellbio.23.090506.123516

91. Wu, D. *et al.* Postsynaptic synaptotagmins mediate AMPA receptor exocytosis during LTP. *Nature* **544,** 316–321 (2017).

92. Ehlers, M. D. *Reinsertion or Degradation of AMPA Receptors Determined by Activity-Dependent Endocytic Sorting the accumulation and half-life of postsynaptic AMPARs at synapses (O'Brien et al suggesting activity-dependent regula-tion of AMPAR degradation. More rapid loss of synaptic AMPARs has been observed following synaptic stimula*. *Neuron* **28,** (2000).

93. Esteban, J., Shi S., Wilson, C., Nuriya, M., Huganir, R., Malinow, R. PKA phosphorilation of AMPA receptor subunits controls synaptic trafficking underlying plasticity. *Nat. Neurosci.* **6,** 136–143 (2003).

94. Chowdhury, D. & Hell, J. W. Homeostatic synaptic scaling: molecular regulators of synaptic AMPA-type glutamate receptors. *F1000Research* **7,** 234 (2018).

95. Hanley, J. G. *Trafficking Pathways During LTP, LTD and Constitutive Cycling*. *Cell adhesion & migration* **2,** (2008).

96. Traynelis, S. F. *et al.* Glutamate receptor ion channels: structure, regulation, and function. *Pharmacol. Rev.* **62,** 405–96 (2010).

97. Lu, W. *et al.* Subunit Composition of Synaptic AMPA Receptors Revealed by a Single-Cell Genetic Approach. *Neuron* **62,** 254–268 (2009).

98. Oh, M. C., Derkach, V. A., Guire, E. S. & Soderling, T. R. Extrasynaptic Membrane Trafficking Regulated by GluR1 Serine 845 Phosphorylation Primes AMPA Receptors for Long-term Potentiation *. (2005). doi:10.1074/jbc.M509677200

99. Esteban, J. A. *et al.* PKA phosphorylation of AMPA receptor subunits controls synaptic trafficking underlying plasticity. *Nat. Neurosci.* **6,** 136–143 (2003).

100. Banke, T. G. *et al. Control of GluR1 AMPA Receptor Function by cAMP-Dependent Protein Kinase*. (1999).

101. Olivito, L. *et al.* Phosphorylation of the AMPA receptor GluA1 subunit regulates memory load capacity. *Brain Struct. Funct.* **221,** 591–603 (2016).

102. Lee, H.-K. *et al. Phosphorylation of the AMPA Receptor GluR1 Subunit Is Required for Synaptic Plasticity and Retention of Spatial Memory*. *Cell* **112,** (2003).

103. Lee, H.-K., Takamiya, K., He, K., Song, L. & Huganir, R. L. Specific Roles of AMPA Receptor Subunit GluR1 (GluA1) Phosphorylation Sites in Regulating Synaptic Plasticity in the CA1 Region of Hippocampus. *J Neurophysiol* **103,** 479–489 (2010).

104. Boehm, J. *et al.* Synaptic Incorporation of AMPA Receptors during LTP Is Controlled by a PKC Phosphorylation Site on GluR1. *Neuron* **51,** 213–225

(2006).

105. Lin, D.-T. *et al.* Regulation of AMPA receptor extrasynaptic insertion by 4.1N, phosphorylation and palmitoylation. *Nat. Neurosci.* **12,** 879–87 (2009).

106. Sheng, M. & Hoogenraad, C. C. The Postsynaptic Architecture of Excitatory Synapses: A More Quantitative View. (2007). doi:10.1146/annurev.biochem.76.060805.160029

107. Kim, E. & Sheng, M. PDZ DOMAIN PROTEINS OF SYNAPSES. *Nat. Rev.* | *Neurosci.* **5,** 1 (2004).

108. Henley, J. M. & Wilkinson, K. A. Synaptic AMPA receptor composition in development, plasticity and disease. *Nat. Publ. Gr.* **17,** (2016).

109. O'brien, R. J. *et al. Synaptic Clustering of AMPA Receptors by the Extracellular Immediate-Early Gene Product Narp*. *Neuron* **23,** (1999).

110. Colledge, M. *et al.* Targeting of PKA to glutamate receptors through a MAGUK-AKAP complex. *Neuron* **27,** 107–119 (2000).

111. Schlimgen, A. K., Helms, J. A., Vogel, H. & Perin, M. S. *Neuronal Pentraxin, a Secreted Protein with Homology to Acute Phase Proteins of the Immune System*. *Neuron* **14,** (1995).

112. Abad, M. A., Enguita, M., DeGregorio-Rocasolano, N., Ferrer, I. & Trullas, R. Neuronal Pentraxin 1 Contributes to the Neuronal Damage Evoked by Amyloid- and Is Overexpressed in Dystrophic Neurites in Alzheimer's Brain. *J. Neurosci.* **26,** 12735–12747 (2006).

113. García-Nafría, J., Herguedas, B., Watson, J. F. & Greger, I. H. The dynamic AMPA receptor extracellular region: a platform for synaptic protein interactions. *J. Physiol.* **594,** 5449–58 (2016).

114. Xu, D. *et al. Narp and NP1 Form Heterocomplexes that Function in Developmental and Activity-Dependent Synaptic Plasticity*. *Neuron* **39,** (2003).

115. Sia, G. M. *et al.* Interaction of the N-Terminal Domain of the AMPA Receptor

GluR4 Subunit with the Neuronal Pentraxin NP1 Mediates GluR4 Synaptic Recruitment. *Neuron* **55,** 87–102 (2007).

116. Pelkey, K. A. *et al.* Pentraxins coordinate excitatory synapse maturation and circuit integration of parvalbumin interneurons. *Neuron* **85,** 1257–72 (2015).

117. Ma, Q.-L. *et al.* Neuronal pentraxin 1: A synaptic-derived plasma biomarker in Alzheimer's disease. *Neurobiol. Dis.* **114,** 120–128 (2018).

118. DeGregorio-Rocasolano, N., Gasull, T. & Trullas, R. Overexpression of neuronal pentraxin 1 is involved in neuronal death evoked by low K+in cerebellar granule cells. *J. Biol. Chem.* **276,** 796–803 (2001).

119. DeKosky, S. T. & Scheff, S. W. Synapse loss in frontal cortex biopsies in Alzheimer's disease: Correlation with cognitive severity. *Ann. Neurol.* **27,** 457–464 (1990).

120. Forner, S., Baglietto-Vargas, D., Martini, A. C., Trujillo-Estrada, L. & Laferla, F. M. Synaptic Impairment in Alzheimer's Disease: A Dysregulated Symphony. **40,** (2017).

121. Scheff, S. W. *et al.* Synaptic alterations in CA1 in mild Alzheimer disease and mild cognitive impairment. *Neurology* **68,** 1501–8 (2007).

122. Blennow, K. Bogdanovic, N. Alafuzoff, R. Ekman, R. and Davidsson, P. SYnaptic pathology in ALzheimer's disease: relation to severity of dementia, but not senile plaques, neurofibrillary tangles, or the ApoE4 allele. *J. Neural Transm.* **104,** 931–941 (1996).

123. E. Masliah, MD; M. Mallory, BS; M. Alford, BS; R. DeTeresa, BS; L.A. Hansen, MD; D.W. McKeel, Jr., MD; and J.C. Morris, M. Altered expression of synaptic proteins occurs early during progression of Alzheimer ' s disease. *Neurology* 127–130 (2001).

124. Bereczki, E. *et al.* Synaptic proteins predict cognitive decline in Alzheimer's disease and Lewy body dementia. *Alzheimers. Dement.* **12,** 1149–1158 (2016).

125. Bereczki, E. *et al.* Synaptic markers of cognitive decline in neurodegenerative diseases: A proteomic approach. *Brain* **141,** 582–595 (2018).

126. Reddy, P. H. *et al.* Differential loss of synaptic proteins in Alzheimer's disease: implications for synaptic dysfunction. *J. Alzheimers. Dis.* **7,** 103-17; discussion 173-80 (2005).

127. Miñano-Molina, A. J. *et al.* Soluble oligomers of amyloid-β peptide disrupt membrane trafficking of α-amino-3-hydroxy-5-methylisoxazole-4-propionic acid receptor contributing to early synapse dysfunction. *J. Biol. Chem.* **286,** 27311–27321 (2011).

128. Gong, Y. *et al.* Alzheimer's disease-affected brain: presence of oligomeric A beta ligands (ADDLs) suggests a molecular basis for reversible memory loss. *Proc. Natl. Acad. Sci. U. S. A.* **100,** 10417–22 (2003).

129. Townsend, M., Shankar, G. M., Mehta, T., Walsh, D. M. & Selkoe, D. J. Effects of secreted oligomers of amyloid beta-protein on hippocampal synaptic plasticity: a potent role for trimers. *J. Physiol.* **572,** 477–92 (2006).

130. Walsh, D. M. *et al.* Naturally secreted oligomers of amyloid β protein potently inhibit hippocampal long-term potentiation in vivo. *Nature* **416,** 535–539 (2002).

131. Wang, H., Megill, A., He, K., Kirkwood, A. & Lee, H.-K. Consequences of Inhibiting Amyloid Precursor Protein Processing Enzymes on Synaptic Function and Plasticity. *Neural Plast.* **2012,** 1–24 (2012).

132. Zhao, W.-Q. *et al.* Inhibition of Calcineurin-mediated Endocytosis and-Amino-3-hydroxy-5-methyl-4-isoxazolepropionic Acid (AMPA) Receptors Prevents Amyloid Oligomer-induced Synaptic Disruption. *J. Biol. Chem.* **285,** 7619–7632 (2010).

133. Snyder, E. M. *et al.* Regulation of NMDA receptor trafficking by amyloid-β. *Nat. Neurosci.* **8,** 1051–1058 (2005).

134. Hsieh, H. *et al.* AMPAR removal underlies Abeta-induced synaptic depression

and dendritic spine loss. *Neuron* **52,** 831–43 (2006).

135. Tackenberg, C. *et al.* NMDA receptor subunit composition determines beta-amyloid-induced neurodegeneration and synaptic loss. *Cell Death Dis.* **4,** e608 (2013).

136. Parameshwaran, K., Dhanasekaran, M. & Suppiramaniam, V. Amyloid beta peptides and glutamatergic synaptic dysregulation. *Exp. Neurol.* **210,** 7–13 (2007).

137. Lacor, P. N. *et al.* Ab Oligomer-Induced Aberrations in Synapse Composition, Shape, and Density Provide a Molecular Basis for Loss of Connectivity in Alzheimer's Disease. (2007). doi:10.1523/JNEUROSCI.3501-06.2007

138. Li, S. *et al.* Soluble oligomers of amyloid Beta protein facilitate hippocampal long-term depression by disrupting neuronal glutamate uptake. *Neuron* **62,** 788–801 (2009).

139. Liu, S.-J., Gasperini, R., Foa, L., Small, D. H. & Butterfield, D. A. Amyloid-β Decreases Cell-Surface AMPA Receptors by Increasing Intracellular Calcium and Phosphorylation of GluR2. *J. Alzheimer's Dis.* **21,** 655–666 (2010).

140. Walsh, D. M. & Selkoe, D. J. Aβ oligomers - A decade of discovery. *Journal of Neurochemistry* **101,** 1172–1184 (2007).

141. Tu, S., Okamoto, S., Lipton, S. A. & Xu, H. Oligomeric Aβ-induced synaptic dysfunction in Alzheimer's disease. *Mol. Neurodegener.* **9,** 48 (2014).

142. Masliah, E. & Terry, R. The Role of Synaptic Proteins in the Pathogenesis of Disorders of the Central Nervous System. *Brain Pathol.* **3,** 77–85 (1993).

143. Lacor, P. N. *et al.* Synaptic Targeting by Alzheimer's-Related Amyloid Oligomers. (2004). doi:10.1523/JNEUROSCI.3432-04.2004

144. Yu, W. & Lu, B. Synapses and dendritic spines as pathogenic targets in Alzheimer's disease. *Neural Plast.* **2012,** (2012).

145. Klein, W. L., Krafft, G. A., Finch, C. E. & Andrus, E. P. *Targeting small Aβ β*

oligomers: the solution to an Alzheimer's disease conundrum? TRENDS in Neurosciences **24,** (2001).

146. Bredt, D. S. & Nicoll, R. a. AMPA receptor trafficking at excitatory synapses. *Neuron* **40,** 361–379 (2003).

147. Hayashi, Y. *et al.* Driving AMPA receptors into synapses by LTP and CaMKII: Requirement for GluR1 and PDZ domain interaction. *Science (80-.).* **287,** 2262–2267 (2000).

148. Baglietto-Vargas, D. *et al.* Impaired AMPA signaling and cytoskeletal alterations induce early synaptic dysfunction in a mouse model of Alzheimer's disease. *Aging Cell* **17,** e12791 (2018).

149. Almeida, C. G. *et al.* Beta-amyloid accumulation in APP mutant neurons reduces PSD-95 and GluR1 in synapses. *Neurobiol. Dis.* **20,** 187–198 (2005).

150. Bilousova, T. *et al.* Parallel age-associated changes in brain and plasma neuronal pentraxin receptor levels in a transgenic APP/PS1 rat model of Alzheimer's disease. *Neurobiol. Dis.* **74,** 32–40 (2015).

151. Horvitz, H. R. & Sulston, J. E. Isolation and genetic characterization of cell-lineage mutants of the nematode Caenorhabditis elegans. *Genetics* **96,** 435–54 (1980).

152. Wightman, B., Ha, I. & Ruvkun, G. Posttranscriptional regulation of the heterochronic gene lin-14 by lin-4 mediates temporal pattern formation in C. elegans. *Cell* **75,** 855–862 (1993).

153. Lee, Rosalind C, Rhonda L. Feinbaum, V. A. The C . elegans Heterochronic Gene lin-4 Encodes Small RNAs with Antisense Complementarity to lin-14. *Cell* **75,** 843–854 (1993).

154. Kozomara, A. & Griffiths-Jones, S. miRBase Search Results for human. Available at: http://www.mirbase.org/cgi-bin/query.pl?terms=hsa&submit=Search. (Accessed: 9th September 2018)

155. Kozomara, A. & Griffiths-Jones, S. MiRBase: Annotating high confidence

microRNAs using deep sequencing data. *Nucleic Acids Res.* **42,** (2014).

156. Daugaard, I. & Hansen, T. B. Biogenesis and Function of Ago-Associated RNAs. *Trends Genet.* **33,** 208–219 (2017).

157. Jones-Rhoades, M. W., Bartel, D. P. & Bartel, B. MicroRNAs and Their Regulatory Roles in Plants. *Annu. Rev. Plant Biol* **57,** 19–53 (2006).

158. Filipowicz, W., Bhattacharyya, S. N. & Sonenberg, N. Mechanisms of post-transcriptional regulation by microRNAs: Are the answers in sight? *Nature Reviews Genetics* **9,** 102–114 (2008).

159. Grimson, A. *et al.* MicroRNA Targeting Specificity in Mammals: Determinants beyond Seed Pairing. *Mol. Cell* **27,** 91–105 (2007).

160. Vasudevan, S. & Steitz, J. A. AU-Rich-Element-Mediated Upregulation of Translation by FXR1 and Argonaute 2. *Cell* **128,** 1105–1118 (2007).

161. Winter, J., Jung, S., Keller, S., Gregory, R. I. & Diederichs, S. Many roads to maturity: microRNA biogenesis pathways and their regulation. *Nat. Cell Biol.* (2009).

162. Meister, G. Argonaute proteins: functional insights and emerging roles. *Nat. Rev.* | *Genet.* **14,** 447 (2013).

163. Nguyen, T. A., Jo, M. H., Kim, V. N. & Correspondence, J.-S. W. Functional Anatomy of the Human Microprocessor. *Cell* **161,** 1374–1387 (2015).

164. Wahid, F., Shehzad, A., Khan, T. & Kim, Y. Y. MicroRNAs: Synthesis, mechanism, function, and recent clinical trials. *Biochimica et Biophysica Acta - Molecular Cell Research* **1803,** 1231–1243 (2010).

165. Miyoshi, K., Miyoshi, T. & Siomi, H. Many ways to generate microRNA-like small RNAs: Non-canonical pathways for microRNA production. *Molecular Genetics and Genomics* **284,** 95–103 (2010).

166. Wang, Y., Medvid, R., Melton, C., Jaenisch, R. & Blelloch, R. DGCR8 is essential for microRNA biogenesis and silencing of embryonic stem cell self-

renewal. *Nat. Genet.* **39,** 380–385 (2007).

167. Schwarz, D. S. *et al.* Asymmetry in the Assembly of the RNAi Enzyme Complex. *Cell* **115,** (2003).

168. Stagsted, L. V. W., Daugaard, I. & Hansen, T. B. The agotrons: Gene regulators or Argonaute protectors? *BioEssays* **39,** (2017).

169. Hansen, T. B. *et al.* Argonaute-associated short introns are a novel class of gene regulators. *Nat. Commun.* **7,** (2016).

170. Smibert, P., Yang, J.-S., Azzam, G., Liu, J.-L. & Lai, E. C. Homeostatic control of Argonaute stability by microRNA availability. *Nat. Publ. Gr.* **20,** (2013).

171. Forman, J. J., Legesse-Miller, A. & Coller, H. A. *A search for conserved sequences in coding regions reveals that the let-7 microRNA targets Dicer within its coding sequence*. (2008).

172. Yang, W. *et al.* Modulation of microRNA processing and expression through RNA editing by ADAR deaminases. *Nat. Struct. Mol. Biol.* **13,** 13–21 (2006).

173. Kawahara, Y. *et al.* Frequency and fate of microRNA editing in human brain. *Nucleic Acids Res.* **36,** 5270–5280 (2008).

174. Schratt, G. M. *et al.* A brain-specific microRNA regulates dendritic spine development. *Nature* **439,** 283–289 (2006).

175. Chen, W. & Qin, C. General hallmarks of microRNAs in brain evolution and development. (2015). doi:10.1080/15476286.2015.1048954

176. Fineberg, S. K., Kosik, K. S. & Davidson, B. L. MicroRNAs Potentiate Neural Development. *Neuron* **64,** 303–309 (2009).

177. Ludwig, N. *et al.* Distribution of miRNA expression across human tissues. *Nucleic Acids Res.* **44,** 3865–3877 (2016).

178. Landgraf, P. *et al.* A Mammalian microRNA Expression Atlas Based on Small RNA Library Sequencing. *Cell* **12,** 1401–1414 (2007).

179. O'Carroll, D. & Schaefer, A. General principals of miRNA biogenesis and regulation in the brain. *Neuropsychopharmacology* **38,** 39–54 (2013).

180. Weiß, K., Antoniou, A. & Schratt, G. Non-coding mechanisms of local mRNA translation in neuronal dendrites. *European Journal of Cell Biology* **94,** 363–367 (2015).

181. Olde Loohuis, N. F. M. *et al.* MicroRNA networks direct neuronal development and plasticity. *Cell. Mol. Life Sci.* **69,** 89–102 (2012).

182. Cogswell, J. P. *et al.* Identification of miRNA changes in Alzheimer's disease brain and CSF yields putative biomarkers and insights into disease pathways. *J. Alzheimer's Dis.* **14,** 27–41 (2008).

183. Zeng, Y. Regulation of the mammalian nervous system by microRNAs. *Mol. Pharmacol.* **75,** 259–264 (2009).

184. Lugli, G., Torvik, V. I., Larson, J. & Smalheiser, N. R. Expression of microRNAs and their precursors in synaptic fractions of adult mouse forebrain. *J. Neurochem.* **106,** 650–661 (2008).

185. Kye, M. J. *et al.* Somatodendritic microRNAs identified by laser capture and multiplex RT-PCR. *RNA* **13,** 1224–1234 (2007).

186. Smalheiser, N. R. The RNA-centred view of the synapse: Non-coding RNAs and synaptic plasticity. *Philosophical Transactions of the Royal Society B: Biological Sciences* **369,** (2014).

187. Dajas-Bailador, F. *et al.* MicroRNA-9 regulates axon extension and branching by targeting Map1b in mouse cortical neurons. *Nat. Neurosci.* **15,** 697–699 (2012).

188. Eljo, X. *et al.* An Image-Based miRNA Screen Identifies miRNA-135s As Regulators of CNS Axon Growth and Regeneration by Targeting Krüppel-like Factor 4. *Dev.* (2018). doi:10.1523/JNEUROSCI.0662-17.2017

189. Davis, T. H. *et al.* Conditional Loss of Dicer Disrupts Cellular and Tissue Morphogenesis in the Cortex and Hippocampus. *J. Neurosci.* **28,** 4322–4330

(2008).

190. De Pietri Tonelli, D. *et al.* miRNAs are essential for survival and differentiation of newborn neurons but not for expansion of neural progenitors during early neurogenesis in the mouse embryonic neocortex. *Development* **135,** 3911–3921 (2008).

191. Schaefer, A. *et al.* Cerebellar neurodegeneration in the absence of microRNAs. *J. Exp. Med.* **204,** 1553–1558 (2007).

192. Kim, H. H., Kim, P., Phay, M. & Yoo, S. Identification of precursor microRNAs within distal axons of sensory neuron. *J. Neurochem.* **134,** 193–199 (2015).

193. Bicker, S. *et al.* The DEAH-box helicase DHX36 mediates dendritic localization of the neuronal precursor-microRNA-134. *Genes Dev.* **27,** 991–996 (2013).

194. Lugli, G., Larson, J., Martone, M. E., Jones, Y. & Smalheiser, N. R. Dicer and eIF2c are enriched at postsynaptic densities in adult mouse brain and are modified by neuronal activity in a calpain-dependent manner. *J. Neurochem.* **94,** 896–905 (2003).

195. Rajman, M. *et al.* A microRNA-129-5p/Rbfox crosstalk coordinates homeostatic downscaling of excitatory synapses. *EMBO J.* **36,** 1770–1787 (2017).

196. Cohen, J. E., Lee, P. R., Chen, S., Li, W. & Fields, R. D. MicroRNA regulation of homeostatic synaptic plasticity. *Proc. Natl. Acad. Sci.* **108,** 11650–11655 (2011).

197. Saba, R. & Schratt, G. M. MicroRNAs in neuronal development, function and dysfunction. *Brain Res.* **1338,** 3–13 (2010).

198. Gao, J. *et al.* A novel pathway regulates memory and plasticity via SIRT1 and miR-134. *Nature* **466,** 1105–1109 (2010).

199. Van Rooij, E. & Kauppinen, S. Development of microRNA therapeutics is coming of age. *EMBO Mol Med* **6,** 851–864 (2014).

200. Bronze-Da-Rocha, E. MicroRNAs Expression Profiles in Cardiovascular Diseases. (2014). doi:10.1155/2014/985408

201. Roser, A. E., Caldi Gomes, L., Schünemann, J., Maass, F. & Lingor, P. Circulating miRNAs as Diagnostic Biomarkers for Parkinson's Disease. *Front. Neurosci.* **12,** 625 (2018).

202. Saito, Y. & Saito, H. MicroRNAs in cancers and neurodegenerative disorders. *Front. Genet.* **3,** 1–5 (2012).

203. Mitchell, P. S. *et al. Circulating microRNAs as stable blood-based markers for cancer detection*. *PNAS* **105,** (2008).

204. Fortunato, O. *et al.* Assessment of Circulating microRNAs in Plasma of Lung Cancer Patients. *Molecules* **19,** 3038–3054 (2014).

205. Lau, P. *et al.* Alteration of the microRNA network during the progression of Alzheimer's disease. *EMBO Mol. Med.* **5,** 1613–1634 (2013).

206. Hébert, S. S. *et al.* MicroRNA regulation of Alzheimer's Amyloid precursor protein expression. *Neurobiol. Dis.* **33,** 422–428 (2009).

207. Salta, E. & De Strooper, B. MicroRNA-132: A key noncoding RNA operating in the cellular phase of Alzheimer's disease. *FASEB J.* **31,** 424–433 (2017).

208. Banzhaf-Strathmann, J. *et al.* MicroRNA-125b induces tau hyperphosphorylation and cognitive deficits in Alzheimer's disease. *EMBO J.* **33,** 1667–1680 (2014).

209. Smith, P. Y. *et al.* MiR-132/212 deficiency impairs tau metabolism and promotes pathological aggregation in vivo. *Hum. Mol. Genet.* **24,** 6721–6735 (2015).

210. Lugli, G. *et al.* Plasma Exosomal miRNAs in Persons with and without Alzheimer Disease: Altered Expression and Prospects for Biomarkers. *PLoS One* **10,** e0139233 (2015).

211. Hebert, S. S. *et al.* Loss of microRNA cluster miR-29a/b-1 in sporadic

Alzheimer's disease correlates with increased BACE1/ -secretase expression. *Proc. Natl. Acad. Sci.* **105,** 6415–6420 (2008).

212. Yang, G. *et al.* MicroRNA-29c targets β-site amyloid precursor protein-cleaving enzyme 1 and has a neuroprotective role in vitro and in vivo. *Mol. Med. Rep.* **12,** 3081–3088 (2015).

213. Schonrock, N. *et al.* Neuronal microrna deregulation in response to Alzheimer's disease amyloid-β. *PLoS One* **5,** (2010).

214. Zhang, J., Hu, M., Teng, Z., Tang, Y.-P. & Chen, X. C. Synaptic and Cognitive Improvements by Inhibition of 2-AG Metabolism Are through Upregulation of MicroRNA-188-3p in a Mouse Model of Alzheimer's Disease. *Neurobiol. Dis.* (2014). doi:10.1523/JNEUROSCI.1165-14.2014

215. Zhang, Y. *et al.* MicroRNA-135b has a neuroprotective role via targeting of β-site APP-cleaving enzyme 1. *Exp. Ther. Med.* **12,** 809–814 (2016).

216. Barbato, C. *et al.* A lentiviral sponge for miR-101 regulates RanBP9 expression and amyloid precursor protein metabolism in hippocampal neurons. (2014). doi:10.3389/fncel.2014.00037

217. Liu, W. *et al.* MicroRNA-16 targets amyloid precursor protein to potentially modulate Alzheimer's-associated pathogenesis in SAMP8 mice. *Neurobiol. Aging* **33,** 522–534 (2012).

218. Zhang, B., Chen, C.-F., Wang, A.-H. & Lin, Q.-F. MiR-16 regulates cell death in Alzheimer's disease by targeting amyloid precursor protein. *Eur. Rev. Med. Pharmacol. Sci.* **19,** 4020–7 (2015).

219. Delay, C., Calon, F., Mathews, P. & Hébert, S. S. Alzheimer-specific variants in the 3'UTR of Amyloid precursor protein affect microRNA function. *Mol. Neurodegener.* **6,** 70 (2011).

220. Wang, W.-X. *et al.* The Expression of MicroRNA miR-107 Decreases Early in Alzheimer's Disease and May Accelerate Disease Progression through Regulation of-Site Amyloid Precursor Protein-Cleaving Enzyme 1. (2008).

doi:10.1523/JNEUROSCI.5065-07.2008

221. Li, K. *et al.* Synaptic Dysfunction in Alzheimer's Disease: Aβ, Tau, and Epigenetic Alterations. *Mol. Neurobiol.* **55,** 3021–3032 (2017).

222. Idda, M. L., Munk, R., Abdelmohsen, K. & Gorospe, M. Noncoding RNAs in Alzheimer's disease. *Wiley Interdisciplinary Reviews: RNA* **9,** (2018).

223. Rajgor, D. Macro roles for microRNAs in neurodegenerative diseases. *Non-coding RNA Res.* **3,** 154–159 (2018).

224. Müller, M., Kuiperij, H. B., Claassen, J. A., Küsters, B. & Verbeek, M. M. MicroRNAs in Alzheimer's disease: differential expression in hippocampus and cell-free cerebrospinal fluid. (2014). doi:10.1016/j.neurobiolaging.2013.07.005

225. Lee, K. *et al.* Replenishment of microRNA-188-5p restores the synaptic and cognitive deficits in 5XFAD Mouse Model of Alzheimer's Disease. *Nat. Publ. Gr.* (2016). doi:10.1038/srep34433

226. Zhang, J., Hu, M., Teng, Z., Tang, Y.-P. & Chen, X. C. Neurobiology of Disease Synaptic and Cognitive Improvements by Inhibition of 2-AG Metabolism Are through Upregulation of MicroRNA-188-3p in a Mouse Model of Alzheimer's Disease. (2014). doi:10.1523/JNEUROSCI.1165-14.2014

227. Ross, S. P. *et al.* miRNA-431 Prevents Amyloid-β-Induced Synapse Loss in Neuronal Cell Culture Model of Alzheimer's Disease by Silencing Kremen1. *Front. Cell. Neurosci.* **12,** 87 (2018).

228. Li, F. *et al.* MicroRNA-574 is involved in cognitive impairment in 5-month-old APP/PS1 mice through regulation of neuritin. *Brain Res.* **1627,** 177–188 (2015).

229. Kao, Y.-C., Wang, I.-F. & Tsai, K.-J. miRNA-34c Overexpression Causes Dendritic Loss and Memory Decline. *Mol. Sci.* (2018). doi:10.3390/ijms19082323

230. Boese, A. S. *et al.* MicroRNA abundance is altered in synaptoneurosomes

during prion disease. *Mol. Cell. Neurosci.* **71,** 13–24 (2016).

231. Ma, Q. L. *et al.* Neuronal pentraxin 1: A synaptic-derived plasma biomarker in Alzheimer's disease. *Neurobiol. Dis.* **114,** 120–128 (2018).

232. Fang, M. R. *et al.* The miR-124 regulates the expression of BACE1/beta-secretase correlated with cell death in Alzheimer's disease. *Toxicol. Lett.* **209,** 94–105 (2012).

233. Wang, X. *et al.* A Novel MicroRNA-124/PTPN1 Signal Pathway Mediates Synaptic and Memory Deficits in Alzheimer's Disease. *Biol. Psychiatry* **83,** 395–405 (2017).

234. Sperling, R. A. *et al.* Toward defining the preclinical stages of Alzheimer's disease: recommendations from the National Institute on Aging-Alzheimer's Association workgroups on diagnostic guidelines for Alzheimer's disease. *Alzheimers. Dement.* **7,** 280–92 (2011).

235. Jack, C. R. *et al.* Tracking pathophysiological processes in Alzheimer's disease: an updated hypothetical model of dynamic biomarkers. *Lancet. Neurol.* **12,** 207–16 (2013).

236. El Kadmiri, N., Said, N., Slassi, I., El Moutawakil, B. & Nadifi, S. Biomarkers for Alzheimer Disease: Classical and Novel Candidates' Review. *Neuroscience* **370,** 181–190 (2018).

237. Dubois, B. *et al.* Advancing research diagnostic criteria for Alzheimer's disease: the IWG-2 criteria. *Lancet Neurol.* **13,** 614–629 (2014).

238. Gallo, A., Tandon, M., Alevizos, I. & Illei, G. G. The Majority of MicroRNAs Detectable in Serum and Saliva Is Concentrated in Exosomes. *PLoS One* **7,** 30679 (2012).

239. Arroyo, J. D. *et al.* Argonaute2 complexes carry a population of circulating microRNAs independent of vesicles in human plasma. *Proc. Natl. Acad. Sci.* **108,** 5003–5008 (2011).

240. Turchinovich, A., Weiz, L., Langheinz, A. & Burwinkel, B. Characterization of

extracellular circulating microRNA. doi:10.1093/nar/gkr254

241. Riancho, J. *et al.* MicroRNA Profile in Patients with Alzheimer's Disease: Analysis of miR-9-5p and miR-598 in Raw and Exosome Enriched Cerebrospinal Fluid Samples. *J. Alzheimer's Dis.* **57,** 483–491 (2017).

242. Sheinerman, K. S., Tsivinsky, V. G., Abdullah, L., Crawford, F. & Umansky, S. R. Plasma microRNA biomarkers for detection of mild cognitive impairment: Biomarker validation study. *Aging (Albany. NY).* **5,** 925–938 (2013).

243. Kayano, M. *et al.* Plasma microRNA biomarker detection for mild cognitive impairment using differential correlation analysis. *Biomark. Res.* **4,** 22 (2016).

244. Nagaraj, S. *et al.* Profile of 6 microRNA in blood plasma distinguish early stage Alzheimer's disease patients from non-demented subjects. *Oncotarget* **8,** 16122–16143 (2017).

245. Geekiyanage, H., Jicha, G. A., Nelson, P. T. & Chan, C. Blood serum miRNA: Non-invasive biomarkers for Alzheimer's disease. *Exp. Neurol.* **235,** 491–496 (2012).

246. Hara, N. *et al.* Serum microRNA miR-501-3p as a potential biomarker related to the progression of Alzheimer's disease. *Acta Neuropathol. Commun.* **5,** 10 (2017).

247. Denk, J. *et al.* MicroRNA Profiling of CSF Reveals Potential Biomarkers to Detect Alzheimer`s Disease. *PLoS One* **10,** e0126423 (2015).

248. Cosín-Tomás, M. *et al.* Plasma miR-34a-5p and miR-545-3p as Early Biomarkers of Alzheimer's Disease: Potential and Limitations. *Mol. Neurobiol.* **54,** 5550–5562 (2017).

249. Rascovsky, K. *et al.* behavioural variant of frontotemporal dementia. 2456–2477 (2011). doi:10.1093/brain/awr179

250. Gorno-Tempini, M., Hillis, A. E. & Weintraub, S. Classification of primary progressive aphasia and its variants Classification of primary progressive aphasia and its variants. (2011). doi:10.1212/WNL.0b013e31821103e6

251. Brooks, B. R., Miller, R. G., Swash, M. & Munsat, T. L. El Escorial revisited: Revised criteria for the diagnosis of amyotrophic lateral sclerosis. *Amyotroph. Lateral Scler.* **1,** 293–299 (2000).

252. Mucke, L. *et al.* High-level neuronal expression of abeta 1-42 in wild-type human amyloid protein precursor transgenic mice: synaptotoxicity without plaque formation. *J. Neurosci.* **20,** 4050–8 (2000).

253. España, J. *et al.* b-Amyloid Disrupts Activity-Dependent Gene Transcription Required for Memory through the CREB Coactivator CRTC1. (2010). doi:10.1523/JNEUROSCI.2154-10.2010

254. Hsia, A. Y. *et al.* Plaque-independent disruption of neural circuits in Alzheimer's disease mouse models. *Proc. Natl. Acad. Sci. U. S. A.* **96,** 3228–33 (1999).

255. Dahlgren, K. N. *et al. Amyloid-β peptides induce neurotoxicity Oligomeric and Fibrillar Species of Amyloid-β β β β Peptides Differentially Affect Neuronal Viability Downloaded from*. **24,** (JBC Papers in Press, 2002).

256. Klein, W. L. *A toxicity in Alzheimer's disease: globular oligomers (ADDLs) as new vaccine and drug targets*. *Neurochemistry International* **41,** (2002).

257. Lambert, M. P. *et al. Diffusible, nonfibrillar ligands derived from A 1-42 are potent central nervous system neurotoxins*. **95,** (1998).

258. Bradford, M. M. A rapid and sensitive method for the quantitation of microgram quantities of protein utilizing the principle of protein-dye binding. *Anal. Biochem.* **72,** 248–254 (1976).

259. Moldovan, L. *et al.* Methodological challenges in utilizing miRNAs as circulating biomarkers. *J. Cell. Mol. Med.* **18,** 371–390 (2014).

260. Vennemann, M. & Koppelkamm, A. Postmortem mRNA profiling II: Practical considerations. *Forensic Sci. Int.* **203,** 76–82 (2010).

261. Bustin, S. A. *et al.* The MIQE guidelines: minimum information for publication of quantitative real-time PCR experiments. *Clin. Chem.* **55,** 611–22 (2009).

262. Ruijter, J. M. *et al.* Amplification efficiency: linking baseline and bias in the analysis of quantitative PCR data. *Nucleic Acids Res.* **37,** e45 (2009).

263. Pfaffl, M. W. A new mathematical model for relative quantification in real-time RT-PCR. *Nucleic Acids Res.* **29,** 45e–45 (2001).

264. Andersen, C. L., Jensen, J. L. & Ørntoft, T. F. Normalization of real-time quantitative reverse transcription-PCR data: a model-based variance estimation approach to identify genes suited for normalization, applied to bladder and colon cancer data sets. *Cancer Res.* **64,** 5245–50 (2004).

265. Vandesompele, J. *et al.* Accurate normalization of real-time quantitative RT-PCR data by geometric averaging of multiple internal control genes. *Genome Biol.* **3,** 34–1 (2002).

266. Silver, N., Best, S., Jiang, J. & Thein, S. L. Selection of housekeeping genes for gene expression studies in human reticulocytes using real-time PCR. *BMC Mol. Biol.* **7,** (2006).

267. Pfaffl, M. W., Tichopad, A., Prgomet, C. & Neuvians, T. P. *Determination of stable housekeeping genes, differentially regulated target genes and sample integrity: BestKeeper-Excel-based tool using pair-wise correlations*. *Biotechnology Letters* **26,** (2004).

268. RefFinder. Available at: http://leonxie.esy.es/RefFinder/?type=reference#. (Accessed: 16th September 2018)

269. miRWalk2.0: a comprehensive atlas of predicted and validated miRNA-target interactions. Available at: http://zmf.umm.uni-heidelberg.de/apps/zmf/mirwalk2/genepub.html. (Accessed: 15th September 2018)

270. Dweep, H., Sticht, C., Pandey, P. & Gretz, N. MiRWalk - Database: Prediction of possible miRNA binding sites by ‘ walking’ the genes of three genomes. *J. Biomed. Inform.* **44,** 839–847 (2011).

271. Pichler, S. *et al.* The miRNome of Alzheimer’s disease: consistent

downregulation of the miR-132/212 cluster. *Neurobiol. Aging* **50,** 167.e1-167.e10 (2017).

272. Lau, P. *et al.* Alteration of the microRNA network during the progression of Alzheimer's disease. *EMBO Mol. Med.* **5,** 1613–1634 (2013).

273. Schonrock, N. *et al.* Neuronal MicroRNA Deregulation in Response to Alzheimer's Disease Amyloid-b. (2010). doi:10.1371/journal.pone.0011070

274. Millan, M. J. Linking deregulation of non-coding RNA to the core pathophysiology of Alzheimer's disease: An integrative review. *Prog. Neurobiol.* **156,** 1–68 (2017).

275. Geekiyanage, H. & Chan, C. MicroRNA-137/181c Regulates Serine Palmitoyltransferase and In Turn Amyloid , Novel Targets in Sporadic Alzheimer's Disease. *Neurobiol. Dis.* (2011). doi:10.1523/JNEUROSCI.3883-11.2011

276. Hajian-Tilaki, K. *Receiver Operating Characteristic (ROC) Curve Analysis for Medical Diagnostic Test Evaluation*. *Caspian J Intern Med* **4,** (2013).

277. Pepe, M. S., Cai, T. & Longton, G. Combining Predictors for Classification Using the Area under the Receiver Operating Characteristic Curve. *Biometrics* **62,** 221–229 (2006).

278. Mazure, C. M. & Swendsen, J. Sex differences in Alzheimer's disease and other dementias. *Lancet Neurol* **15,** 451–452 (2016).

279. Teresa Ferretti, M. *et al.* Sex differences in Alzheimer disease — the gateway to precision medicine. *Nat. Rev. Neurol.* (2018). doi:10.1038/s41582-018-0032-9

280. Mariani, E., Monastero, R. & Mecocci, P. Mild cognitive impairment: a systematic review. *J. Alzheimers. Dis.* **12,** 23–35 (2007).

281. Nudelman, A. S. *et al.* Neuronal activity rapidly induces transcription of the CREB-regulated microRNA-132, in vivo. *Hippocampus* **20,** 492–498 (2010).

282. Bicker, S., Lackinger, M., Weiß, K. & Schratt, G. MicroRNA-132, -134, and -138: a microRNA troika rules in neuronal dendrites. *Cell. Mol. Life Sci.* **71,** 3987–4005 (2014).

283. Hu, Z. & Li, Z. miRNAs in synapse development and synaptic plasticity. *Current Opinion in Neurobiology* **45,** 24–31 (2017).

284. Chai, S., Cambronne, X. A., Eichhorn, S. W. & Goodman, R. H. MicroRNA-134 activity in somatostatin interneurons regulates H-Ras localization by repressing the palmitoylation enzyme, DHHC9. *Proc. Natl. Acad. Sci.* **110,** 17898–17903 (2013).

285. Giménez-Llort, L. *et al.* Modeling behavioral and neuronal symptoms of Alzheimer's disease in mice: a role for intraneuronal amyloid. *Neurosci. Biobehav. Rev.* **31,** 125–47 (2007).

286. Cummings, J. L., Morstorf, T. & Zhong, K. Alzheimer's disease drug-development pipeline: few candidates, frequent failures.

287. Sperling, R. A., Jack, C. R. & Aisen, P. S. Testing the right target and right drug at the right stage. *Sci. Transl. Med.* **3,** 1–10 (2011).

288. Sheinerman, K. S. & Umansky, S. R. Circulating cell-free microRNA as biomarkers for screening, diagnosis and monitoring of neurodegenerative diseases and other neurologic pathologies. *Front. Cell. Neurosci.* **7,** (2013).

289. Erson, A. E., Petty, E. M. & Petty, E. M. microRNAs in development and disease. *Blackwell Munksgaard Clin. Genet.* **74,** 296–306 (2008).

290. Rupaimoole, R. & Slack, F. J. MicroRNA therapeutics: towards a new era for the management of cancer and other diseases. *Nat. Publ. Gr.* **16,** (2017).

291. Diagnostics Accelerator | Alzheimer's Drug Discovery Foundation. Available at: https://www.alzdiscovery.org/research-and-grants/diagnostics-accelerator. (Accessed: 22nd September 2018)

292. Sheinerman, K. S. *et al.* Circulating brain-enriched microRNAs as novel biomarkers for detection and differentiation of neurodegenerative diseases.

Alzheimers. Res. Ther. **9,** 89 (2017).

293. Le Carré, J., Lamon, S. & Léger, B. Validation of a multiplex reverse transcription and pre-amplification method using TaqMan® MicroRNA assays. *Front. Genet.* **5,** 1–7 (2014).

294. Mattsson, N. *et al.* Revolutionizing Alzheimer's disease and clinical trials through biomarkers. *Alzheimer's Dement. Diagnosis, Assess. Dis. Monit.* **1,** 1–8 (2015).

295. Ma, C. *et al.* A comprehensive meta-Analysis of circulation miRNAs in glioma as potential diagnostic biomarker. *PLoS One* **13,** 1–13 (2018).

296. Holohan, K. N., Lahiri, D. K., Schneider, B. P., Foroud, T. & Saykin, A. J. Functional microRNAs in Alzheimer's disease and cancer: Differential regulation of common mechanisms and pathways. *Front. Genet.* **3,** 1–16 (2013).

297. Schonrock, N., Humphreys, D. T., Preiss, T. & Götz, J. Target gene repression mediated by miRNAs miR-181c and miR-9 both of which are down-regulated by amyloid-β. *J. Mol. Neurosci.* **46,** 324–335 (2012).

298. Li, J. J., Dolios, G., Wang, R. & Liao, F. F. Soluble beta-amyloid peptides, but not insoluble fibrils, have specific effect on neuronal MicroRNA expression. *PLoS One* **9,** (2014).

299. Sturchler-Pierrat, C. *et al. Two amyloid precursor protein transgenic mouse models with Alzheimer disease-like pathology*. **94,** (1997).

300. Parra-Damas, A. *et al.* Crtc1 Activates a Transcriptional Program Deregulated at Early Alzheimer's Disease-Related Stages. *J. Neurosci.* **34,** 5776–5787 (2014).

301. Hansen, K. F., Sakamoto, K., Wayman, G. A., Impey, S. & Obrietan, K. Transgenic miR132 alters neuronal spine density and impairs novel object recognition memory. *PLoS One* **5,** 15497 (2010).

302. Li, Y. Y. *et al.* Increased expression of miRNA-146a in Alzheimer's disease

transgenic mouse models. *Neurosci. Lett.* **487,** 94–98 (2011).

303. Kreth, S., Hübner, M. & Hinske, L. C. MicroRNAs as Clinical Biomarkers and Therapeutic Tools in Perioperative Medicine. *Anesth. Analg.* **126,** 1 (2017).

304. Velagapudi, S. P., Vummidi, B. R. & Disney, M. D. Small molecule chemical probes of microRNA function. *Current Opinion in Chemical Biology* **24,** 97–103 (2015).

305. Bader, A. G. miR-34 – a microRNA replacement therapy is headed to the clinic. (2012). doi:10.3389/fgene.2012.00120

306. Hébert, S. S. & De Strooper, B. Alterations of the microRNA network cause neurodegenerative disease. *Trends in Neurosciences* **32,** 199–206 (2009).

307. Twine, N. A., Janitz, K., Wilkins, M. R. & Janitz, M. Whole Transcriptome Sequencing Reveals Gene Expression and Splicing Differences in Brain Regions Affected by Alzheimer's Disease. *PLoS One* **6,** 16266 (2011).

308. Liang, W. S. *et al.* Altered neuronal gene expression in brain regions differentially affected by Alzheimer's disease: a reference data set NIH Public Access Author Manuscript. *Physiol Genomics* **33,** 240–256 (2008).

309. Saura, C. A., Parra-Damas, A. & Enriquez-Barreto, L. Gene expression parallels synaptic excitability and plasticity changes in Alzheimer's disease. *Front. Cell. Neurosci.* **9,** (2015).

310. Phillips, H. S. *et al.* BDNF mRNA is decreased in the hippocampus of individuals with Alzheimer's disease. *Neuron* **7,** 695–702 (1991).

311. Lee, S.-J. *et al.* Presynaptic Neuronal Pentraxin Receptor Organizes Excitatory and Inhibitory Synapses. *J. Neurosci.* **37,** 1062–1080 (2017).

312. Tan, L. L. *et al.* Circulating miR-125b as a biomarker of Alzheimer's disease. *J. Neurol. Sci.* **336,** 52–56 (2014).

313. Leidinger, P. *et al.* A blood based 12-miRNA signature of Alzheimer disease patients. *Genome Biol.* **14,** R78 (2013).

314. Guo, R. *et al.* A 9-microRNA Signature in Serum Serves as a Noninvasive Biomarker in Early Diagnosis of Alzheimer's Disease. *J. Alzheimer's Dis.* **60,** 1365–1377 (2017).

315. Dong, H. *et al.* Serum MicroRNA Profiles Serve as Novel Biomarkers for the Diagnosis of Alzheimer's Disease.1 Dong Hui, Li Jialu, Huang Lei, et al. Serum MicroRNA Profiles Serve as Novel Biomarkers for the Diagnosis of Alzheimer's Disease. Dis Markers 2015; 2015:625659. D. *Dis. Markers* **2015,** 625659 (2015).

316. Millan, M. J. Linking deregulation of non-coding RNA to the core pathophysiology of Alzheimer's disease: an integrative review. *Prog. Neurobiol.* (2017). doi:10.1016/j.pneurobio.2017.03.004

ANNEXES

Accession	Transcript ID (Array Design)	Control Bi-weight Avg Signal (log2)	ADI-II Bi-weight Avg Signal (log2)	ADIII-IV Bi-weight Avg Signal (log2)	ADV-VI Bi-weight Avg Signal (log2)	Control Standard Deviation	ADI-II Standard Deviation	ADIII-IV Standard Deviation	ADV-VI Standard Deviation	Fold Change (ADI-II vs. Control)	ANOVA p-value (ADI-II vs. Control)	Fold Change (ADIII-IV vs. Control)	ANOVA p-value (ADIII-IV vs. Control)	Fold Change (ADV-VI vs. Control)	ANOVA p-value (ADV-VI vs. Control)
MIMAT0004502	hsa-miR-145-5p	12.52	11.21	11.17	11.43	0.05	0.45	0.27	0.25	**-2.49**	**0.007464**	**-2.55**	**0.001379**	**-2.13**	**0.004025**
MIMAT0005593	hsa-miR-3120-3p	2.02	0.69	0.55	0.53	0.31	0.46	0.6	0.07	**-2.5**	**0.024995**	**-2.76**	**0.048682**	**-2.81**	**0.01136**
MIMAT0027399	hsa-miR-143-5p	5.52	2.36	1.58	2.84	0.35	1.64	1.69	0.87	**-8.89**	**0.041**	**-15.3**	**0.032599**	**-6.4**	**0.014586**
MIMAT0016921	hsa-miR-143-3p	12.3	10.77	11.05	11.14	0.27	0.4	0.27	0.39	**-2.89**	**0.00667**	**-2.38**	**0.00456**	**-2.24**	**0.027238**
MIMAT0004813	hsa-miR-3065-3p	4.25	5.44	4.99	5.41	0.56	0.24	0.2	0.14	**2.28**	**0.012867**	**1.66**	**0.039402**	**2.22**	**0.040101**
MIMAT0021080	hsa-miR-642a-3p	4.38	3.02	2.66	2.19	0.64	0.99	0.83	0.92	**-2.58**	**0.046396**	**-3.31**	**0.026054**	**-4.56**	**0.048816**
MIMAT0015041	hsa-miR-6508-5p	4.36	4.92	5.53	5.4	0.13	0.44	0.33	0.07	**1.48**	**0.094582**	**2.26**	**0.007002**	**2.05**	**0.002134**
HBII-115	hsa-miR-584-5p	8.26	7.37	7.2	7.22	0.16	1.37	0.41	0.03	**-1.85**	**0.283181**	**-2.09**	**0.011159**	**-2.05**	**0.003091**
MIMAT0026720	hsa-miR-5571-5p	6.05	6.45	7.25	7.08	0.28	0.33	0.39	0.01	**1.33**	**0.373274**	**2.3**	**0.020894**	**2.04**	**0.024022**
MIMAT0018072	hsa-miR-338-5p	8.76	8.25	8.06	8.17	0.21	1.07	0.27	0.09	**-1.43**	**0.366691**	**-1.62**	**0.021559**	**-1.5**	**0.035564**
MIMAT0000427	hsa-miR-1973	6.87	6.15	5.99	5.79	0.33	0.74	0.58	0.48	**-1.64**	**0.276474**	**-1.85**	**0.022213**	**-2.11**	**0.03642**

Microarray Results for entorhinal cortex: miRNA levels during the pathology progression compared to healthy subjects. Changes in ADI-II mantained in later stages and changes starting in ADIII-IV stage mantained until ADV-VI. p-value < 0.05 and Fold change ≥ 1.5 was considered significant.

Accession	Transcript ID (Array Design)	Control Bi-weight Avg Signal (log2)	ADI-II Bi-weight Avg Signal (log2)	ADIII-IV Bi-weight Avg Signal (log2)	ADV-VI Bi-weight Avg Signal (log2)	Control Standard Deviation	ADI-II Standard Deviation	ADIII-IV Standard Deviation	ADV-VI Standard Deviation	Fold Change (linear) (ADI-II vs. Control)	ANOVA p-value (ADI-II vs. Control)	Fold Change (linear) (ADIII-IV vs. Control)	ANOVA p-value (ADIII-IV vs. Control)	Fold Change (linear) (ADV-VI vs. Control)	ANOVA p-value (ADV-VI vs. Control)
MIMAT0020924	**hsa-miR-642a-3p**	4,56	3	3,32	3,37	0,09	0,56	0,47	0,9	**-2,95**	**0,008009**	**-2,36**	**0,011232**	**-2,29**	**0,028282**
MIMAT0019019	**hsa-miR-4485**	8,85	7,32	6,76	6,83	0,83	0,1	0,26	0,03	**-2,88**	**0,031617**	**-4,27**	**0,017016**	**-4,05**	**0,013002**
MIMAT0028213	**hsa-miR-7151-3p**	2,34	1,14	1,09	0,81	0,63	0,41	0,19	0,24	**-2,29**	**0,038289**	**-2,37**	**0,011856**	**-2,88**	**0,012209**
MIMAT0018076	**hsa-miR-3656**	11,25	10,36	10,09	10,28	0,21	0,45	0,38	0,37	**-1,85**	**0,049757**	**-2,24**	**0,013239**	**-1,96**	**0,024701**
MIMAT0015090	**hsa-miR-1273d**	2,61	1,04	1,42	0,66	0,48	1,59	0,48	0,52	**-2,99**	**0,364548**	**-2,28**	**0,019188**	**-3,88**	**0,009274**
MIMAT0019022	**hsa-miR-4488**	11,53	11,09	10,45	10,79	0,26	0,63	0,42	0,21	**-1,36**	**0,292227**	**-2,12**	**0,043264**	**-1,68**	**0,020079**
MIMAT0027574	**hsa-miR-6836-5p**	6,74	6,29	5,89	5,6	0,3	0,47	0,16	0,65	**-1,37**	**0,3429**	**-1,8**	**0,006155**	**-2,2**	**0,015472**
MI0022645	**hsa-mir-6800**	10,76	9,99	9,97	9,82	0,39	0,37	0,22	0,15	**-1,7**	**0,252224**	**-1,73**	**0,043523**	**-1,93**	**0,02982**
MIMAT0031016	**hsa-miR-8089**	7,26	6,77	6,5	6,34	0,38	0,24	0,04	0,38	**-1,4**	**0,19395**	**-1,69**	**0,033665**	**-1,9**	**0,04733**
MIMAT0027542	**hsa-miR-6821-5p**	10,13	9,38	9,42	9,32	0,33	0,37	0,23	0,17	**-1,69**	**0,257556**	**-1,64**	**0,046708**	**-1,76**	**0,0271**
MIMAT0019871	**hsa-miR-4741**	8,89	8,38	8,23	7,78	0,32	0,34	0,25	0,34	**-1,43**	**0,099952**	**-1,58**	**0,045402**	**-2,17**	**0,025624**
MIMAT0004609	**hsa-miR-149-3p**	10,51	10,26	9,88	9,85	0,26	0,48	0,23	0,18	**-1,19**	**0,258972**	**-1,56**	**0,019152**	**-1,59**	**0,013471**
MIMAT0027614	**hsa-miR-6857-5p**	1,18	1,47	0,57	0,57	0,22	0,3	0,04	0,15	**1,22**	**0,323313**	**-1,53**	**0,018778**	**-1,52**	**0,033243**
MIMAT0019074	**hsa-miR-378i**	6,05	6,12	6,7	6,63	0,13	0,42	0,22	0,08	**1,05**	**0,296141**	**1,57**	**0,024925**	**1,5**	**0,003462**
14qII-26	**14qII-26**	6,46	6,71	7,13	7,4	0,27	0,46	0,25	0,24	**1,19**	**0,439023**	**1,6**	**0,042544**	**1,92**	**0,012553**
MIMAT0004599	**hsa-miR-143-5p**	4,73	4,93	5,56	5,87	0,35	0,21	0,32	0,21	**1,15**	**0,742999**	**1,78**	**0,019959**	**2,21**	**0,008375**
MIMAT0019843	**hsa-miR-4725-5p**	2,18	4,05	3,81	3,38	0,51	1,48	0,52	0,36	**3,67**	**0,339526**	**3,1**	**0,037429**	**2,3**	**0,031175**
MIMAT0002805	**hsa-miR-489-3p**	3,18	4,17	4,84	5,69	0,99	2,47	0,17	0,38	**2**	**0,626397**	**3,17**	**0,041306**	**5,71**	**0,015328**
MIMAT0022485	**hsa-miR-4666b**	2,11	2,87	3,96	4,73	0,69	0,61	0,48	0,51	**1,69**	**0,333356**	**3,6**	**0,018377**	**6,12**	**0,006082**
MIMAT0000264	**hsa-miR-203a**	1,24	2,14	4,76	2,92	0,35	1,38	1,03	0,9	**1,87**	**0,398098**	**11,5**	**0,005673**	**3,2**	**0,038308**

Microarray Results for hippocampus: miRNA levels during the pathology progression compared to healthy subjects. Changes in ADI-II mantained in later stages and changes starting in ADIII-IV stage mantained until ADV-VI. p-value < 0.05 and Fold change ≥ 1.5 was considered significant.

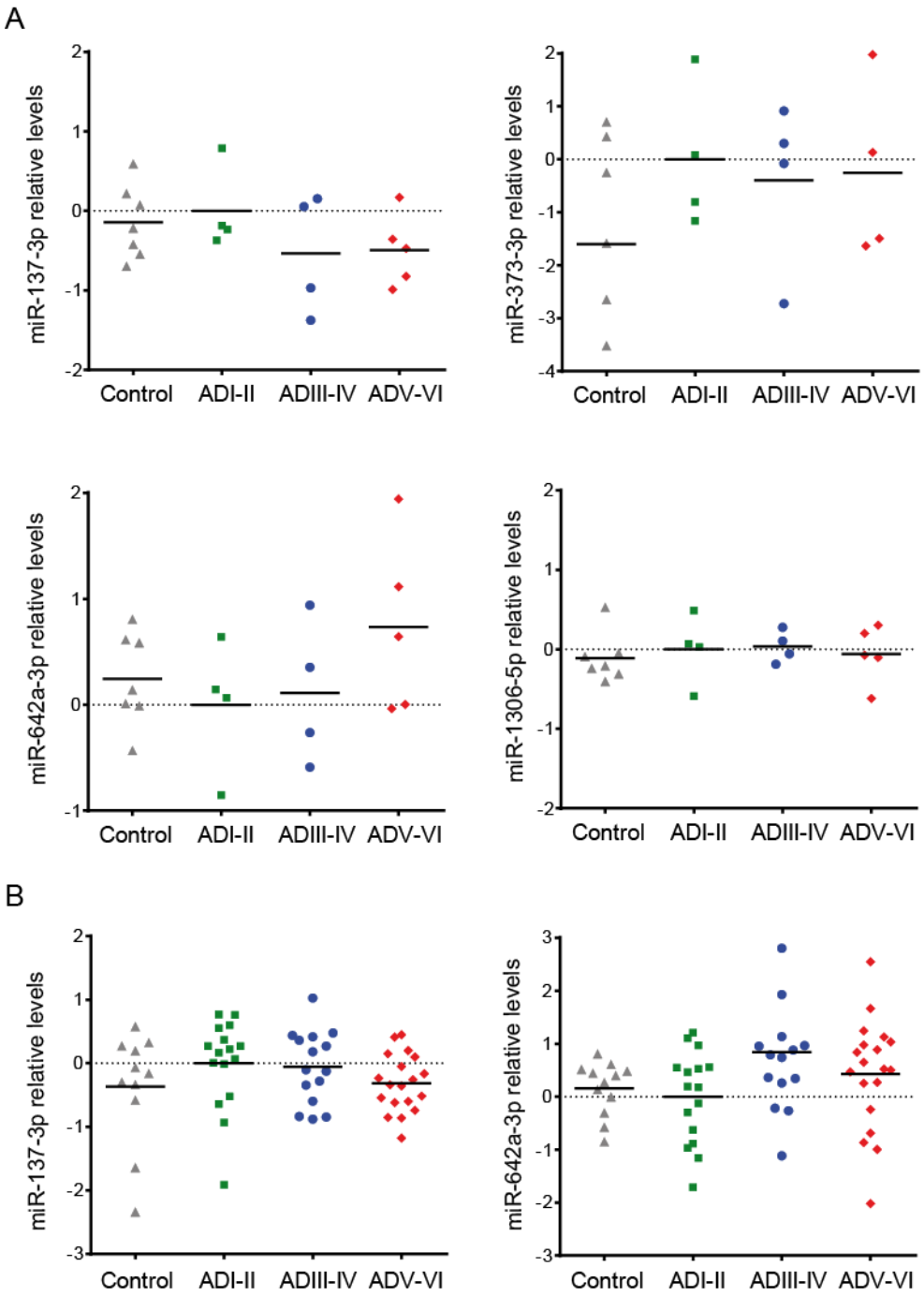

Figure I: Other candidates miRNA levels in entorhinal cortex (A) and hippocampus (B). Selected miRNAs levels were analyzed at different Braak stages of AD pathology and were compared with cognitively normal subjects. Log2 transformed data were normalized versus the geometric mean of U18 and U48 levels. p-value <0.05 was considered significant.

INDEX

INTRODUCTION 1

1. Alzheimer's disease 4

The numbers of the disease 4

AD genetics and neuropathological aspects 5

Synaptic plasticity and glutamatergic synaptic transmission 12

Synaptic dysfunction in AD 15

2. microRNAs 18

miRNAs biogenesis 19

miRNAs in synaptic plasticity 24

miRNAs in AD 26

miRNAs as biomarkers 27

AIMS 31

METHODS 35

1. Human samples 37

Human plasma samples 37

Human tissue samples 37

2. Experimental models 39

$APP_{Sw,Ind}$ transgenic mice 39

Primary hippocampal neuronal cultures 40

Cell lines 41

3. Cell treatments 41

OAβ oligomerization 41

Chemical stimulation of hippocampal neurons 42

4. Biochemical methods 43

Tissue and cell lysis and protein quantification 43

SDS-PAGE and Western Blotting 44

5. Molecular biology methods 45

Samples processing and miRNA extraction 45
Reverse transcription 47
Quantitative real-time PCR 49
Droplet digital PCR 51
Generation of lentiviral vectors 52
Luciferase assay 56
6. Microarray analysis 58
7. Statistical analysis 61
RESULTS 63
1. miRNA levels deregulation during AD progression in different brain areas: Microarray results 65
2. Microarray validation: human brain 74
snoRNAs RNU18 and RNU48 were selected for miRNA levels normalization in brain samples 74
Determination of the control group 75
miR-132-3p levels decrease during AD progression in all studied brain areas 75
miR-92a-3p and miR-181c-5p levels increase in AD entorhinal cortex 76
miR-92a-3p, miR-143-5p and miR-7151-3p levels increase in early AD hippocampus 77
miR-181c-5p levels are increased in prefrontal cortex in late AD stages 77
miR-92a-3p and miR-584-5p levels are altered in cerebelum of AD patients 78
3. Microarray validation: human plasma 83
miR-191 and miR-484 were selected for miRNA levels normalization in plasma 83
miR-92a-3p, miR-181c-5p and miR-210-3p are increased in plasma levels from MCI and AD patients. 83
Majority of evaluated MCI patients progress to AD 90
Expression levels of miR-92a-3p, miR-181c-5p and miR-210-3p are not affected in FTD patients 91
4. Study of selected-miRNAs protein target levels during AD progression 93
Bcl-2 levels increase in entorhinal cortex during AD progression 93
Total GluA1 levels decrease in hippocampus during AD progression 93
5. Study of selected miRNA levels *in vitro* 96
oAβ exposure increase miR-181c-5p and miR-210-3p levels 96

miR-92a-3p levels are no significantly affected by neuronal activity induction with bicuculline.. 97
miRNAs silencing and overexpression.... 98
Potential targets are not affected by oAβ nor LNA miRNA inhibitors.... 101
LNA miRNA inhibitors efficiency in not clear.... 102
6. Study of selected miRNA levels in the hippocampus of $APP_{Sw,Ind}$ transgenic mice 104
APPSw,Ind 104
DISCUSSION 109
CONCLUSIONS 123
REFERENCES 127
ANNEX 160